Stringent response regulation and its impact on *ex vivo* survival in the commensal pathogen *Neisseria meningitidis*

Regulation der stringenten Kontrolle und ihre Auswirkungen auf das *ex vivo* Überleben des kommensalen Erregers *Neisseria meningitidis*

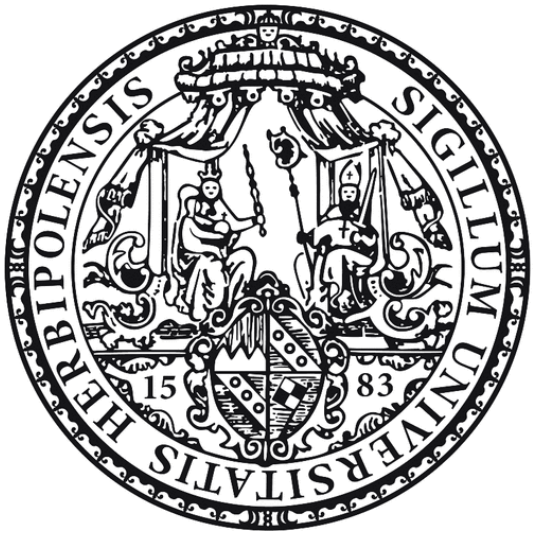

Dissertation zur Erlangung des
naturwissenschaftlichen Doktorgrades
der Julius-Maximilians-Universität Würzburg

vorgelegt von

Laura Violetta Hagmann (geb. Kischkies)

Frankfurt am Main

Würzburg, 2016

Eingereicht am: ……

Mitglieder der Promotionskommission:

Vorsitzender: ……..

Gutachter: PD Dr. rer. nat. Dr. med. Christoph U. Schoen

Gutachter: PD Dr. rer. nat. Knut Ohlsen

Tag des Promotionskolloquiums: ……...

Doktorurkunde ausgehändigt am: ……...

EIDESSTATTLICHE ERKLÄRUNG

Hiermit versichere ich, dass ich die vorliegende Dissertation selbstständig angefertigt und nur die angegebenen Quellen und Hilfsmittel verwendet habe. Ich versichere zudem, dass diese Arbeit in dieser oder ähnlicher Form in keinem anderen Prüfungsverfahren vorgelegen hat. Bis auf den Titel der Diplom-Biologin habe ich bislang keinen anderen akademischen Grad erworben oder zu erwerben versucht.

Würzburg, den 13.10.2016

…….

Laura Violetta Hagmann

Table of Content

1 Summary

Neisseria meningitidis is a commensal bacterium which sometimes causes serious disease in humans. Recent studies in numerous human pathogenic bacteria have shown that the stringent response contributes to bacterial virulence. Therefore, this study analyzed the regulation of the stringent response in meningococci and in particular of RelA as well as its contribution to *ex vivo* fitness in a strain- and condition- dependent manner by using the carriage strain α522 and the hyperinvasive strain MC58 in different *in vitro* and *ex vivo* conditions.

Growth experiments revealed that both wild-type strains were almost indistinguishable in their *ex vivo* phenotypes. However, quantitative real time PCR (qRT-PCR) found differences in the gene expression of *relA* between both strains. Furthermore, in contrast to the MC58 RelA mutant strain α522 deficient in RelA was unable to survive in human whole blood, although both strains showed the same *ex vivo* phenotypes in saliva and cerebrospinal fluid. Moreover, strain α522 was depended on a short non-coding AT-rich repeat element (ATR_{relA}) in the promoter region of *relA* to survive in human blood. Furthermore, cell culture experiments with human epithelial cells revealed that in both strains the deletion of *relA* resulted in a significantly decreased invasion rate while not significantly affecting adhesion. In order to better understand the conditional lethality of the *relA* deletion, computational and experimental analyses were carried out to unravel differences in amino acid biosynthetic pathways between both strains. Whereas strain MC58 is able to synthesize all 20 amino acids, strain α522 has an auxotrophy for cysteine and glutamine. In addition, the *in vitro* growth experiments found that RelA is required for growth in the absence of external amino acids in both strains. Furthermore, the mutant strain MC58 harboring an ATR_{relA} in its *relA* promoter region showed improved growth in minimal medium supplemented with L-cysteine and/or L-glutamine compared to the wild-type strain. Contrary, in strain α522 no differences between the wild-type and the ATR_{relA} deletion mutant were observed.

Together this indicates that ATR_{relA} interferes with the complex regulatory interplay between the stringent response pathway and L-cysteine as well as L-glutamine metabolism. It further suggests that meningococcal virulence is linked to *relA* in a strain- and condition- depended manner. In conclusion, this work highlighted the role of the stringent response and of non-coding regulatory elements for bacterial virulence and indicates that virulence might be related to the way how meningococci accomplish growth within the host environments.

2 Zusammenfassung

Neisseria meningitidis ist ein kommensal lebendes, fakultativ pathogenes Bakterium, welches unter nicht vollständig verstandenen Umständen lebensbedrohliche Krankheitsbilder bei Menschen verursacht. Aktuelle Studien haben gezeigt, dass die stringente Antwort einen Einfluss auf die bakterielle Virulenz haben kann. Aus diesem Grund untersucht diese Arbeit die Regulation der stringenten Antwort, insbesondere die Rolle von RelA, sowie den Einfluss der stringenten Antwort auf die *Ex-vivo*-Fitness der Meningokokken. Die Ergebnisse wurden für den Trägerstamm α522 und den hyperinvasiven Stamm MC58 erhoben und miteinander verglichen.

Wachstumsexperimente zeigten, dass sich beide Wildtyp-Stämme in ihren *Ex-vivo*-Phänotypen nicht unterscheiden. Jedoch wurden mittels quantitativer Echtzeit-PCR (qRT-PCR) Unterschiede zwischen beiden Stämmen in der Genexpression von *relA* gefunden. Zudem war die α522 *relA* Mutante im Gegensatz zu der MC58 *relA* Mutante nicht in der Lage, in menschlichem Vollblut zu überleben. Allerdings zeigten in Saliva und Liquor beide Stämme den gleichen Phänotyp. Außerdem war der Trägerstamm auf eine kurze, nicht-codierende AT-reiche Region (ATR_{relA}) in der Promotorregion von *relA* angewiesen, um im menschlichen Blut überleben zu können. Darüber hinaus zeigten Zellkulturexperimente mit humanen Epithelzellen, dass die Deletion *relA* die Invasionsrate in beiden Stämmen signifikant verringerte, obwohl die Adhäsionsrate durch die Deletion unbeeinflusst blieb.

Um besser verstehen zu können, weshalb die Deletion von *relA* unter bestimmten Bedingungen letal ist, wurden mit *In-silico*- und experimentellen Analysen nach Unterschieden in den Aminosäurebiosynthesewegen beider Stämme gesucht. Es zeigte sich, dass Stamm MC58 in der Lage ist alle 20 Aminosäuren zu synthetisieren, während Stamm α522 eine Auxotrophie für Cystein und Glutamin aufweist. Ferner zeigten die *In-vitro*-Wachstumsversuche, dass RelA bei Aminosäuremangel essentiell für beide Stämme ist. Darüber hinaus zeigte eine MC58 Mutante mit einer ATR_{relA} –Kopie in der *relA* Promotorregion ein im Vergleich zum Wildtyp-Stamm verbessertes Wachstum in mit L-Cystein und/oder L-Glutamin angereichertem Minimalmedium. Gegensätzlich dazu zeigte der Stamm α522 keine Unterschiede im Wachstum zwischen dem Wildtyp und einer ATR_{relA} Deletions-Mutante.

Dies deutet darauf hin, dass ATR_{relA} an dem komplexen regulatorischen Zusammenspiel der stringenten Antwort und dem L-Cystein- beziehungsweise dem L-Glutamin-Metabolismus beteiligt ist. Es lässt sich vermuten, dass RelA zu der Virulenz von

Meningokokken in einer stamm- und umgebungsspezifischen Weise beiträgt. Abschließend hebt diese Arbeit die Rolle von kleinen regulatorischen Elementen für die bakterielle Virulenz hervor und postuliert, dass die Virulenz der Meningokokken auf ihrer Fähigkeit basiert, sich der durch den Wirt gegebenen Umgebung anzupassen.

3 Introduction

3.1 The commensal pathogen *Neisseria meningitidis*

Neisseria meningitidis is a gram-negative diplococcus and belongs to the ß-proteobacteria. It lives as a commensal bacterium in the upper airways of humans and can be found in the nasopharynx of up to 10% of the healthy population [2, 3]. Humans are the exclusively hosts and the bacteria can be transmitted from person to person by direct contact or via inhalation of airborne droplets [4]. The colonization process starts with the adhesion of the bacteria to the epithelial cell layer of the human nasopharynx [5]. In this environment the microorganisms, as other bacterial commensals, can form a biofilm which provides a 'shield' against the host immune system and mechanical forces [6]. Meningococci can sometimes penetrate the epithelial layer of the nasopharynx, enter into the bloodstream, multiply and evade the immune system of the host and thus can cause life-threatening sepsis. If they reach and adhere to the endothelial cell layer of brain vessels, they can cross the blood-brain barrier and finally replicate in the human cerebrospinal fluid (CSF) in the subarachnoidal space [7] causing acute bacterial meningitis [5, 8]. Invasive meningococcal disease (IMD) can occur as an endemic disease with sporadic cases or in form of global epidemics [4] and leads to death in about 10% of the cases [9]. On the basis of their capsular polysaccharides thirteen serogroups can be distinguished, however, only six serogroups of *N. meningitidis* (A, B, C, W-135, Y and X) are responsible for most IMD cases around the world [10, 11].

Unfortunately, the reasons why these bacteria sometimes cause IMD is still poorly understood and the genetic factors which contribute to bacterial invasiveness remain unclear [5]. In fact, IMD is an evolutionary dead end for this species as bacteria residing in the bloodstream or CSF are rarely transmitted to new hosts.

3.2 Pathogenomics of *N. meningitidis*

Research over the past decades has shown that meningococci possess numerous factors that are involved in host interaction and that might coincidentally contribute to virulence: (i) the capsule polysaccharide expression, (ii) expression of adhesines, such as pili, porin A and B, (iii) endotoxins, like lipopolysaccharides (LPS) and (iv) the high genome flexibility, resulting from its natural competence for the uptake of DNA [12].

However, in contrast to pathogenic *Escherichia coli* there is no defined set of virulence genes in *N. meningitidis* that would allow for a clear separation between pathogenic and non-pathogenic bacteria [13]. With respect to gene content meningococcal strains isolated from healthy carriers and IMD patients are almost indistinguishable [14], and many of the so called meningococcal virulence genes have also been found in purely commensal neisserial species [15]. The analysis of meningococcal population genetic structure by multilocus sequence typing (MLST) demonstrated yet that disease-causing meningococci do belong to particular groups of related sequence types (STs), termed clonal complexes (CCs), which are overrepresented in disease isolates relative to their carriage prevalences and are responsible for most disease [16]. This indicates that invasive disease is somehow associated with the genetic background of hyperinvasive lineages. Experimental studies further indicate that differences in gene expression patterns [17] and metabolism [18] might have a central role in the virulence differences among different lineages. Together, this suggests that genetic differences affecting metabolism among meningococcal strains contribute to meningococcal virulence in a yet to define manner.

Most experimental work has focused almost exclusively on invasive strains to identify so called virulence factors responsible for disease. Recent investigations revealed particular large and blood-specific expression differences between a strain that was isolated from a healthy carrier and a strain isolated from a case of invasive disease. These two meningococcal serogroup B strains are geno- and phenotypically very similar, except for their epidemiology (Table 3.1).

Table 3.1 *Comparison of the two meningococcal strains used in this study*

Strain	**α522**	**MC58**
Genome characteristics		
GenBank accession number	FR845693 to FR845718	AE002098
Genome size[a]	≥ 2,066,193 bp	2,272,360 bp
GC content[a]	51.78%	51.53%
Predicted number of coding sequences[a]	≥ 2002	2063
Reference	This work, Ampattu & Hagmann *et al*., 2016 (submitted)	Tettelin *et al*., 2000 [19]
Molecular epidemiology		
Lineage[b]	carriage	invasive
Source[b]	carrier	IMD[c]
Country[b]	Germany	United Kingdom
Year of isolation[b]	2000	1983
Sequence type (ST)[b]	ST-35	ST-74
Clonal complex (CC)[b]	ST-35	ST-32
Serogroup	B	B
Reference	Claus *et al.,* 2005 [2]	McGuiness *et al.,* 1991 [20]

[a]Calculated by using the ARTEMIS tool from Sanger, [21]

[b]Based on ref. [2]

[c]Invasive meningococcal disease

Strain MC58 belongs to the hyperinvasive ST-32 CC and the carriage strain α522 belongs to the ST-35 CC, and both strains share about 95.9% of their genes [22].

The *N. meningitidis* model strain MC58 has a 2,272,351-base pair genome, with an average G+C content of 51.5% and contains 2158 predicted coding genes, of which 1158 open reading frames (ORFs) were assigned to have a biological role [19]. In addition, *Neisseria* genomes contain approximately 10-50 insertion sequences (IS) and IS remnants [15]. Additionally, *N. meningitidis* is able to modify its gene content via horizontal acquisition of DNA from the same or related species [23].

Neisserial genomes are characterized by a high abundance and variety of repetitive DNA sequences which play diverse roles in meningococcal biology [24]. The *N. meningitidis*

genome contains with 2% Correia elements (CE) a very large amount of repetitive DNA [19, 25]. Furthermore, the chromosome of strain MC58 contains 1910 copies of the 10 bp DNA uptake sequence (DUS), which is the most abundant repeat sequence, 689 replica of a 20 bp duplicated repeat sequence 3 (dRS3), 316 of the dRS3 neisserial filamentous phage (Nf)1 subtype (dRS3 Nf1) and 261 correia repeat elements [26].

3.3 Genomic flexibility and repeated DNA sequences in *N. meningitidis*

DUSs are not equally distributed over the chromosome and potentially function in mediating replication, recombination and restriction modification and are involved in DNA repair [27]. Furthermore, the high occurrence of these DUSs in bacterial genomes promote the integration of DNA form the same or related species via homologues recombination [28-30]. The second most abundant class is dRS3, and inverted dRS3 flank different 50-150 bp repeat sequences [25], known as neisserial intergenic mosaic elements (NIMEs). dRS3 seem to be points for genome rearrangements [31] and can bear potential integration sites for the neisserial filamentous phages [1, 32]. CE often flank a conserved repeat region of 50-150 bp and form Correia repeat enclosed elements (CREE). They were found many times inserted in 5'-UTR of genes and have been shown to affect gene expression [24, 32] (described below).

Another group of repeat sequences belongs to the class of miniature inverted transposable elements (MITEs). MITEs are widely distributed among bacteria, but the exact function of these elements remains unclear. MITEs or the so-called neisseria miniature insertion sequences (nemis) are found in all *Neisseria* species. Nemis account up to 2% of *N. meningitidis* genomes [33] and about one third of these elements occur in the chromosome within repeated DNA sequences, the remaining are associated with coding regions and are often found at the start or the end of an ORF [34].

MITEs can be further sub-divided into to two classes which either are a result of a deletion within an IS element (type I or *Tourist-type*) or which share the same terminal inverted repeats (TIRs) with those of a known transposon (type II or *Stowaway-type*) [35-37]. MITEs have been reported across different species in plants, animals, fungi, and bacteria [38]. They are usually 50-500 bp long, occur in high copy numbers within the chromosome, are structurally characterized by an AT-rich sequence and probably do not code for any known gene.

These elements are often found close to or sometimes also within genes where they may affect gene expression [37]. Additionally, they can fold into long stem loop structures at the RNA level and thus are highly stable thermodynamically [38]. Another

characteristic feature is their conserved architecture. They carry two TIRs and flanking direct repeats (DR) or the also named target site duplications (TSDs). The TIRs and the TSDs are potentially important for the mobility within the genome. It is known that transposases use the TIRs as binding sites which enables transposition whereby the direct repeat sequences of 2-20 bp are generated [39]. In *Neisseria,* there are two potential MITE candidates, the AT-rich repeat (ATR) and the already mentioned CREE repeat elements, which are potentially type II MITEs.

In contrast to the ATR, CREEs are already well-described in *N. meningitidis* and in the closely related pathogen *Neisseria gonorrhoeae.* Correia *et al.* identified 1988 a family of small repeated elements in the genome of *N. gonorrhoeae* [40], which is now called CE, CREE or NEMIS. Here we refer to the repeat as the CREE. CREE have features, such as an integration host factor (IHF) binding and transcriptional start signals that may play a role in altering gene expression. Parkhill *et al*. 2000 characterized the occurrence of repetitive DNA in more detail in the invasive *N. meningitidis* strain Z2491 [25]. In contrast to the low copy number of ATRs, strain Z2491 contains 286 copies of three different CREE repeat types: (i) 173 full length CREEs with 150-159 bp (ii) 84 with an internal deletion of approximately 50 bp, which usually harbors a IHF-binding site and thus has a length of ~104 bp (iii) 29 CREEs with a partial repeat type of varying length from 37 to 145 bp [25]. Of note, comparable numbers of each repeat type were also found in strain MC58. This strain harbors 13 ATRs, 161 full-length CREEs, 82 CREEs with internal deletion and 19 partial CREE repeat types [32]. The insertion of these elements is facilitated by a duplication of the direct repeat signal 'TA' at the target site [41] and Snyder *et al*. 2009 provided evidence for the mobility of CREEs in *N. gonorrhoeae* by a chromosomal comparison of differences in the locations of CREEs to a closely related strain [42].

Moreover, CREEs might have functional roles by influencing gene expression at the transcriptional level. Two functional promoters have been reported as being created by CREE insertion 5' of genes [43]. Black *et al.* 1995 showed that a σ^{70} binding site was located within the neisserial repeat element [43]. The study described that the insertion of a CREE into the 5'-UTR of *uvrB* generated an almost perfect σ^{70} promoter, comprised by a full -35 and a partial -10 element within the one end of CREE closest to the gene [43]. At the other end of the CREE a second σ^{70} promoter was identified. Snyder *et al*. 2003 described the second promoter 5' of *dcaC* in *Neisseria lactamica* [44]. Here, the -35 region comes from the native sequence and the -10 box was completely given by the first bases of the CREE [44]. Both of these promoters would drive transcription in the same direction and through the inverted sequences it might be possible to generate both promoters on the opposite strand as well.

Siddique *et al.* 2011 presented a more detailed description of the promoter regions within the CREE [45]. They divided the Correia element into eight subtypes according to the combination of the left and right end TIRs and the presence or absence of the internal IHF-binding site. They showed that two subtypes encode strong promoters. Additionally, they tested the effect of the IHF-binding site on transcription and showed that the elements lacking the IHF-binding sites were very similar to the wild-type expression profiles [45].

Another function of these kinds of MITEs is probably at the post-transcriptional level. There is evidence that the stem-loop structures generated by the TIRs of the CREE regulate the half-live of the mRNA. Gregorio *et al.* 2002 demonstrated that the hairpins created by the inverted repeats of the CREEs were binding targets for RNase III [46]. Additionally, they described that binding of RNase III regulates cleavage or protection of a transcript, depending on the Correia inverted repeat sequence [34].

Taken together, MITEs and CREEs in particular are multifunctional elements with still unknown features, and like CREEs also ATRs might affect the transcription of adjacent genes. Moreover, it remains unclear what effect such integrations in intergenic regions could have on the regulation of cellular functions such as metabolism and in particular virulence in meningococci.

3.4 Gene regulation in *N. meningitidis*

Proper regulation of gene expression is mandatory for a pathogen to survive within the host and often is a crucial step in establishing disease. Bacterial species typically respond to stresses by altering the level or activity of two-component systems (TCSs), transcription factors and/or of alternative sigma factors [47].

TCSs contain two central enzymatic components, a histidine kinase sensing environmental stimuli and a transcriptional response regulator [48]. In contrast to *E. coli*, which possesses around 30 TCSs [49, 50], *N. meningitidis* contains only four putative TCSs [51, 52]. Probably NtrY/NtrX (NMB0114/NMB0115) regulates nitrogen metabolism, NMB1606/NMB1607 regulates piliation and the NarQ/NarP (NMB1249/NMB1250) might respond to anaerobic growth [52]. Experimental evidence for a regulatory function is only available for the fourth TCS. The magnesium dependent MisR (NMB0595) / MisS (NMB0594) (or PhoP/PhoQ) regulatory system modulates outer membrane structures and senses virulence control [53-55].

Whereas *E. coli* expresses about 200 regulators [56], meningococci only encode for 35 putative regulators according to current genome annotations [57]. Until now there are only a few transcriptional regulators that have been experimentally verified in meningococci, for instance Fur, OxyR and AsnC. Delany *et al*. 2004 showed that Fur (NMB0205), encoding for a ferric uptake regulation protein, can act as a repressor as well as an activator for putative virulence genes *in vivo* and *in vitro* [58]. In response to oxidative stress OxyR (NMB0173) is required to activate the expression of genes which are responsible for the detoxification of intracellular hydrogen peroxide, crucial for the survival in the human host [59, 60]. AsnC (NMB0573) responds to nutrient poor conditions, and regulates the expression of cell surface proteins and components of aerobic metabolism [61].

Finally, transcription can also be regulated by alternative sigma factors. The meningococcal chromosome appears to harbor only three alternative sigma factors, RpoH (σ^{32}), RpoN (σ^{54}) and RpoE (σ^{E}) [62] - compared to seven in *E. coli* [63, 64]. RpoH has been described more closely in *N. gonorrhoeae* [65] and RpoN seems to be inactive in gonococci and meningococci [66]. The RpoE regulon in meningococci was described in detail [67, 68] and is known to be essential for the response to environmental challenges in many pathogens [69-72].

Bacterial regulatory circuits can differ among species and strains by the presence or absence of a specific binding site for a conserved transcription factor, horizontally-acquired genes under regulation of a specific transcription factor, rearrangement of the promoters controlled by a transcription factor and modifications in the transcription factors themselves [73]. These changes enable the bacteria to expand or modify cellular functions controlled by transcriptional factor(s).

Together, this indicates that regulatory circuits are constantly being modified and that these changes contribute significantly to the generation of phenotypic diversity within and across species [74]. Consequently, the regulation and the expression of genes or virulence-associated genes are likely to depend on the genetic background and the environment [75, 76].

3.5 Adaption to environmental changes: the stringent response

One strategy to metabolically adapt to and survive within the host niche is linked to the so-called stringent response. Many bacteria rely on their hosts for nutrients necessary for survival, for instance for many potential pathogens amino acids are critical nutrients [77]. There is evidence, that human host cells are able to starve bacteria of amino acids, and bacteria have developed mechanisms to respond to host-mediated amino acid starvation [77].

Since the discovery in 1969 [78], extensive analyses in *E. coli* revealed that guanosine tetra- or pentaphosphate ((p)ppGpp), seems to be a key player in regulatory networks in prokaryotes and is linked to the stringent response or also known as stringent control [79-82]. In *E. coli,* the machinery of the stringent response controls stress responses, such as amino acid starvation [82, 83], fatty acid limitation [84], iron limitation [85], heat shock and other stress conditions, mainly by the two enzymes RelA and SpoT (Figure 3.1).

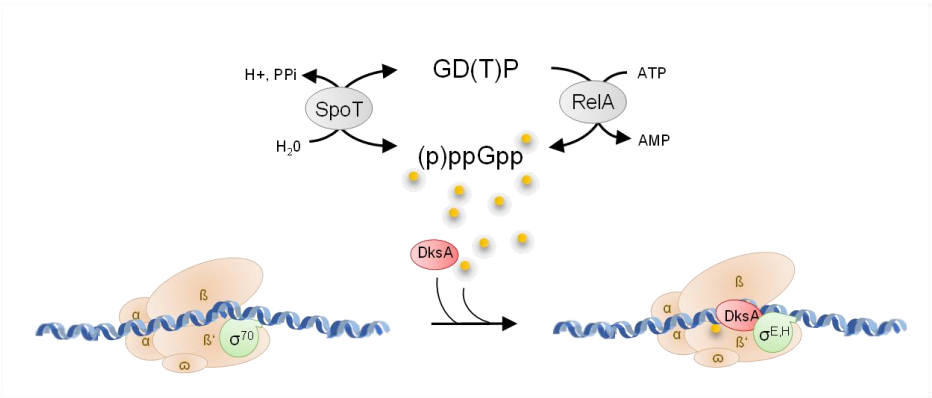

Figure 3.1 Control of the cellular pool of (p)ppGpp

Depicted is the graphical representation of the stringent response in *E. coli*. During particular stresses, SpoT and RelA produce (p)ppGpp by catalyzing PPi transfer from ATP to GDP or GTP. (p)ppGpp together with DksA directly interacts with RNA polymerase and initiate transcription of promoters for stress resistance through alterative sigma factors such as σ^E or σ^H. In nutrient high conditions, SpoT degrades (p)ppGpp and 'housekeeping' sigma factor σ^{70} drives transcription of genes important for vegetative growth. Adapted from ref. [80].

Under amino acid limiting conditions, uncharged tRNAs bring the ribosomes to a halt, which activates ribosome associated RelA to generate (p)ppGpp by catalyzing pyrophoshoryl transfer from ATP to GTP or GPD. These nucleotides, together with DnaK suppressor (DksA), amplify direct transcription initiation at particular promoters through direct interaction between the two RNA polymerase subunits ß' and ω [79, 80, 86]. (p)ppGpp and DksA can also regulate transcription indirectly by a process called 'sigma factor competition'. During logarithmic growth in nutrient high conditions, transcription is mainly initiated from strong σ^{70} factor. Moreover, when bacteria enter the stringent

response high concentrations of (p)ppGpp accumulate in the cell and inhibit RNA polymerase to bind to σ^{70}-dependent promoters. In consequence, more RNA polymerases bind alternative sigma factors such as σ^{H} and σ^{E} and transcription from promoters promoted by alternative sigma factors increases thus mediating particular stress responses [87]. In contrast to RelA, SpoT senses other stress conditions, such as limiting phosphate, fatty acids or carbon stress and is additionally characterized by its bifunctionality [88]. Beside (p)ppGpp synthetase function, SpoT has also hydrolase activity, by degrading guanosine tetra- or pentaphosphate which is essential to a cell, as high concentrations of (p)ppGpp abolish replication. In these species, the functionality of SpoT can only be studied in the background of *relAspoT* double mutants (often annotated as $ppGpp^0$ cells), which lack all synthetase activity.

Together, the complex control and the regulation of the pool of the alarmone (p)ppGpp allows the cell to rapidly adapt to environmental changes. Different species of bacteria harbor specific stringent response machineries and encode for a variety of synthetase and hydrolase enzymes to control the levels of (p)ppGpp. For instance, the model organism *E. coli* possess SpoT and RelA, whereas *Bacillus subtilis* has only one enzyme named Rel for this activity [89] and *Vibrio cholerae* holds a stringent response machinery consisting of RelA, SpoT and RelV [90]. Mittenhuber *et al.* 2001 presented a classification of the Rel, RelA and SpoT orthologues comprising only four groups, which indicates a very high conservation of (p)ppGpp metabolism among bacteria [89].

As mentioned above, RelA produces (p)ppGpp and thus could act as a global regulator, by changing the metabolic status of the cell via the stringent response and thus might be important for the survival of meningococci in the human host. Therefore, RelA and the stringent response are a main focus of the present work.

3.6 Stringent response and virulence

In many pathogenic bacteria, (p)ppGpp plays an important role in colonization and invasive infection via coordination of environmental signals with global regulators involved in pathogenesis [88, 91-93]. For instance, a *Salmonella typhimurium* strain deficient in *relA* and *spoT* was found to be highly attenuated *in vivo* and non-invasive *in vitro*. The $(p)ppGpp^0$ mutant showed reduced expression of transcriptional regulators required for pathogenicity island 1 (SPI-1) gene expression, which codes for the type III secretion apparatus required for invasion into host cells [91]. Mice infected with a *relAspoT* mutant strain contained no recoverable bacteria in spleen cell lysates, and *in vitro* invasion assays with colon epithelial cell lines showed no significant levels of

invasion compared to the wild-type strain, confirming the results from the *in vivo* experiments [91].

Another example is the requirement of the stringent response in tuberculosis infection. Klinkenberg *et al.* 2010 showed that (p)ppGpp is essential for full virulence of *Mycobacterium tuberculosis* in guinea pigs [92]. During tuberculosis infection, the bacterium resides within the nutrient-starved environment of lung granulomas and accordingly (p)ppGpp is synthesized by the Rel enzyme, thus enabling the cells to restrict growth by down regulating metabolism in a coordinated fashion. The study revealed that Rel deficient strains showed impaired survival relative to the wild-type strain and decreased colony forming units (CFU) counts measured by lung and spleen cell lysates from guinea pigs [92].

Moreover, *Pseudomonas aeruginosa*, which is mainly responsible for chronic lung infections in patients with cystic fibrosis, was unable to establish chronic infection *in vivo* and *in vitro* in a *relAspoT* double mutant [93]. The (p)ppGpp-devoid *relAspoT* strain showed that the stringent response is important for full virulence in both the fly (*Drosophila melanogaster*) feeding model and rat lung agar bead model of infection. The synthesis of virulence factors, such as the toxin pyocyanin, elastase, protease and siderophores was abolished in the mutant strain which might be therefore less able to outlast stresses, e.g. heat shock and oxidative stress than the wild-type strain. Together, the results indicate that the stringent response is a critical regulator of the pathogenicity in *P. aeruginosa* [93].

These examples demonstrate that the stringent response machineries are important for the adaptation of the pathogen to its ecological niche within mammalian, animal and plant hosts. The stringent response can give the bacterium the opportunity to alter the metabolism and protein repertoire in response to local conditions. In response to changes in the nutrient supply, contact with new surfaces or alterations in immune responses pathogenic bacteria might in turn modulate the host cell biology, the immune response or invade into more favorable compartments by activating, for instance, secretion systems, toxins, adhesins or motility organelles. The expression and regulation of many of such virulence factors are modulated by (p)ppGpp, thereby coupling virulence to metabolic status.

Unfortunately, nothing is known about the stringent response and its contribution to fitness under infection mimicking conditions in *N. meningitidis* so far.

3.7 Aims of this study

The aim of this work was the characterization of the stringent response and its regulation in two different meningococci strains. Consequently, the focus of thus work was (i) the analysis of the stringent response and in particular the characterization of stringent response related genes with respect to meningococcal pathogenicity, and (ii) the impact of ATR on *relA* and meningococcal fitness *in vitro* and *ex vivo*.

In order to define the physiological role of the stringent response and its contribution to meningococcal virulence, *relA* as well as *relAspoT* double mutants were generated in strain MC58 and α522 and phenotypically characterized for growth deficiencies under various *in vitro* conditions as well as in an *ex vivo* infection model. In addition, intracellular ppGpp concentrations were quantified in wild-type and mutant strains as well as transcriptional changes during SHX-mediated amino acid starvation using microarrays.

To assess the biological role of ATRs in meningococcal virulence and their impact on meningococcal genome structure and gene expression, computational genome comparisons between strain MC58 and α522 were performed with particular emphasis on intergenic regions and the *relA* locus. ATR knock-in and knock-out mutants, respectively, were generated at the *relA* locus and the phenotypic properties of mutant and wild-type strains in both genetic backgrounds compared under various *in vitro* as well as in an *ex vivo* infection model.

4 Materials

4.1 Laboratory equipment

The laboratory equipment used in this study is listed in Table 4.1.

Table 4.1 *List of devices and laboratory equipment*

Device	**Type**	***Manufacturer****
10 µl pipette	Research plus, 0,5 – 10 µl	*Eppendorf*, Hamburg
100 µl pipette	Research plus, 10 – 100 µl	*Eppendorf*, Hamburg
1000 µl pipette	Research plus,100 – 1000 µl	*Eppendorf*, Hamburg
Agarose gel electrophoresis chamber	MINI-BASIC	*Cti*, Idstein
Agarose gel electrophoresis chamber	Electrophoresis chamber 'Maxi'	*Von Keutz*, Reiskirchen
Agarose gel electrophoresis chamber	SubCell® GT	*Bio-Rad*, Dreieich
Analytical balance	P – 1200	*Mettler-Toledo*, Greifensee, CH
Analytical balance	ABT 120-5DM	*Kern & Sohn*, Balingen
Bunsen burner	Fireboy (electric)	*Tecnomara*, Zürich, Ch
Centrifuge (4 ºC)	Megafuge 1.0 R	*Heraeus*, Hanau
Centrifuge (benchtop, 4 ºC)	Mikro Rapid	*Hettich*, Tuttlingen
Centrifuge (benchtop)	Biofuge pico	*Heraeus*, Hanau
Centrifuge (-Mini)	SproutTM	*Biozym*, Hessisch Oldendorf
Centrifugal vacuum concentrator	SC110A Speed Vac® Plus	*Savant*, Holbrook, USA
Colony counter	ProtoCOL	*Meintrup DWS*, Lähden
OD_{600} photometer	WPA biowave	*Biochrom,* Berlin
Diaphragm pump	Membrane vacuum pump MD 4C	*Vacuubrand*, Wertheim
Fluorescence activated cell sorting	BD FACSCalibur™	*BD Biosciences*, *Heidelberg*
Heating block	VLM Q1	*VLM*, Bielefeld
Imaging system	ChemiDoc MP	*Bio-Rad*, Dreieich
Incubator (37 ºC)	Heraeus Kelvitron ® t	*Heraeus*, Hanau
Incubator (37 ºC/5% CO_2)	Heraeus 6000	*Heraeus*, Hanau
Incubation hood	CERTOMAT® H	*B. Braun*, Melsungen
Magnetic stirrer	IKAMAG® RCT	*IKA*®, Staufen
Microarray hybridization station	HS 4800 Pro	*TECAN*, Männedorf, Ch
Microarray scanner	GenePix Professional 4200A	*Sunnyvale*, USA
Microplate reader	Infinite F200® PRO	*TECAN*, Männedorf, Ch
Microplate reader	Multiskan® EX	*Thermo Scientific*, Frankfurt
Microscope	Wilovert®	*WILL*, Wetzlar
Oven	OV 5	*Biometra*, Göttingen
PCR thermocycler	T3 Thermocycler	*Biometra*, Göttingen

Device	Type	*Manufacturer**
Pipette controller	Accu-jet®	*BRAND*, Wertheim
Pipette controller	Accu-jet® pro	*BRAND*, Wertheim
Power supply	EV243 Consort Power Supply	*Consort*, Turnhout Be
Power supply	Standard Power Pack P25	*Biometra*, Göttingen
Protein gel electrophoresis	Mini-Protean	*Bio-Rad*, Dreieich
Real-time PCR system	StepOnePlus™	Applied *Biosystems*, Darmstadt
Safety cabinet	Safe 2020	*Thermo Scientific*, Frankfurt
Semi-dry-blotter	PEGASUS S	*PHASE*, Lübeck
Shaker	CERTOMAT® U	*B. Braun*, Melsungen
Shaker	Phero Shaker	*Biotec-Fischer*, Reiskirchen
Spectrophotometer	PEQLAB, ND-1000	*VWR*, Erlangen
Thermo shaker	Thermomixer 5436	*Eppendorf*, Hamburg
UV crosslinker	18000	*Life Technologies,* Darmstadt
Vortex mixer	REAX 2000	*Heidolph*, Schwabach
Waterbath	Type WB7	*Memmert*, Schwabing

*Unless stated otherwise, Manufacturers come from Germany.

4.2 Chemicals and consumables

Standard laboratory chemicals were purchased from AppliChem (Darmstadt), Merck (Darmstadt), Carl Roth (Karlsruhe), Roche (Mannheim) and Sigma-Aldrich (Schnelldorf). All specific reagents are listed in Table 4.2.

Table 4.2 *Specific reagents*

Reagent	*Source*
3-propanesulfonic acid (MOPS)	*AppliChem*
Ammonium persulfate (APS)	*Roth*
Anti-Digoxigenin-AP Fab fragments (Anti-DIG-ATP)	*Roche*
Bromphenol blue	*Merck*
ß-mercaptoethanol (ß-ME)	*Roth*
Chloroform ultra pure	*AppliChem*
Crystal violet	*Difco*
CSPD	*Roche*
Cy™3-dCTP / Cy™5-dCTP, 25 nmol	*GE Healthcare*
Diethylpyrocarbonate (DEPC)	*AppliChem*
DIG DNA labeling mix (10X)	*Roche*
Dithiothreitol (DTT)	*AppliChem*
Ethylenediaminetetraacetic acid (EDTA)	*AppliChem*
Ethanol absolute	*AppliChem*

Reagent	***Source***
Formaldehyde solution, 36.5-38%	*Sigma-Aldrich*
Formamide, deionized	*AppliChem*
GelRed™	*Biotum*
Hexanucleotide mix (10X)	*Roche*
Nonfat dried milk powder	*AppliChem*
Nuclease-free water	*Ambion*
Phenol	*Roth*
Phenol/chloroform/isomylacohol (P:C:I)	*Roth*
Phenol/chloroform/isomylacohol (25:24:1)	*AppliChem*
Polyacrylamid (PAA): Rotiphorese Gel 30	*Roth*
Polyacrylamid (PAA): Rotiphorese Gel 40	*Roth*
Power SYBR Green PCR master mix	*Applied Biosystems*
Sodium dodecyl sulfate (SDS) pellets	*Roth*
Tetramethylethylendiamine (TEMED)	*Roth*
Triton-X 100%	*Roth*
Xylene Cyanole	*Sigma-Aldrich*

Standard consumables were supplied from Ambion, Biozym, Eppendorf, Greiner bio-one, Hartenstein and Sarstedt, and special consumables and their sources are listed in Table 4.3.

Table 4.3 *Special consumables*

	Application	**Product**	***Source***
	Agarose-gels	UltraPure™ agarose	*Life Technologies,* Darmstadt
dNTPs			
	cDNA transcription	100 mM dNTP set (dATP, dCTP, dGTP, dTTP)	*Life Technologies,* Darmstadt
	PCR/amplification	100 mM dNTP set (dATP, dCTP, dGTP, dTTP)	*Sigma-Aldrich,* Schnelldorf
Oligos			
	PCR/amplification	DNA oligonucleotides	*Sigma-Aldrich,* Schnelldorf
Ladders			
		DNA HyperLadder™ 1kb	*Bioline,* Luckenwalde
		DNA Molecular Weight Marker VII, DIG-labeled	*Roche,* Mannheim
		PageRuler™ Prestained Protein Ladder, 10 to 180 kDa	*Life Technologies,* Darmstadt
		RNA ladder 0.16-1.77 Kb	*Life Technologies,* Darmstadt
		RNA Molecular Weight Marker I, DIG-labeled	*Roche,* Mannheim

	Application	Product	*Source*
Ladders			
		RNA Molecular Weight Marker III, DIG-labeled	*Roche,* Mannheim
Blotting			
	Southern/Northern blot	Amersham Hybond™-N+	*GE Healthcare,* Freiburg
	Northern blot	Whatman TurboBlotter	*GE Healthcare,* Freiburg
	Western blot	Whatman Protran nitrocellulose transfer membrane	*GE Healthcare,* Freiburg
	Western blot	Pierce™ ECL Western Blotting Substrate	*Thermo Fisher,* Frankfurt
Antibodies			
	First antibody	Anti-Mouse IgG–Peroxidase antibody produced in rabbit	*Sigma-Aldrich,* Schnelldorf
	Second antibody	Monoclonal Anti-polyHistidine antibody produced in mouse	*Sigma-Aldrich,* Schnelldorf
Varying Applications			
	Collecting human saliva specimen	CRT paraffin	*Ivoclar Vivadent GmbH*, Ellwangen
	Collecting human saliva specimen	0.2 µm filter	*SARSTEDT*, Nümbrecht
	Static biofilm formation96	Well microtiter plate	*SARSTEDT*, Nümbrecht
	Cell invasion/adhesion	24-well cell culture plates	*SARSTEDT*, Nümbrecht
	Cell culturing	TC Flask T75 standard	*SARSTEDT*, Nümbrecht
	ppGpp extraction	Filtropur S 0.2 µm	*Sarstedt,* Nümbrecht
	Promoter analysis	5'/3' RACE Kit, 2nd Generation	*Roche,* Mannheim

4.3 Kits and enzymes

All kits used in this study are listed in Table 4.4.

Table 4.4 *Kits*

Application	**Product**	***Source***
cDNA purification	MSB Spin PCRapace	*STRATEC Biomedical AG,* Birkenfeld
cDNA purification	Illustra AutoSeq G-50	*GE Healthcare,* Freiburg
DNA extraction	Invisorb Spin DNA Extraction Kit	*STRATEC Biomedical AG,* Birkenfeld
gDNA isolation	QIAamp DNA Mini Kit	*Qiagen,* Hilden
PCR purification	MSB Spin PCRapace	*STRATEC Biomedical AG,* Birkenfeld
Plasmid isolation	QIAprep Spin Miniprep Kit	*Qiagen,* Hilden
Plasmid isolation	QIAGEN Plasmid Midi Kit	*Qiagen,* Hilden

All restriction endonucleases for DNA digestion and polymerases for PCR were supplied from New England Biolabs (Frankfurt). Enzymes for RNA transcription were from *Roche* (Mannheim) and Life Technologies (Darmstadt). For the digestion of single- or double stranded DNA, DNaseI from Thermo Scientific (Schwerte) was used. The enzymes are listed in Table 4.5.

Table 4.5 *Enzymes*

Enzyme	***Source***
DNase I, RNase-free	*Thermo Scientific,* Schwerte
Klenow Enzyme, labeling grade, 500U	*Roche,* Mannheim
Lysozyme	*Roth,* Karlsruhe
Restriction endonucleases	*New England Biolabs,* Frankfurt
Ribonuclease A from bovine pancreas (RNase A)	*Sigma-Aldrich,* Schnelldorf
RNase, DNase-free	*Roche,* Mannheim
RNaseOUT™ recombinant ribonuclease inhibitor	*Life Technologies,* Darmstadt
SuperScript® II reverse transcriptase	*Life Technologies,* Darmstadt
T4 DNA ligase	*New England Biolabs,* Frankfurt
Taq DNA polymerase	*New England Biolabs,* Frankfurt
Q5® High-Fidelity DNA polymerase	*New England Biolabs,* Frankfurt

4.4 Buffers and solutions

All reagents used in this work were purchased from Carl Roth (Karlsruhe), Difco (Heidelberg), Merck (Darmstadt), und Sigma-Aldrich (Steinheim), if not indicated otherwise. Buffers and solutions were prepared by using (Aqua ad iniectabilia) ddH_2O (B. Braun).

For microbiological methods 1x Phosphate-buffered saline (PBS, Table 4.6) was used in cell culture and for the preparation of dilution series.

Unless stated otherwise, all solutions and buffers were sterilized by autoclaving at 121 °C, with 1 bar for 20 minutes.

Table 4.6 *Phosphate-buffered saline*

	Content	Preparation
10x PBS		
	Gibco Dulbecco's Buffered Saline	for 1x 10 l
	ddH_2O	ad 1000 ml
1x PBS		
	10x PBS	100 ml
	ddH_2O	ad 1000 ml, adjust pH to 7.4

The 1x PBS buffer has a final concentration of 2.6 mM potassium chloride (KCl), 1.4 mM potassium phosphate monobasic (KH_2PO_4), 137.9 mM sodium chloride (NaCl) and 8.0 mM sodium phosphate dibasic (Na_2HPO_4).

For the long-term storage of bacterial clones a freezing medium was used as described in Table 4.7.

Table 4.7 *Conventional freezing media*

	Content	Preparation
Freezing media		
	Glycerol, 86%	233 ml
	Caso-Bouillon (Becton Dickinson)	15 g
	ddH_2O	ad 500 ml

Table 4.8 *Electrophoretic separation of DNA in agarose gels*

	Content	Preparation
50x TAE (TRIS-acetate-EDTA)		
	TRIS (trishydroxymethylaminomethane)	242 g
	100% Acetic acid	57.1 ml
	0.5M EDTA (pH 8.0)	100 ml
	ddH_2O	ad 1000 ml, pH to 8.3
1x TAE		
	50x TAE	40 ml
	ddH_2O	ad 2000 ml
6x DNA loading buffer		
	Saccharose	40 g
	Glycine	30 ml
	Bromphenolblue	100 mg
	Xylencyanol	100 mg
	ddH_2O	ad 100 ml

	Content	Preparation
GelRed™ solution /bath		
	ddH_2O	150 ml
	GelRed™	15 µl

TAE buffer was used for all DNA agarose gels and as running buffer (Table 4.8). The 6x agarose buffer was aliquoted 1 ml each in a 1.5 ml microcentrifuge tube and was stored at 4 °C until use. The components (Table 4.8) of the GelRed™ bath solution were mixed and the gels were stained for 30-45 minutes.

The composition of all buffers used for Southern blot analysis is given in Table 4.9.

Table 4.9 *Buffers and solutions used for Southern blots*

	Content	Preparation
20x Saline-Sodium-Citrate (SSC)		
	NaCl	175.5 g
	Sodium citrate	88.2 g
	ddH_2O	ad 1000 ml, to pH 7.0
10x Blocking reagent		
	Blocking reagent	10 g
	1x Maleic acid buffer	ad 100 ml
		Storage at -20 °C
1x Maleic acid buffer		
	Maleic acid	23.2 g
	NaCl	17.53 g
	ddH_2O	ad 2000 ml, pH to 7.5
Washing buffer		
	1x Maleic acid buffer	1000 ml
	Tween 20	3 ml
	ddH_2O	ad 2000 ml
High SDS hybridisation buffer		
	20XSSC	125 ml
	10XBlocking reagent	100 ml
	SDS	35 g
	10% N-Lauroylsarcosine	0.5 ml
	5x Sodium phosphate buffer, pH 7.0	25 ml
	ddH_2O	ad 500 ml
		Storage at -20 °C

	Content	Preparation
Stringent washing buffer I: 2x SSC/0.1% SDS		
	20x SSC	100 ml
	10x SDS	10 ml
	ddH_2O	ad 1000 ml
Stringent washing buffer II: 0.1x SSC/0.1% SDS		
	20x SSC	5 ml
	10x SDS	10 ml
	ddH_2O	ad 1000 ml
1x Blocking solution		
	10x Blocking reagent	10 ml
	1x Maleic acid buffer	90 ml
	Final volume	100 ml
Detection buffer		
	1M TRIS/HCl, pH 9.6	100 ml (0.1M)
	5M NaCl	20 ml (0.1M)
	Final volume	ad 1000 ml
Antibody solution		
	Anti-DIG-AP 1:10.000 in 1x Blocking solution	
		Storage at 4 °C
CSPD working solution		
	CSPD 1:100 in detection buffer	
		Storage at 4 °C

The buffers and reagents used for the electrophoretic separation of proteins under denaturing conditions using SDS polyacrylamide electrophoresis (SDS PAGE) is given in Table 4.10.

Table 4.10 *SDS PAGE*

	Content	Preparation
Upper TRIS		
	TRIS	30.3 g
	10% SDS	20 ml
	ddH_2O	ad 500 ml
		Storage at 4 °C
Lower TRIS		
	TRIS	90.85 g
	10% SDS	20 ml
	ddH_2O	ad 500 ml

	Content	Preparation
		Storage at 4 °C
Sample buffer		
	ß-mercaptoethanol	5 ml
	20% SDS	10 ml
	Glycerol	25 ml
	Bromophenol blue	A spatula tip
	0.5M TRIS/HCl pH 6.8	ad 100 ml
		Storage at -20 °C
10x Lämmli		
	TRIS	30 g
	Glycine	144 g
	ddH_2O	ad 1000 ml, pH to 8.3
1x Electrophoresis buffer		
	10x Lämmli	200 ml
	10% SDS	10 ml
	ddH_2O	ad 2000 ml
	Content	**2 Gels**
Separation gel 12.5%		
	Lower TRIS	3 ml
	PAA 30	5 ml
	10% APS	60 µl
	TEMED	20 µl
	ddH_2O	4 ml
Loading gel		
	Upper TRIS	1.25 ml
	PAA 30	0.75 ml
	10% APS	35 µl
	TEMED	20 µl
	ddH_2O	

The reagents and buffers used for Western blotting are given in Table 4.11.

Table 4.11 *Western blot buffers*

	Content	Preparation
Blotting buffer		
	10x Lämmli	100 ml
	Methanol	200 ml
	ddH_2O	ad 1000 ml

	Content	Preparation
Washing buffer (PBS-T)		
	0.1% Tween20 in 1x PBS	

The buffers used for the electrophoretic separation of RNA under denaturing conditions are given in Table 4.12.

Table 4.12 *Electrophoretic separation of RNA in agarose gels*

	Content	Preparation
10x TBE (Tris-Borate-EDTA)		
	TRIS	121.4 g
	Boric acid	61.8 g
	EDTA	7.3 g
	ddH_2O	ad 1000 ml
1x TBE		
	50x TBE	100 ml
	ddH_2O	900 ml
RNA loading buffer		
	Glycerol	50%
	EDTA	1 mM
	Bromphenol blue	0.25%
	Xylene cyanole	0.25%

For Northern blots, all buffers and solutions were prepared with DEPC water (Table 4.13). To inhibit nucleases and to inactivate enzymes, 2 ml DEPC (diethyl pyrocarbonate) was added to 2 L ddH_2O, incubated overnight at 37 °C and was 2 times autoclaved.

Table 4.13 *Buffers and solutions used for Northern blot*

	Content	Preparation
Sample buffer		
	Formamide, deionized	750 µl
	10x MOPS	150 µl
	Formaldehyde (37%)	262 µl
10x MOPS		
	MOPS	40.5 g
	NaAc (sodium acetate)	4.1 g
	0.5 M EDTA (pH 8.0)	20 ml
	10 N NaOH (sodium hydroxide)	4 ml

	Content	Preparation
	DEPC ddH_2O	ad 1000 ml
1x MOPS		
	10x MOPS	100 ml
	DEPC ddH_2O	ad 900 ml
2x RNA loading dye		
	95% Formamide	
	0.02% SDS	
	0.02% Bromphenol blue	
	0.01% Xylene cyanol	
	1 mM EDTA	
		Aliquots at -20 °C
Formaldehyde gel for RNA		
	Agarose	0.8 g
	DEPC H_2O	68 ml
	10x MOPS	8 ml
	Formaldehyde	4 ml
30:1 Mix		
	100% Ethanol	290 ml
	3 M NaOAc (sodium acetate) pH 5.2	

The sample buffer used for Northern blots was always prepared fresh (Table 4.13). The components of the10x MOPS buffer were mixed, not autoclaved and stored protected from light. For the formaldehyde RNA gel (Table 4.13), agarose and DEPC H_2O was melt, cooled down and finally 10x MOPS and formaldehyde was added. For the detection and development the digoxigenin (DIG) Wash and Block Buffer Set (*Roche*) was used. The washing, blocking and detection buffers are specific for the detection of DIG labeled probes. The kit contains 10x concentrated washing buffer, 10x concentrated maleic acid buffer, 10x concentrated blocking solution and 10x concentrated detection buffer. Except for the blocking solution, the 10x concentrated buffers were diluted to 1x concentrations with DEPC water. The blocking solution was diluted in 1x malic acid buffer. According to the manufacturer's instructions, the buffers were autoclaved, filtered and tested for the absence of DNases and RNases. All buffers and solutions used for the hybridization of spotted oligonucleotide microarrays with dye-labeled cDNAs are given in Table 4.14.

Table 4.14 *Buffers and solutions used for microarray hybridization*

	Content	**Preparation**
20x SSC		
	NaCl	175.5 g
	Sodium citrate	88.2 g
	ddH_2O	ad 1000 ml, to pH 7.0
10% SDS		
	SDS	100 g
	ddH_2O	ad 1000 ml
1% SDS		
	10% SDS	5 ml
	ddH_2O	ad 45 ml
Pre-Hybridization		
0.1% Triton X-100		
	Triton X-100	2 ml
	ddH_2O	ad 2000 ml
1 mM HCl		
	25% HCl	292 µl
	ddH_2O	ad 2000 ml
100 mM KCl		
	1M KCl	200 ml
	ddH_2O	ad 2000 ml
Hybridization		
2x Blocking solution		
	2M TRIS/HCl, pH 9.0	100 ml
	Ethanolamine	6.2 ml
	ddH_2O	ad 1000 ml
Working solution		
	2x Blocking solution	500 ml
	10% SDS	10 ml
	ddH_2O	ad 1000 ml
Post-Hybridization		
2x SSC/0.2% SDS		
	20x SSC	100 ml
	10% SDS	20 ml
	ddH_2O	ad 1000 ml
2x SSC		
	20x SSC	100 ml
	ddH_2O	ad 1000 ml

	Content	Preparation
Post-Hybridization		
0.2% SSC		
	20% SSC	10 ml
	ddH_2O	ad 1000 ml
0.1% SSC		
	20% SSC	5 ml
	ddH_2O	ad 1000 ml

The working solution (Table 4.14) was always prepared fresh.

4.5 Culture media

4.5.1 Proteose peptone medium composition

Proteose peptone medium (PPM, Table 4.15) medium was used as rich medium for all *N. meningitidis* strains tested in this study. Unless stated otherwise, all media were sterilized by autoclaving at 121 °C, with 1 bar for 20 minutes or were sterilized by filtration through 0.2 µm membrane filters (Sarstedt).

Table 4.15 *Composition of PPM*

Content	Preparation
Bacto™ proteose peptone	15 g
NaCl	5 g
Starch from potatoes (Fluka)	0.5 g
KH_2PO_4	4 g
K_2HPO_4 (dipotassium phosphate)	1 g
ddH_2O	ad 1000 ml, pH 7.8

PPM was supplemented shortly before use with 500 µl of 8.4% sodium bicarbonate ($NaHCO_3$), 500 µl of 2 M magnesium chloride ($MgCl_2$), and 1 ml PolyVitex (bioMerieux) per 100 ml to obtain PPM^+, the final medium used for cultivation. Table 4.16 lists the PPM-supplements. The final composition of the PolyVitex components is in mg/l.

Table 4.16 *Supplements of PPM^+ medium*

Supplement	Preparation
8.4% $NaHCO_3$	
$NaHCO_3$	21 g
ddH_2O	ad 250 ml

Supplement	Preparation
2M $MgCl_2$	
$MgCl_2x6H_2O$	101.7 g
ddH_2O	ad 250 ml
PolyVitex	
Vitamin B12/cobalamin	0.1
L-glutamine	100
Adenine	10
Guaninchlorhydrate	0.3
4-Aminobenzoic acid (PABA)	0.13
L-cystine	11
Diphosphopyridinnucleotid, oxidized	2.5
Cocarboxylase	1.04
Iron(III) nitrate	0.2
Thiamine chlorhydrate	0.03
Cysteine chlorhydrate	259

4.5.2 **GCBL medium composition**

N. gonorrhoeae liquid medium ($GCBL^{++}$) was used for transformation of *N. meningitidis*. In Table 4.17 the composition of liquid GCBL medium is given.

Table 4.17 *Composition of GCBL*

Content	Preparation
Proteose peptone	15 g
K_2HPO_4	4 g
KH_2PO_4	1 g
NaCl	1 g
ddH_2O	ad 1000 ml

Table 4.18 *Supplements of $GCBL^{++}$ medium*

Supplement	Preparation
Kellogg's supplement I (100x)	
Glucose	40 g
L-glutamine	1 g
Thiamine pyrophosphate	2 mg
ddH_2O	ad 100 ml
Kellogg's supplement II (1000x)	
Iron(III) nitrate	50 mg
ddH_2O	ad 100 ml

Supplement	Preparation
Sodium bicarbonate ($NaHCO_3$)	
$NaHCO_3$	0.42 g
ddH_2O	ad 100 ml

100 ml Kellogg's supplement I and 10 ml Kellogg's supplement II (Table 4.18) were mixed, sterile filtrated and stored in 10 ml aliquots at –20 °C until use. One ml of this solution and 1 ml $NaHCO_3$ (also sterile filtrated) were added to 100 ml GCBL to obtain $GCBL^{++}$.

4.5.3 GCB^{++} agar

For the cultivation of *N. meningitidis* on solid media, GCB^{++} agar plates (Table 4.19) or Columbia agar plates with 5% sheep blood (COS plates from Becton Dickinson) were used.

Table 4.19 *Composition of GCB agar*

Content	Preparation
Difco™ GC Medium Base (GCB)	36.25 g
Agar	1.25 g
ddH_2O	ad 1000 ml

After autoclaving 1 ml Kellogg's supplement I and II was added per 100 ml to obtain GCB^{++} agar.

4.5.4 LB medium composition

LB medium was used for routine cultivation of *E. coli*. Table 4.20 lists all components of the LB medium.

Table 4.20 *Composition of LB medium*

Content	Preparation
Peptone	10 g
Yeast extract	5 g
NaCl	10 g
ddH_2O	ad 1000 ml

Generally, for agar plates, 1.5% agar was added to the liquid medium before autoclaving.

4.5.5 **Super Optimal Broth (SOB) medium**

Super Optimal Broth (SOB) was used for chemical transformation of *E. coli*.

Table 4.21 *Composition of SOB medium*

Component	**Concentration**
Bacto tryptone 2% Bacto™ Yeast extract	0.5%
NaCl	10 mM
KCl	2.5 mM

SOC medium (SOB added with glucose) was prepared freshly by adding 25 µl 2M $MgCl_2$, 50 µl 1M $MgSO_4$ and 100 µl 1M glucose to 5 ml SOB medium (Table 4.21).

4.5.6 **Minimal medium for meningococci (MMM)**

A minimal medium for meningococci (MMM) was prepared according to Lappann *et al*., 2006 [94] and Baart *et al*., 2007 [95] with some modifications (Table 4.22).

Table 4.22 *Composition of MMM*

Component[a]	**Concentration**
NaCl	140 mM
TRIS	40 mM
D-glucose-monohydrate	35 mM
NH_4Cl	25 mM
KCl	2.0 mM
NaH_2PO_4	1 mM
$CaCl_2$ $2H_2O$	0.5 mM
$MgSO_4$	0.2 mM
$Na_2S_2O_3$ $5H_2O$	0.4 mM
$FeCl_3$ $6H_2O$	0.1 mM
$ZnSO_4$ $7H_2O$	0.34 µM
Na_2MoO_4 $2H_2O$	0.16 µM
$MnCl_2$ $4H_2O$	0.08 µM
$CoCl_2$ $6H_2O$	0.08 µM
$CuSO_4$ $5H_2O$	0.08 µM
$NaHCO_3$	5 mM
	The pH was adjusted to 7.6.

4.5.7 **Modified Neisseria Defined Medium (mNDM)**

A chemically defined rich medium (Table 4.23) for the cultivation of meningococci was prepared according to Archibald *et al*., 1978 [96].

Table 4.23 *Composition of mNDM*

Component[a]	**Concentration**
L-glutamic acid	10 mM
D-glucose-monohydrate	10 mM
L-cysteine	1 mM
Uracil	1 mM
L-arginine	1 mM
NaCl	140 mM
TRIS	40 mM
NH_4Cl	10 mM
NaH_2PO_4	1 mM
Na_2SO_4	2.3 mM
KCl	2.0 mM
$CaCl_2x2H_2O$	0.5 mM
$MgSO_4$	0.2 mM
$FeNO_3$	1 mg/l
$ZnSO_4x7H_2O$	0.2 µM
$MnCl_2x4H_2O$	0.2 µM
$CoCl_2x6H_2O$	0.2 µM
$CuSO_4x5H_2O$	0.2 µM
$NaHCO_3$	5 mM
10 ml PolyVitex (Biomerieux, 55652) per liter	

4.5.8 **Cell culture solutions and media**

As a standard cell culture medium MEM Eagle (EMEM) supplemented with 10% fetal calf serum (FCS), 1% nonessential amino acids (NEAA) and 1% Sodium pyruvate (NaPyr) was used ($EMEM^{+++}$, Table 4.24).

Table 4.24 *EMEM^{+++} composition*

Name	Application	*Source*
MEM Eagle (EMEM)	Standard cell culture medium and for cell invasion/adhesion assays	*LONZA*, Basel (Ch)
FCS	Medium supplement (EMEM^{+++})	*Thermo Fisher,* Frankfurt
NEAA	Medium supplement (EMEM^{+++})	*LONZA*, Basel (Ch)
NaPyr	Medium supplement (EMEM^{+++})	*LONZA*, Basel (Ch)

Table 4.25 lists general solutions and media used for cell culture.

Table 4.25 *Solutions and media used for cell culture*

Name	Application	*Source*
MEM Eagle (EMEM)	Standard cell culture medium and for cell invasion/adhesion assays	*LONZA*, Basel (Ch)
FCS	Medium supplement (EMEM^{+++})	*Thermo Fisher,* Frankfurt
NEAA	Medium supplement (EMEM^{+++})	*LONZA*, Basel (Ch)
NaPyr	Medium supplement (EMEM^{+++})	*LONZA*, Basel (Ch)
Trypsin-EDTA (0.05%)	Dissociation of cells	*Thermo Fisher,* Frankfurt
Gentamycin (10 mg/ml)	Antibacterial agent	*Biochrom,* Berlin
Saponin (20%)	Permeabilization of cells	*SERVA,* Heidelberg
RPMI 1640 + GlutaMAX^{TM}-1	Standard cell culture medium	*Thermo Fisher,* Frankfurt
Dimethyl sulfoxide (DMSO)	Cell cryopreservation	*Roth,* Mannheim

For long-term storage, approximately 1x 10^6 cells were resuspended in a special freezing media (RPMI 1640 + GlutaMAX^{TM}-1, 10% FCS, 12% DMSO, Table 4.26) and stored in liquid nitrogen.

Table 4.26 *Cell freezing medium composition*

Component	Preparation
RPMI 1640 + GlutaMAX^{TM}-I	50 ml
FCS	30 ml
DMSO	20 ml
	Storage at -80 °C

4.7 Antibiotic supplements

Antibiotics were used when appropriate of concentrations given in Table 4.27.

Table 4.27 *Preparation of antibiotics*

Antibiotic	**Final concentration (µg/ml)**		**Stock concentration (mg/ml)**		**Solvent**
	E. coli	*N. meningitidis*	*E. coli*	*N. meningitidis*	
Ampicillin	**100**	**-**	100	-	ddH_2O
Kanamycin	**30**	**100**	30	100	ddH_2O
Erythromycin	**250**	**7**	100	7	100% Ethanol
Chloramphenicol	**30**	**7**	30	7	70% Ethanol

4.8 Oligonucleotides

All Oligonucleotides used in this work were purchased from Sigma-Aldrich and described in Table 4.28.

Table 4.28 *Oligonucleotides used in this study*

ID[a]	**Sequence (5'-3')**[b]	**Target site**	**Description**
310	gcgcgcGGATCC$_{BamHI}$GATGCCGTCTGAAGCACCGTCCAT	*relA* locus	α522/MC58 *relA* knock-out
311	gcgcgcCTGCAG$_{PstI}$GATGGGGTCTTCCGTTCCGATAAA	*relA* locus	α522/MC58 *relA* knock-out
312	gcgcgcCTGCAG$_{PstI}$ATACAAAAATGCCGTCTGAAAGCC	*relA* locus	α522/MC58 *relA* knock-out
313	gcgcgcGAATTC$_{EcoRI}$TGTTTCATCCAAATAAACGCGTTG	*relA* locus	α522/MC58 *relA* knock-out
324	gcgcgcGGATCC$_{BamHI}$CGATTCCGCCGTTGATGCCGTCTGA	ATR$_{relA}$	α522 ATR$_{relA}$ knock-out
325	CCGATAAAAACGAGTTTATTGTAACAGCTTATTTATTTACGGTGCATAGGCGGG	ATR$_{relA}$	α522 ATR$_{relA}$ knock-out
326	CACCGTAAATAAATAAGCTGTTACAATAAACTCGTTTTTATCGGAACGGAAG	ATR$_{relA}$	α522 ATR$_{relA}$ knock-out
327	gcgcgcgGAATTC$_{EcoRI}$GGTTTCTTTGGCGACGGCGCGTTTTTC	ATR$_{relA}$	α522 ATR$_{relA}$ knock-out
354	gcgcgcGGATCC$_{BamHI}$ACATTTGAAGCCATTGACCCTGT	*spoT* locus	α522/MC58 *spoT* knock-out
355	gcgcgcAAGCTT$_{HindIII}$AGCAGGTAAAACGGGTTGCCTT	*spoT* locus	α522/MC58 *spoT* knock-out
356	gcgcgcAAGCTT$_{HindIII}$TTCAGACGGCTTTCGGTATGT	*spoT* locus	α522/MC58 *spoT* knock-out
357	gcgcgcATCGATC$_{ClaI}$AGGCTATGACGTGATTTTGGA	*spoT* locus	α522/MC58 *spoT* knock-out
360	AGTGGGTGAGTTTCTGCACTTCGT	*relA* TSS	Specific primer
361	TACTGTTGCAGCGTTCGGAAACCA	*relA* TSS	Nested primer
410	gcgcgcGGATCC$_{BamHI}$ATGCCGTCTGAATCAAATTGGCGGAAAAGCTGCCGATGCTT	ATR$_{relA}$	ATR$_{relA}$ knock-in

ID[a]	Sequence (5'-3')[b]	Target site	Description
411	TAACAGACTATTTTTGCAAAGGTCTCAGCTTATTTATTTACGGTGCATA	ATR_{relA}	ATR_{relA} knock-in
412	TATGCACCGTAAATAAATAAGCTGAGACCTTTGCAAAAATAGTCTGTTA	ATR_{relA}	ATR_{relA} knock-in
413	TCCGATAAAAACGAGTTTATTGTAACAGCTTGAGACCTTTGCAATAACAT	ATR_{relA}	ATR_{relA} knock-in
414	ATGTTATTGCAAAGGTCTCAAGCTGTTACAATAAACTCGTTTTTATCGGA	ATR_{relA}	ATR_{relA} knock-in
415	gcgcgcAAGCTT$_{HindIII}$ATGCCGTCTGAAATCGCCAGTTTGATTAACACGACGCGGATG	ATR_{relA}	ATR_{relA} knock-in
449	gcgcgcGAATTC$_{EcoRI}$CAGCTTGAGACCTTTGCAATAA	ATR_{relA}	Complementation
448	gcgcgcGAATTC$_{EcoRI}$AAGCTGAGACCTTTGCAAAAATA	ATR_{relA}	Complementation
865	TTCCGGATTTATGGACACCGAAA	*spoT* locus	*spoT* knock-out verification
866	CAGGAAGCTTTTTTGGAATACGC	*spoT* locus	*spoT* knock-out verification
896	gttttGGATCC$_{BamHI}$AACCTGCAAGAGCTTGCCGAAAATCT	*relA*	$relA_{flagtag}$
897	gttttGAATTC$_{EcoRI}$TTACTATTTATCGTCGTCATCTTTGTAGTCGATATCATGATCTTTATAATCACCGTCATGGTCTTTGTAGTCAAGCCGGGTAACGCTCAATAC	*relA*	$relA_{flagtag}$
898	gttttGAATTC$_{EcoRI}$ATACAAAAATGCCGTCTGAAAGCC	intergenic region	$relA_{flagtag}$
899	gttttCTCGAG$_{NotI}$ACGCGTTGGTAGTCAGAAAATTCG	intergenic region	$relA_{flagtag}$
900	AAGCACTGGTATTTCGGCCA	*relA* locus	*relA* knock-out verification
901	CTTGTGCGGACACCAGAGAT	*relA* locus	*relA* knock-out verification
1145	GCGGCTTTTGGAACACGATT	*cysT*	Transcription
1146	ATAAAGGGCAGGCTGACGAC	*cysT*	Transcription
1147	ACCCGTTTTGATTTTCGCGG	*cysT*	Transcription
1148	GCTTGCGCCGAGTATCAATG	*cysW*	Transcription
1149	ATCAACCTCAACGTCCCCAC	*cysW*	Transcription
1150	CAAACCGAAAGCGACGTTGT	*cysA*	Transcription
1151	GTGGGGACGTTGAGGTTGAT	intergenic region	CREE

General primers

ID[a] / Name	Sequence (5'-3')[b]	Target site
242/KB 9	AATACGACTCACTATAGGGC	Amplification of an insert within pBS
243/329	ACCATGATTACGCCAAGC	Amplification of an insert within pBS
244/Kana1	CACGAGGCAGACCTCAG	Amplification of down region of kanamycin resistance cassette
245/Kana2	GATTTTGAGACACAACGTGG	Amplification of up region of the kanamycin resistance cassette
459/API	CGGCATTTATCAGATATTTGTT	Amplification of an insert within pAP1
460/APII	CGTCAGAGCATGGCTTTAT	Amplification of an insert within pAP1
837/Nona	NNN NNN NNN	universal, non-specific primer

qRT-PCR primers		
ID[a] / Name	**Sequence (5'-3')[b]**	**Target site**
282	GGATGATTATGGATGTGCTGCCG	*rpoC*_RT (F)
283	CGCATGCAGTTCCAACAGACGTT	*rpoC*_RT (R)
306	ACCTATTGGTTTCCGAACGCTGC	*relA*_RT (F)
307	GCCAGCAGCATTTTCCGCATAGT	*relA*_RT (R)
308	AATATGCGGACGCTCGGTTCGAT	*spoT*_RT (F)
309	TGGGATGCAGGTTTTGGAACGAT	*spoT*_RT (R)
400	GACGAACTCATCGAAAATGCTTCC	*dksA*_RT (F)
401	GGTCGCCTGTATTTTACTGAGAAG	*dksA*_RT (R)
434	TCGAGGTATTGGGCGGTTTTATTC	*grxB*_RT (F)
435	TACAACGACAAACTGGTGCAGCC	*grxB*_RT (R)

[a]ID according to the AG Schoen oligonucleotide collection

[b]Restriction sites are underlined, small letters indicate nonsens-nucleotides

4.9 Plasmids

The backbones of plasmids used for all cloning work in this study are depicted in Figure 4.1. All plasmid constructs obtained in this study are listed in Table 4.29.

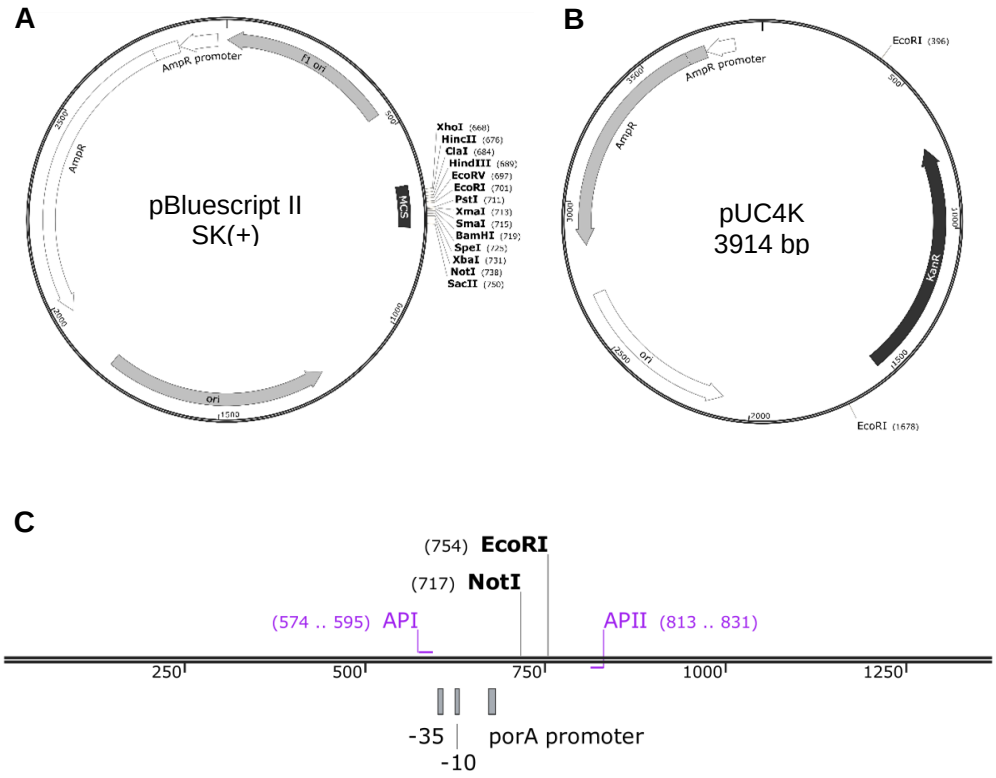

Figure 4.1 Backbone and delivery plasmids used in this study.

As a standard cloning vector pBluescript II SK (+) (A) or pBluescript-SK (pBS-SK) was used. The standard cloning plasmid pUC4K (B) functioned as a source for the kanamycin resistance cassette. (C) Internal fragment of pAP1 comprising the *porA* promoter and the cloning region. The plasmid maps were created by snap gene (Table 5.12).

Table 4.29 *Plasmids used in this study*

ID[a]	Plasmid	Description	Resistance	Reference
-	pAP1	Neisserial expression vector derived from pEG2-Ery by deletion of rs-gfp	Ery^r	Lappann *et al*., 2006 [94]
-	pBluescript II SK (+)	Standard cloning vector	Amp^r	Stratagene
315	pBS-SK	Standard cloning vector	Amp^r	Stratagene
58	pUC4K	Delivery plasmid harboring kanamycin resistance cassette	Amp^r/Km^r	GE Healthcare
2304	pBS-CM	Delivery plasmid harboring chloramphenicol resistance cassette	Cm^r	IHM
WUE4713	pKE1	Kanamycin resistance cassette with *PstI* sites from pUC4K cloned between PCR product 310/311 comprising MC58 *relA* UP fragment and *relA* DOWN PCR fragment 312/313 in *BamHI* and *EcoRI* sites of pBS-SK	Amp^r/Km^r	This study
WUE4714	pKE2	Kanamycin resistance cassette with *PstI* sites from pUC4K cloned between PCR product 310/311 comprising α522 *relA* UP fragment and *relA* DOWN PCR fragment 312/313 in *BamHI* and *EcoRI* sites of pBS-SK	Amp^r/Km^r	This study
WUE4736	pKE4	Chloramphenicol resistance cassette with *HindIII* sites from pBS-CM cloned between PCR product 354/355 comprising α522/MC58 *spoT* UP fragment and *spoT* DOWN PCR fragment 356/357 in *BamHI* and *ClaI* sites of pBS-SK	Amp^r/Cm^r	This study
WUE4734	pKE3	PCR product 324/325 and PCR product 326/327 comprising α522 ATR_{relA} UP and DOWN fragments fused to each other by using megaprimer PCR cloned into *BamHI* and *EcoRI* sites of pBS-SK	Amp^r	This study
WUE4754	pKB1	PCR product 412/413 comprising α522 ATR_{relA} inserted between PCR product 410/411 (MC58 UP) and PCR product 414/415 (MC58 DOWN) by using megaprimer PCR cloned into *BamHI* and *EcoRI* sites of pBS-SK	Amp^r	This study
WUE5269	pLK4	PCR product $896/897_{flagtag}$ and 898/899 comprising MC58 regions which leads to C-terminal fusion of an 6x his-flagtag to *relA* cloned into pBluescript II SK (+)	Amp^r	This study
WUE5260	pLK13	PCR product 448/1095 comprising α522 ATR_{relA} cloned between the *EcoRI* and the *NotI* sites of pAP1 ATR_{relA} is cloned downstream P_{porA} in wt direction (I) to *grxB*	Ery^r	This study
WUE5263	pLK14	PCR product 449/1094 comprising α522 ATR_{relA} cloned between the *EcoRI* and the *NotI* sites of pAP1 ATR_{relA} is cloned downstream P_{porA} in wt direction (II) to *relA*	Ery^r	This study
WUE5266	pLK17	PCR product $896/897_{flagtag}$ and 898/899 comprising α522 regions which leads to C-terminal fusion of an 6x his-flagtag to *relA* cloned into pBluescript II SK (+)	Km^r	This study

[a]According to the strain collection of the Institute for Hygiene and Microbiology (IHM), Würzburg

4.10 Microorganisms

4.10.1 **Strains used in this study**

All strains used in this study are given in Table 4.30 along with their relevant characteristics and sources.

Table 4.30 *Strains used in this study*

ID[a]	Microorganism	Strain	Genotype/relevant characteristics	Source/Reference
	E. coli			
		XL1-Blue MRF'	*Δ((mcrA)183Δ(mcrCB-hsdSMR-mrr)173 recA1 endA1 gyrA96 thi-1 hsdR17 supE44 relA1 lac F´ proAB lacIqZΔM15 Tn10 Tetr fhuA2 lac(del)U169 phoA glnV44 Φ80' lacZ(del)M15 gyrA96 recA1 relA1 endA1 thi-1 hsdR17*	Stratagene
		DH5α		Invitrogen
	N. meningitidis			
-		α522	wild-type	IHM
WUE2135		MC58	wild-type	McGuiness *et al.*, 1991 [20]
WUE4715		α522	Δ*relA*::Km^r	this study
WUE4716		MC58	Δ*relA*::Km^r	this study
WUE4733		α522	ΔATR$_{relA}$	this study
WUE4737		MC58	*relA*1 Δ*spoT*::Cm^r	this study
WUE4739		MC58	Δ*relA*::Km^{r}Δ*spoT*::Cm^r	this study
WUE4740		α522	Δ*relA*::Km^{r}Δ*spoT*::Cm^r	this study
WUE4755		MC58	*relAp*::ATR$_{relA}$	this study
WUE5258		α522	pAP1	this study
WUE5259		α522ΔATR$_{relA}$	pAP1	this study
WUE5261		α522	pLK13	this study
WUE5262		α522ΔATR$_{relA}$	pLK13	this study
WUE5264		α522	pLK14	this study
WUE5265		α522ΔATR$_{relA}$	pLK14	this study
WUE5267		α522	*relA*$_{flag\text{-}tag}$	this study
WUE5270		MC58	*relA*$_{flag\text{-}tag}$	this study

[a]According to the strain collection of the Institute for Hygiene and Microbiology (IHM), Würzburg

4.11 Cell lines

For the cell invasion and adhesion assays a nasopharyngeal epithelial cell line (Detroit562, ATCC® number CCL-138™) was used [97, 98].

5 Methods

5.1 Cultivation of bacteria

N. meningitidis strains were cultivated overnight on COS or on GCB^{++} agar plates (Table 4.19) at 37 °C with 5% CO_2 in an incubator. For selection of recombinant strains, the GCB^{++} agar medium was supplemented with chloramphenicol (7 µg/ml), erythromycin (7 µg/ml), kanamycin (100 µg/ml), or with combinations of these antibiotics (Table 4.27). For cultivation in liquid culture, the strains were inoculated in PPM^{+} (Table 4.15 and 4.16) with or without antibiotics, and were incubated for the appropriate time at 37 °C and 200 rpm.

E. coli were cultivated overnight on LB agar plates (Table 4.20) in an incubator at 37 °C or in LB media at 37 °C while shaking at 200 rpm in an incubator shaker. For growth of recombinant clones the solid or liquid medium was supplemented with ampicillin (100 µg/ml), chloramphenicol (30 µg/ml), erythromycin (250 µg/ml) or kanamycin (30 µg/ml) (Table 4.27).

5.2 Estimation of bacterial cell number by determination of the optical density at 600 nm

Liquid medium was inoculated with the bacteria from an agar plate, followed by pre-incubation, at 37 °C unless stated otherwise in an incubator shaker for a specific period of time (45'-1 h). After pre-incubation, 1 ml of the bacterial suspension was pipetted in a cuvette and the absorption at 600 nm (OD_{600}) was measured with a photometer (WPA biowave) against the blank medium. The bacterial suspension was adjusted to the desired optical density if appropriate.

For calculation of the cell number, an OD_{600} 1.0 is equivalent to approximately $1x10^9$ cells/ml for *N. meningitidis* and to approximately $2x10^8$ cells/ml for *E. coli*.

5.3 Preparation of chemically competent *E. coli* cells

XL-1 Blue MRF' or DH5α frozen glycerol stocks were streaked out onto an LB agar plate and incubated at 37 °C overnight. A 15 ml starter culture of LB medium was inoculated with a single colony from the fresh agar plate and grown overnight at 37 °C. 25 ml LB medium was inoculated with 1 ml starter culture and was incubated at 37 °C in a shaker (Thermomixer 5436). After approximately 1-2 h when the OD_{600} reached 0.5-0.7, the cells were chilled 10-20 minutes on ice. Subsequently, cells were harvested in

pre-cooled tubes at 4 °C via centrifugation for 5 minutes at 4000 rpm. The supernatant was decanted, the pellet chilled on ice for 1 minute and then resuspended and washed with 10 ml of ice cold 80 mM $MgCl_2$/20 mM $CaCl_2$. The cell suspension was centrifuged at 4 °C for 5 minutes at 4000 rpm and the pellet was resuspended with 10 ml 80 mM $MgCl_2$/20 mM $CaCl_2$ and chilled on ice for another 30 minutes. A third centrifugation step was done to resuspend the pellet in 800 µl of 100 mM $CaCl_2$/20% glycerol, and aliquots of 100 µl were shock frozen in liquid nitrogen and stored at -80 °C until use.

5.4 Transformation of *E. coli*

A 100 µl aliquot of chemically competent *E. coli* DH5α or *E. coli* XL-1 Blue MRF' was thawed slowly on ice. 10 µl of the ligation reaction was added to the bacteria and chilled on ice for approximately 30 minutes. Subsequently, the cells were incubated at 42 °C for 90 seconds and immediately cooled on ice for 2 minutes. Then, 800 µl SOC medium (Table 4.21) was added and the cells were incubated for 1 h at 37 °C at 200 rpm. Afterwards, bacteria were plated on LB agar plates supplemented with the appropriate antibiotic(s) for selection of transformants and incubated overnight at 37 °C.

5.5 Transformation of *N. meningitidis*

The strain to be transformed was grown overnight on COS agar plates at 37 °C with 5% CO_2 in an incubator. Bacteria were grown in PPM^+ (Table 4.15 and 4.16) for 1 h at 37 °C at 200 rpm. After the pre-culture, bacterial suspensions were adjusted to an OD_{600} 0.1 in a final volume of 1 ml PPM^+. For the transformation, 600 ng - 1 µg of the DNA (plasmid preparation, chapter 5.7), were added to the culture and incubated for 5 to 6 hours at 37 °C and 200 rpm. One hundred µl of the bacterial suspension were directly plated on GCB^{++} agar supplemented with the required antibiotic for selection of transformants. The remaining 900 µl were pelleted at 5000 rpm for 5 minutes at room temperature. The supernatant was discarded, the pellet was resuspended in the remaining medium and plated on GCB^{++} agar plates. The plates were incubated overnight at 37 °C with 5% CO_2.

5.6 Preparation of meningococcal genomic DNA

For the isolation of meningococcal genomic DNA the QIAamp DNA Mini Kit (*Qiagen*, Hilden/Table 4.4) was used with some modification of the manufacturer's protocol. Meningococci were streaked onto two agar plates and grown overnight at 37 °C with 5% CO_2 in an incubator (Heraeus 6000). Next day, the entire bacterial lawn/culture was harvested with a cotton swab and resuspended in 1.25 ml PBS (Table 4.6). Subsequently, the bacterial suspension was centrifuged for 5 minutes at 8000 rpm, the supernatant discarded and the pellets resuspened in 180 µl ATL buffer with 20 µl Proteinase K (20 mg/ml) and mixed. Afterwards, the suspensions were incubated at 56 °C for 2-3 hours and vortexed every thirty minutes. After the incubation time, the tubes were briefly centrifuged, 80 µl RNase A (5 mg/ml) was added and vortexed 10 times. 200 µl AL buffer was added, the tubes vortexed 10 times and incubated for 10 minutes at 70 °C. The suspensions were spinned down, 200 µl ethanol was added, vortexed 10 times and centrifuged shortly. The whole material was pipetted onto a QIAamp spin column and was centrifuged for 1 minute at 8000 rpm. To remove residual contaminants, DNA bound to the QIAamp membrane was washed in two centrifugation steps. The column was transferred into a fresh tube, 500 µl AW1 buffer was added and centrifuged for 1 minute at 8000 rpm, the flow-through was discarded and the column was washed with 500 µl AW2 buffer 3 minutes at 13000 rpm. Afterwards, the column was dried with a 1 minute centrifugation step at 13000 rpm and then transferred into a fresh 2 ml microcentrifuge tube. To elute the DNA, 100 µl 1xTE buffer was applied to the column, incubated at room temperature for at least one minute and then centrifuged for 1 minute at 8000 rpm. Concentration and purity of the DNA was measured using a spectrophotometer (NanoDrop 1000, Peqlab) and stored at -20 °C.

5.7 Isolation of plasmid DNA

For the isolation of plasmid DNA the QIAprep Spin Miniprep Kit or the Qiagen Plasmid Midi Kit (*Qiagen*, Hilden) were used (Table 4.4). For the isolation of smaller amounts of plasmid DNA with the QIAprep Spin Miniprep Kit, a single colony was picked from a freshly streaked selective agar plate and inoculated into 5 ml LB medium containing the appropriate selective antibiotic. These cultures were incubated overnight at 37 °C with shaking at 200 rpm. The next day, the bacterial cells were harvested by centrifugation at 8000 rpm in a microcentrifuge for 5 minutes at room temperature. The bacterial pellet was resuspended in 250 µl Buffer P1 and transferred to a microcentrifuge tupe (Eppendorf cups). Subsequently, 250 µl Buffer P2 was added and thoroughly mixed by inverting the tube 4-6 times. Immediately, 350 µl of Buffer N3 were added and mixed by

inverting 4-6 times. Afterwards the tubes were centrifuged for 10 minutes at 13.000 rpm in a microcentrifuge at room temperature. The supernatants were pipetted to the QIAprep spin columns and centrifuged for 30-60 seconds at 13.000 rpm. After discarding the flow-through, the column was washed by adding 500 µl of Buffer PB and was centrifuged 30-60 seconds at 13.000 rpm. Again, the flow-through was discarded, the QiAprep spin column washed by adding 750 µ of Buffer PE and centrifuged for 30-60 seconds. To remove the ethanol of the PE Buffer, the column was placed into a fresh tube and was centrifuged for 3 minutes at full speed. Finally the the QIAprep column was placed in a clean 1.5 ml microcentrifuge tube, 30-50 µl ddH_2O was added to the center of each column, incubated for 1-5 minutes at room temperature and centrifuged for 1-2 minutes at 13.000 rpm to elute the DNA. The plasmid DNA concentration was measured using a spectrophotometer (NanoDrop 1000) and stored at -20 °C or at 4 °C.
For higher amounts of DNA, the plasmid preparation was carried out with the QIAGEN Plasmid Midi Kit according to the manufacturer's protocol. One colony of the desired strain was picked and was inoculated into a 25 ml LB medium supplemented with the respective antibiotic. The culture was incubated overnight at 37 °C and 200 rpm and the next day the cells were harvested by centrifugation at 4000 rpm for 15 minutes at 4 °C. The supernatant was discarded and the pellet was resuspended in 4 ml pre-cooled buffer P1, 4 ml of buffer P2 was added and mixed by inverting 4-6 times. The reaction was incubated for 5 minutes at room temperature prior to addition of 4 ml ice-cool buffer P3. The suspension was mixed again by inverting the tube 4-6 times and incubated for 15 minutes on ice. Afterwards, the reaction was centrifuged at 14000 rpm for 30 minutes at 4 °C. The supernatant was transferred to a fresh tube and centrifuged again for 15 minutes at 14000 rpm at 4 °C. QIAGEN Tip-100 columns were equilibrated with 4 ml buffer QBT, the supernatant was applied to the membrane and followed by two washing steps with 10 ml buffer QC. The DNA was eluted into a clean tube with 5 ml buffer QF and was precipitated by adding 3.5 ml isopropanol. Subsequently, the mixture was transferred into a fresh tube and the DNA was pelleted at 14000 rpm for 30 minutes at 4 °C. The supernatant was carefully removed and the DNA was washed with 2 ml 70% ethanol. The pellet was dried by vacuum concentration in the Savant SpeedVac®Plus (Thermo Scientific) for 5 minutes at medium temperature and was redissolved in 80 - 100 µl 1xTE buffer, pH 8.0.

5.8 Bacterial lysates

To test bacterial colonies for the correct transformation via PCR, lysates were prepared as follows. A colony was picked from a fresh agar plate and resuspended by pipetting up and down in 20-30 µl 1x PBS. The suspension was incubated for about 5 minutes (*E. coli*) or for 15 minutes (*N. meningitidis*) at 100 °C in a heating block and then immediately cooled on ice for 2-5 minutes. After centrifugation for 1 min at 13000 rpm in a tabletop centrifuge, the lysates were chilled on ice and 1-2 µl per 25 µl PCR mixture was used.

5.9 Polymerase chain reaction (PCR)

PCRs were used to amplify specific DNA fragments and to screen for correct clones after transformation (chapter 5.4, 5.5). Q5® High-Fidelity DNA polymerase (NEB) was used for cloning purposes because of its proof reading activity. *Taq* DNA polymerase (NEB) was used to screen for correct clones or to check if RNA samples are free from DNA. Generally, 100 ng genomic or plasmid DNA was used as template DNA. To screen for transformants, 1-2 µl of a suspension of mutant colonies was used as template DNA or a colony was picked and directly rubbed in.

PCR was performed in modification of the manufacturer's protocol as given in Table 5.1.

Table 5.1 *PCR protocol for Taq DNA polymerase*

Component	25 µl reaction	Final Concentration
10X ThermoPol reaction buffer	2.5 µl	1X
20 mM dNTPs	0.25 µl	200 µM
25 µM forward primer	0.5 µl	0.5 µM
25 µM reverse primer	0.5 µl	0.5 µM
Template DNA	variable	< 1µg
Taq DNA polymerase	0.25 µl	0.05 U/µl
ddH2O	to 25 µl	

PCR reactions for clone testing were prepared on ice and were quickly transferred to a thermocycler (Thermomixer 5436) preheated to the denaturing temperature (95 °C). The standard PCR program is given in Table 5.2.

Table 5.2 *Thermocycling program for Taq DNA polymerase*

Step		Temperature	Time
Initial denaturation		95 °C	30 seconds (5' for lysates)
Denaturation	25-35 Cycles	95 °C	30 seconds
Annealing		50-65 °C	30 seconds
Extention		68 °C	1 minute/kb
Final extension		68 °C	5 minutes
Hold/cooling		4 °C	∞

The annealing temperatures (T_a) of the NEB *Taq* DNA Polymerase were obtained by estimating the melting temperatures (T_m) of each primer with the formula [2× (A+T) + 4× (G+C)], and subtracting 5 °C. The standard reaction used for Q5® High-Fidelity DNA polymerase is shown in Table 5.3.

Table 5.3 *PCR protocol for Q5® High-Fidelity DNA polymerase*

Component	50 µl reaction	Final Concentration
5X Q5 reaction buffer	10 µl	1X
20 mM dNTPs	0.5 µl	200 µM
25 µM forward primer	1 µl	0.5 µM
25 µM reverse primer	1 µl	0.5 µM
Template DNA	variable	< 1µg
Q5® High-Fidelity DNA polymerase	0.5 µl	0.02 U/µl
ddH2O	to 50 µl	

PCR reactions for cloning purposes were prepared on ice and were quickly transferred to a thermocycler preheated to the denaturing temperature (98 °C). The PCR cycling scheme is given in Table 5.4.

Table 5.4 *Thermocycling program for Q5® High-Fidelity DNA polymerase*

Step		Temperature	Time
Initial denaturation		98 °C	30 seconds
Denaturation	25-35 Cycles	98 °C	10 seconds
Annealing		50-72 °C	30 seconds
Extension		72 °C	20-30 seconds/kb
Final extension		72 °C	2 minutes
Hold/cooling		4 °C	∞

The annealing temperature (T_a) of the Q5® High-Fidelity DNA Polymerase was calculated by using the T_m Calculator (http://tmcalculator.neb.com/#!/) from NEB.

5.10 Visualization and purification of PCR products

Agarose gel electrophoresis was performed to visualize PCR products and to estimate the length of the DNA molecule. PCR products were electrophoretically separated in an agarose gel with TAE buffer (chapter 4.4).

Agarose was added to 1X TAE buffer (Table 4.8) at a concentration between 1% and 2% (w/v), depending on the size of the DNA fragment. The mixture of agarose and buffer was heated in a microwave, cooled down and poured into a gel chamber. Five µl of the length standard 'Hyper Ladder I' (Table 4.3) were used as standard molecular weight marker. 6X DNA loading buffer/dye (Table 4.8) was added to each PCR sample to a 1X concentration and pipetted into a well of the gel. DNA samples were separated at 170 V in 1X TAE buffer, for approximately 1 h. Afterwards, for post-staining the agarose gel was incubated in a GelRed™ bath (Table 4.8) for 30-45 minutes, or the gel was pre-stained (e.g. 5 µl stock solution added to 50 ml of gel solution). The Chemi Doc MP System (Bio-Rad) was used to visualize the bands of the DNA fragments via UV light (at 302 nm or 312 nm). Depending on the subsequent treatment, the PCR products were either purified using the Stratec INVISISORB Purification Kit (*Stratec*) or were extracted from the gel with the Stratec Gel Extraction Kit (*Stratec*). For sequencing or cloning procedures, only 3-5 µl of the PCR product was used for electrophoretic detection and the remaining PCR sample was directly purified and eluted in 30 µl ddH_2O.

5.11 Sequencing of PCR products and plasmids

Sequencing reactions were prepared in a final volume of 10 µl in ddH_2O. One µl of the respective primer (25 µM) and 20-80 ng of PCR fragments or 200-400 ng of plasmids were mixed in a 1.5 ml tube and sent to GATC (Köln, Germany) for sequencing.

5.12 Cloning procedure: digestion of DNA, gel extraction and ligation

The digestion of DNA fragments, plasmids or genomic DNA was performed with restriction endonucleases purchased from New England BioLabs. For cloning purposes, purified PCR products or plasmids were enzymatically digested using different restriction endonucleases. Table 5.5 shows the typical restriction digest.

Table 5.5 *Standard restriction digest and gel extraction*

Component	50 µl reaction
Restriction Enzyme	10 U
DNA	1 µg
10X NEBuffer	5 µl (1X)
Total Reaction Volume	50 µl
ddH_2O	to 50 µl
Incubation Time	1-2 h
Incubation Temperature	37 °C

Digested DNA fragments were purified using the MSB Spin PCRapace Kit (*Stratec*). Digested vector DNA was applied to a 1% agarose gel and the separated band was sliced out of the gel and extracted using the Invisorb Spin DNA Extraction Kit (*Stratec*) according to the manufacturer's instructions.

Table 5.6 *Standard ligation protocol with T4 DNA Ligase*

Component	20 µl reaction
10X T4 DNA Ligase Buffer	2 µl
Vector DNA	50 ng
Insert DNA	variable (amount of insert)
T4 DNA Ligase	1 µl
ddH_2O	to 20 µl

A ligation with purified digested DNA fragment and the linearized vector was performed by using the T4 DNA ligase. Generally, a molar ratio of 1:3 vector to insert was used in standard ligation reaction. The proportion of insert to the vector was calculated with the following formula:

$$Amount\ of\ insert\ (ng) = insert/vector\ ratio\ x\ mass\ of\ vector\ (ng) x\ ratio\ insert/vector\ lengths$$

All ligation reactions were performed in a microcentrifuge tube on ice. The ligation buffer was thawed and resuspended at room temperature and all components (Table 5.6) were mixed together by gently pipetting up and down. Subsequently, the ligation reactions were incubated at 16 °C overnight in a thermocycler. Next day, the ligation was heat inactivated at 65 °C for 10 minutes, chilled on ice until chemical transformation using 100 µl competent cells or stored -20 °C.

5.13 Construction of mutants

5.13.1 **Construction of isogenic deletion mutants**

Deletion mutants in *relA* and *relAspoT* were constructed in the strains MC58 and α522 by replacing the respective genes with a kanamycin or a chloramphenicol resistance cassette in frame. Briefly, around 600 bp upstream and downstream fragments of the target gene were amplified with oligonucleotides (Table 4.28) modified to introduce different enzyme restriction sites. The fragments were digested, purified and cloned into the pBluescript-SK vector (chapter 4.8) along with the digested DNA fragment containing the kanamycin or the chloramphenicol resistance cassette to yield the knock-out plasmids (Table 4.29) containing the resistance cassette flanking the upstream region and the downstream region of the respective gene. The meningococcal strains were then transformed with the respective knock-out plasmids (pKE1 and pKE2) and double homologous recombination resulted in the replacement of the target gene with the resistance cassette. Deletion of *relAspoT* double mutant were achieved by deleting the *spoT* gene in the *relA* mutant strain by using pKE4 for both strains.

The MC58 *relA1spoT* mutant was created by the deletion of the *spoT* gene (pKE4) in the wild-type strain MC58 and resulting in a compensatory mutation (11 bp deletion next to catalytic site) in *relA*, which led to a defective *relA1*.

The correct insertion of the resistance cassettes was confirmed by PCR and sequencing as well as by Southern blot analysis (chapter 5.14).

5.13.2 **Construction of mutants using megaprimer PCR**

Deletion of the ATR in the 5´region of *relA* in strain α522 was achieved by restriction free cloning using megaprimer PCR [99]. Around 600 bp regions upstream and downstream of the ATR in α522 were amplified using oligonucleotides (for the upstream fragment oligonucleotides 324 and 325, for the downstream fragment oligonucleotides 326 and 327, Table 4.28) where the 3´oligonucleotide of the upstream fragment had a complementary region of about 25 bp to the 5´region of the downstream fragment and similarly the 5´oligonucleotide of the downstream fragment had a complementary region of about 25 bp to the 3´region of the upstream fragment. These two purified fragments were further used as template for a megaprimer PCR (Table 5.7) to yield a fused DNA fragment containing the upstream and downstream regions of the ATR in the strain α522.

Table 5.7 *Megaprimer PCR thermocycling program*

Step	Cycles	Temperature	Time
Initial denaturation	1	95 °C	30 sec
Denaturation	25	95 °C	30 sec
Annealing		60 °C	1 min
Extention		72 °C	5 min
Final extension	1	72 °C	7 min
Hold/cooling	1	4 °C	∞

This fusion fragment was then purified, cloned into pBS-SK (pKE3) and transformed into the strain α522. The deletion of the ATR in the mutant strain was confirmed by PCR and sequencing.

The insertion of the ATR in the 5' region of *relA* in strain MC58 was also achieved by restriction free cloning using megaprimer PCR, as described above. Around 600 bp regions upstream and downstream of the putative ATR_{relA} insertion site in MC58 were amplified using oligonucleotides (for the upstream fragment oligonucleotides 410 and 411, for the downstream fragment oligonucleotides 414 and 415, Table 4.28) and were cloned flanking α522 ATR_{relA} (primers 412 and 413, Table 4.28) by using megaprimer PCR. The resulting PCR fusion fragment was then ligated into pBS-SK (pKB1), cloned into the strain MC58 and insertion of the ATR in the mutant strain was confirmed by PCR and sequencing.

5.13.3 **Construction of *relA* 6xHis-tagged mutants**

RelA 6xHis-tagged at the C-terminal in the strains MC58 and α522 by homologue recombination. Around 600 bp upstream and downstream fragments of the target insertion site (C-terminal end) were amplified with oligonucleotides (for the upstream fragment oligonucleotides 896 and 897, for the downstream fragment oligonucleotides 898 and 899, Table 4.28) modified to introduce different enzyme restriction sites and the 6xHis-tag sequence. The fragments were digested, purified and cloned into the pBluescript-SK vector (chapter 4.8) along with the digested DNA fragment to yield the cloning plasmids (Table 4.29). The meningococcal strains were then transformed with the respective plasmids (pLK4 and pLK17) and double homologous recombination resulted in the insertion of the 6xHis-tag at the C-terminal end of *relA*. The correct insertion was confirmed by PCR and sequencing as well as by Western blot analysis (chapter 5.23).

5.14 Southern Blot

One microgram of genomic DNA was digested with a suitable restriction enzyme in a 30 µl reaction volume overnight at 37 °C. Digested gDNA mixed with loading buffer as well as the DIG-labeled molecular weight marker were separated in a 0.8% agarose gel at 80 V for 5 – 6 hours, and the gel was stained to monitor DNA digestion. The gel was depurinated by incubation in 0.25 M HCl for 20 minutes, denatured in 5 M NaOH/1.5 M NaCl for 30 minutes, and finally neutralized in 5 M TRIS, pH 7.5/1.5 M NaCl for another 30 minutes. The blotting sandwich was build up and the flow of 20x SSC buffer led to capillary transfer of negatively charged DNA from the agarose gel to the positively charged nylon membrane. After overnight transfer the nylon membrane was dried and UV cross linked in an UV crosslinker (Life technologies) for 1 minute. The membrane was at least 30 minutes pre-hybridized in 50 ml of high SDS hybridization buffer (Table 4.9) at 48 °C in a special oven. In the meantime, 500 ng of the DIG-labeled DNA probe was added to 50 ml of high SDS hybridization buffer. Subsequently, the mixture was boiled in a water bath at 95 °C for 10 minutes and immediately cooled down on ice for 5 – 10 minutes. The pre-hybridization buffer was exchanged against the hybridization solution with the DIG-labeled probe in which the membrane was incubated overnight at 48 °C. The next day, the membrane was washed and developed with ChemiDoc MP System according to the manufacturer's instructions.

5.15 RNA preparation from liquid culture

For extraction of total RNA, bacterial cells from 10 ml of liquid culture were pelleted at the appropriate time point by centrifugation at 4 °C for 10 minutes. The supernatant was discarded, the pellets were frozen in liquid nitrogen and stored -80 °C until the next preparation step.

Total RNA extraction was performed by the hot phenol method, followed by DNA digestion and quantity and quality checks.

The heating block was set to 64 °C, the pellets stored at -80 °C were resuspended in 600 µl 0.5 mg/ml lysozyme and transferred in a fresh 2 ml microcentrifuge tube. 60 µl 10% SDS were added and mixed by inversion. The tubes were heated for 1-2 minutes at 64 °C until they got clear. After the incubation, 66 µl 1M NaOAc was applied and mixed by inversion. The hot phenol extraction started by adding 750 µl phenol to the suspensions, which were mixed by inversion and incubated for 6 minutes at 64 °C. During the incubation the tubes were mixed by inversion 6-10 times. Afterwards, the reactions were cooled on ice and centrifuged for 15 minutes at 13000 rpm at 4 °C. After centrifugation,

the aqueous layer was transferred into a new 2 ml microcentrifuge tube, 750 µl chloroform was added, mixed by inversion and centrifuged at 13000 rpm for 12 minutes at 15 °C. Subsequently, the aqueous layer was dispatched into two 2 ml microcentrifuge tubes, 1.4 ml ethanol was added, mixed and incubated for 2 hours or overnight at -80 °C.

To precipitate the RNA, the tubes were centrifuged for 30 minutes at 13000 rpm at 4 °C and the ethanol was removed carefully. The pellet was next washed with 900 µl pre-cooled (-20 °C) 75% ethanol and centrifuged for 10 minutes at 13000 rpm at 4 °C. Finally, the ethanol was removed carefully and the pellet was air dried for 5-10 minutes. The RNA was eluted by adding 100 µl Rnase-free H_2O and shaking at 800-1000 rpm for 5 minutes at 65 °C.

For complete DNA removal RNA was digested with DNaseI from *Thermo Scientific* (Schwerte). A standard protocol was prepared as described in Table 5.8.

Table 5.8 *DNase digestion*

Component	**100 µl reaction**
DNase I buffer	10 µl
RNase Inhibitor	1 µl
DNase I (1U/µl)	10 µl
RNA	30 µg
Rnase-free H_2O	to 100 µl

RNA was first denatured by incubation for 5 minutes at 65 °C and chilled on ice for 5 minutes, buffers and enzymes were added and the reaction was incubated at 37 °C for 45 minutes. Afterwards, 100 µl P:C:I (Table 4.2) was applied to the mixture, centrifuged at 13000 rpm for 12 minutes at 15 °C and the aqueous layer was transferred into a new tube. Two and a half volumes of a 30:1 mix (Table 4.13) were applied to the suspension and the RNA was precipitated overnight at -20 °C. The next day, samples were centrifuged for 30 minutes at 4 °C and 13000 rpm. The supernatant was discarded and the RNA pellets were washed with 350 µl 75% ethanol by centrifugation at 4 °C for 10 minutes at 13000 rpm. Pellets were air dried and dissolved in 30 µl Rnase-free H_2O by shaking at 800-1000 rpm for 5 minutes at 65 °C.

To check the RNA preparation for quantity and quality the RNA samples were measured with the NanoDrop 1000 (*Peqlab*) to determine the concentration of the RNA. Additionally, the purity was checked by measuring the OD at different wavelength. RNA has a maximum absorption at 260 nm and the A260/A280 ratio is an indication of the level of protein or DNA contaminations in the sample. A260/A280 ratio above 2.0

indicates pure RNA. Furthermore, RNA preparations can contain contaminants such as EDTA and phenol, and the ideal A260/A230 ratio is greater than 1.5.

In addition, a 1% TBE agarose gel was prepared to determine the integrity of RNA samples by electrophoretic separation. A bacterial RNA sample of good quality is indicated by a sharp band for the 23S ribosomal RNA and one band for the 16S rRNA in the stained gel. To ensure complete removal of DNA, a control PCR was carried out with 1 µl of the RNA sample and primers 282 and 283 (chapter 4.7). As a positive control, genomic DNA of the appropriate meningococcal strain was used.

5.16 cDNA synthesis

In modification to the manufacturer's protocol first-strand cDNA synthesis was prepared with SuperScript™ II reverse transcriptase from Invitrogen (Life technologies, Darmstadt). Table 5.9 shows the standard protocol used to transcribe 5 µg total RNA into cDNA.

Table 5.9 *cDNA synthesis – First step*

Component	
RNA	5 µg
NONA primer	1 µl
dNTPs Mix (10 mM each)	1 µl
Rnasefree H_2O	to 12 µl

The mixture was heated to 65 °C for 5 minutes and quickly chilled on ice. The contents of the tube were collected by brief centrifugation and the components given in Table 5.10 were added in a second step.

Table 5.10 *cDNA synthesis – Second step*

Component	
5x First-Strand Buffer	4 µl
0.1 DTT	2 µl
RNaseOUT™	1 µl

The contents of the tube were mixed gently and the samples were incubated for 2 minutes at 25 °C. Finally, 1 µl SuperScript™ II Reverse Transcriptase (Table 4.5) was added to a final volume of 20 µl.

After incubating at 25 °C for 10 minutes, the samples were heated to 42 °C for 50 minutes. The reaction was inactivated at 70 °C for 15 minutes. To digest the remaining RNA 1 µl RNase was added and incubated at 37 °C for 1 h. Subsequently, cDNA was

purified by using MSB Spin PCRapace Kit from *Stratec*. cDNA was eluted in 30-40 µl ddH_2O. Undiluted cDNA was applied for RT-PCRs, 1:10 dilution was used for qRT-PCRs.

5.17 Transcriptional start site mapping

To determine transcriptional start sites (TSSs) in the strains MC58 and α522, the 5'/3' RACE Kit (*Roche*, Table 4.3) was used according to manufacturer's protocol. cDNA was prepared using RNA from both strains and a gene specific primer (oligonucleotide 360, Table 4.28) and the reagents of the 5'/3' RACE Kit. After incorporation of the poly(A) tail at the 5´end of the cDNA using the terminal transferase of the 5'/3' RACE Kit, the tailed cDNA was amplified by PCR using the oligo(dT) anchor primer along with a nested primer (oligonucleotide 361, Table 4.28). The nested primer binds internal on the cDNA generated by the specific primer. After agarose gel electrophoresis, the DNA fragment was purified, sequenced and the last base upstream of the poly-A-tail corresponds to the first nucleotide transcribed (TSS).

5.18 Quantitative real-time PCR (qRT-PCR)

qRT-PCR analysis was performed with the StepOnePlus™ (Applied Biosystems) system. Total RNA was isolated and checked (as described in 5.16) and reverse transcribed into cDNA (as described in 5.17). Primers were first tested in a PCR with chromosomal DNA as well as with cDNA. If PCR products displayed the expected size, primer efficiency and unique melting temperature were tested using relative standard curve experiments of the StepOne software.

qRT-PCR reactions were performed with the Power SYBR Green Master Mix (Applied Biosystems), 15 ng cDNA and primers at a final concentration of 900nM. The gene *rpoC* (NMB0133) was used as a reference, and expression levels of the target genes were normalized to *rpoC* expression. Negative controls without cDNA template were also tested. In each assay, triplicates of each sample were analyzed. Data analysis was done with the StepOnePlus™ software based on the ΔΔcT method [100]. For each gene, relative quantity (RQ) values were calculated that give the fold change of expression of the investigated gene relative to the respective growth phase or the wild-type.

5.19 Northern Blot

First, 5 µg total RNA was mixed with 15 µl sample buffer (Table 4.13), incubated at 65 °C for 15 minutes and 2 µl RNA loading dye (Table 4.13) were added. If necessary, the same was done for the RNA molecular weight marker I or III. RNA samples were separated in 0.8-1% formaldehyde gel for 5 – 6 hours in 1x MOPS running buffer at 80 V. Afterwards, the gel was incubated for 10 - 20 minutes in DEPC H_2O. In the meantime, the blotting apparatus was build using the Turboblotter Transfer System (*Whatman*) according to the manufacturer's protocol. Overnight transfer was required because of the thickness of the gel (>4 mm). The next day, the membrane was neutralized by incubation in 2x SSC for 5 minutes. The membrane was placed on a fresh sheet of dry 3MM blotting paper and the RNA was fixed via UV light (UV crosslinker 8000, Life technologies) to the membrane. A thirty minutes pre-hybridization step was followed by an overnight hybridization in high SDS buffer with dig-labeled probe at 48 °C. The Dig Wash and Block Buffer set (*Roche*) was used for washing, blocking and developing the membrane (chapter 5.21).

5.20 Generation of DIG-labeled DNA probes

The probe was generated via PCR using the Q5® high-fidelity DNA polymerase. The DNA was purified and eluted in 30 µl ddH_2O. Subsequently, 15 µl of the DNA was denatured in a heating block at 95 °C for 10 minutes and then immediately cooled down on ice. Next, 2 µl of the 10x hexanucleotide mix, 2 µl 10x DIG DNA labeling mix and 1 µl of Klenow enzyme were added. The samples were incubated overnight at 37 °C in an incubator. The next day, 2 µl of 0.2M EDTA, pH 8.0, was added to stop the reaction. Two and a half microliter of 3M sodium acetate, pH 4.5, and 75 µl of ice cold 96% ethanol were added to precipitate the DNA at -80 °C for at least 30 min. After a centrifugation step at 4 °C and 13000 rpm for 15 minutes, the supernatant was removed and washed with 1000 µl ice cold 70% ethanol. Following a second centrifugation step at 4 °C and 13000 rpm for 15 minutes, the ethanol was removed carefully and the pellet was dried via vacuum centrifugation for 5 minutes at medium heat. Finally, the probe was resuspended in 50 µl 1x TE buffer.

To quantify the DNA via dot blot, 1 µl of serial dilutions of the DIG-labeled DNA and a DIG-labeled control DNA were pipetted onto a nylon membrane. The DNA was cross linked to the nylon membrane via UV light (UV crosslinker 8000, Life technologies) for 1 minute. Afterwards, the probes were detected by chemiluminescence with the ChemiDoc

MP system and the concentration was determined based on the comparison with the control DNA of known concentration.

5.21 Detection of DIG-labeled DNA by chemiluminescence

Following Southern or Northern blot, the overnight hybridization solution was carefully removed and the membrane was stored at -20 °C until use. For the detection of hybridized DIG-labeled probes, the membrane was washed two times in stringent washing buffer I at room temperature for 5 min (Table 4.9) and two times in stringent washing buffer II (Table 4.9) at 68 °C for 15 min. All subsequent steps were performed at room temperature on a laboratory shaker. First the membrane was incubated in 1x washing buffer for 5 minutes (Table 4.9), then in 1x blocking solution (Table 4.9) for 30 minutes, and finally in antibody solution (Table 4.9) for another 30 min. The membrane was then washed two times for 15 minutes in 1x washing buffer and was incubated in the detection buffer (Table 4.9) for another 5 minutes. Finally, CSPD working solution was pipetted onto the membrane. After 5 minutes of incubation, the membrane was wrapped into a cling film and left in an incubator at 37 °C for 15 minutes.

Subsequently, the membrane was developed with ChemiDoc MP system according to the manufacturer's instructions.

5.22 cDNA microarray

For transcriptome analysis bacterial cultures from two different strains in two conditions and at four time points were used.

MC58 wild-type and MC58Δ*relA* (#4716) were cultivated in 50 ml $GCBL^{++}$ with and without the addition of 100 µg/ml DL-serine hydroxamate (SHX). The cultures were incubated in a shaker at 37℃ at 200 rpm. Four 100 ml polypropylene conical flaks with a screw cap containing 50 ml $GCBL^{++}$ were inoculated with the preculture of the respective strain and grown in the same medium.

Ten ml pellets were taken from these cultures of 4 different time points:

1. Time point (0): 30' after incubation start and SHX addition
2. Time point (10'): 10 minutes after SHX addition
3. Time point (30'): 30 minutes after SHX addition
4. Time point (300'): 5 h after incubation start

On reaching the desired time point, the cultures were transferred into 50 ml Greiner tubes and centrifuged at 4000 rpm at 4℃. The supernatant was discarded and the pellets were shock frozen in liquid N_2 and stored at -80℃ until further processing. Total RNA was prepared as described in 5.16.

Nonamer random primers (Table 4.28) were purchased from Sigma-Aldrich at a concentration of 0.2 µmol and were adjusted with nuclease-free H_2O to a final concentration of 5 µg/µl. For each RNA, 5 µg were adjusted with nuclease-free H_2O to a final volume of 16 µl. Subsequently, 2 µl of the nonamer primer (5 µg/µl) were added and the mixture was incubated at 70 °C for 5 minutes and chilled on ice for 5 minutes. In the meantime, the reverse transcription reaction mix was prepared as described in Table 5.11.

Table 5.11 *Protocol of Cy3-/Cy5-cDNA transcription*

Cy3-labeling (individual sample RNAs)	Component	Cy5-labeling (pooled RNAs)
5.8 µl	ddH_2O	1.8 µl
8 µl	5x First Strand Buffer	8 µl
1 µl	20 mM dATP	1 µl
0.8 µl	10 mM dCTP	0.8 µl
1 µl	20 mM dGTP	1 µl
1 µl	20 mM dTTP	1 µl
0.4 µl	0.1 M DTT	0.4 µl
1 µl	RNaseOUT™	1 µl
1 µl	Superscript II Reverse Transcriptase	1 µl
2 µl	Cy3/Cy5	6 µl

Twenty two microliter of the mix was pipetted to each RNA sample. After vortexing, brief centrifugation and incubation at room temperature for 10 minutes, samples were incubated for 2 h at 42 °C in a heating block. Afterwards, the samples were incubated to 70 °C for 15 minutes to inactivate the transcriptase and chilled on ice. The samples were incubated for 45 minutes at 37 °C with 2 µl DNase-free RNase to digest the RNA template. Because of the instability of the dyes, all incubation steps were performed in the dark. The labeled cDNA was purified using the illustra AutoSeq G-50 dye terminator removal kit from GE Healthcare (Table 4.4) according to the manufacturer's instructions. Individual sample RNAs were Cy-3 labeled, and the reference RNAs (the pooled RNAs)

were Cy5 labeled. Cy3- or Cy5-labelled cDNA samples were used at a final volume of 40 µl.

Finally, the Cy3- or Cy5-labelled cDNAs were pipetted together and 19.5 µl of 20x SSC, 13 µl of 1% SDS and 17.5 µl of ddH_2O were added to reach a final volume of 130 µl. After incubating the samples for 2 minutes at 95 °C and a brief centrifugation step, the samples were ready for hybridization using spotted 70-mer oligonucleotide microarrays based on the genomic sequence of strain MC58 [101]. Therefore, microarray slides were incubated in the following buffers:

1. 5 minutes in 0.1% Triton X-100
2. 2x for 2 minutes in 1 mM HCl
3. 10 minutes in 0.1 M KCl
4. 1 minute in ddH_2O
5. 15 minutes in blocking solution, at 50 °C
6. 1 minute in dH_2O

All incubation steps, except step 5, were prepared at room temperature and the racks were placed on a stirrer to keep the solutions in motion. Slides were then placed in a 50 ml Greiner-tube and dried by centrifugation in the Heraeus Megafuge 1.0 R at 1600 rpm for 5 min. After this pre-hybridized step, the slides were placed into the hybridization chamber of the TECAN HS 4800 Pro microarray hybridization station. The samples were shortly cooled down on ice and loaded carefully onto the pre-hybridized microarray slides. The hybridization solutions were filled in bottles according to the channels of microarray station, as follows:

1. 2x SSC/0.2% SDS
2. 2x SSC
3. 0.2x SSC
4. 0.1x SSC
5. ddH_2O

The hybridization was carried out using the HS Pro Control Manager Software (TECAN) and the following hybridization program:

1. WASH: 60 °C, Channel: 1, Runs: 1, Wash time: 30 sec
2. SAMPLE INJECTION: 60 °C, Agitation
3. HYBRIDISATION: 52 °C, Agitation frequency: High, Time: 17 h
4. WASH: 60 °C, Channel: 1, Runs: 2, Wash time: 1 min

5. HYBRIDISATION: 52 °C, Agitation frequency: High, Time: 1 min
6. WASH: 23 °C, Channel: 2, Runs: 1, Wash time: 1 min, Soak time: 1 min
7. HYBRIDISATION: 23 °C, Agitation frequency: High, Time: 1 min
8. WASH: 23 °C, Channel: 3, Runs: 2, Wash time: 1 min
9. HYBRIDISATION: 23 °C, Agitation frequency: High, Time: 30 sec
10. WASH: 23 °C, Channel: 4, Runs: 2, Wash time: 30 sec
11. SLIDE DRYING: 23 °C, Channel: 5, Time: 2 min, Final manifold cleaning

After completion of the hybridization reaction, the microarray slides were scanned using a GenePix professional 4200A scanner (MDS Analytical Technologies, Ismaning, Germany), and the images were quantified using the GenePix Pro 7.0 gridding software. The raw files were analyzed including Background correction using the Limma package implemented in R version 2.7.0. The scanned images were analyzed and the resulting .gpr files were further processed using the limma package [102, 103]. Two levels of normalization were performed. Within slide normalization using loess method and between slide normalization using 'R Quantile'. Using the normalized data, expression differences for the various contrasts were computed as follows:

a. MC58_0' – MC58Δ*relA*_0'
b. MC58_10' – MC58_shx_10'
c. MC58_10' – MC58Δ*relA* _10'
d. MC58Δ*relA* _10' – MC58Δ*relA* _shx_10'
e. MC58_30' – MC58_shx_30'
f. MC58_30' – MC58Δ*relA* _30'
g. MC58Δ*relA* _30' – MC58Δ*relA* _shx_30'
h. MC58_240' – MC58_shx_240'
i. MC58_240' – MC58Δ*relA* _240'
j. MC58Δ*relA* _240' – MC58Δ*relA* _shx_240'

The data were further filtered based on the adjusted *p*-value or log2 fold change values to generate a list of differentially regulated genes under the various conditions investigated.

Furthermore, the microarray data were analyzed for overrepresented clusters of orthologous groups (COGs) [104]. COG gene enrichment analysis was used to identify statistically overrepresented COG classes in the tested gene collection. Fisher's exact test [105] was used for enrichment analysis, the false discovery rate (FDR) was determined based on *p*-values from Fisher's exact test and the Holm-Bonferroni multiple testing correction [106].

5.23 Western Blot

12.5% SDS-polyacrylamide gels were cast on the previous day and stored until use at 4 °C. Before gel electrophoresis, protein samples were incubated at 95 °C for 10 min and cooled on ice. Ten to twenty µl of protein samples were applied to the gel and 5 µl of the prestained protein marker (Life Technologies, Table 4.3*)* were pipetted into a slot. The separation of proteins was carried out for approximately 1.5 h in electrophoresis buffer (Table 4.10) at 160 V. Afterwards, the gel was carefully transferred into the semi-dry blotting system and the proteins were transferred to a nitrocellulose membrane by semi-dry electroblotting for 1 h at 30 V in blotting buffer (Table 4.11).

Non-specific binding sites were saturated by incubation of the membrane in 5% low fat milk in washing buffer PBS-T (Table 4.11) for 1 h. The blot was then incubated overnight at 4 °C in a dilution of the primary antibody in 1% low fat in PBS-T. The membrane was washed tree times for 10 min in PBS-T, and the secondary antibody diluted in PBS-T was applied for 1 h at RT. After washing in PBS-T three times for 5 min each, the blot was developed with the Pierce ECL chemiluminescence detection system according to the manufacturer's instructions (Table 4.3).

5.24 Phenotypic characterization

5.24.1 *In vitro* growth experiments

For the *in vitro* growth experiments, strains were grown overnight at 37 °C/5% CO_2 on COS agar plates. The next day, wild-type and mutant strains were inoculated in PPM^+, MMM or MMM supplemented with amino acids and grown at 37 °C at 200 rpm on a shaker for 1 h. Afterwards, meningococci were adjusted to an optical density at 600 nm (OD_{600}) of 0.1 and further cultivated at 37 °C and 200 rpm. Growth was determined by measuring the OD_{600} every hour.

5.24.2 Cell adhesion and invasion assay

Cell adhesion and invasion assays were performed with human Detroit562 (ATCC® number CCL-138™) nasopharyngeal epithelial cell lines. Wild-type strains and the respective mutant strains were grown on COS blood plates overnight at 37 °C/5% CO_2. The bacteria were inoculated into 5 ml $EMEM^{+++}$ and cultured at 37 °C at 200 rpm on a shaker for 1 h. In the meantime, 4x 10^4 adherent Detroit cells per well in a 24-well cell culture plate were washed with 1 ml $EMEM^{+++}$ per well to remove all non-adherent cells. After two washing steps 1 ml $EMEM^{+++}$ was added to each well and the Detroit cells were

checked for viability and confluence under an inverted microscope (Wilovert®, WILL). The bacterial cell number was determined by measuring the optical density at 600 nm and the multiplicity of infection (MOI) was adjusted in $EMEM^{+++}$ to 20. The Detroit cells were infected for 4 hours at 37 °C with 5% CO_2. Additionally, the number of CFUs per well was determined by adding the same volume of bacterial suspensions used for infection into 1 ml 1x PBS and followed by plating of serial dilutions in triplicates to yield the 'seeded' bacteria.

After 4 hours of infection, the CFU in the supernatant was determined as described above. The supernatant was carefully removed in the remaining wells and all wells were washed with $EMEM^{+++}$. One group of wells, which were used to determine the number of 'invasive' bacteria, was treated with 0.2 mg/ml gentamicin for 1 h to kill the extracellular bacteria. The other group of wells, which were used to assess the number of 'adherent' bacteria, was treated with 1% saponin for 15 minutes to break up the Detroit cells and the CFU was determined accordingly. After 1 h of gentamicin treatment at 37ºC, the wells were washed twice with 1 ml $EMEM^{+++}$ and the same procedure as for the 'adherent' bacteria was applied to the wells for the invasive bacteria. The CFU of the 'adherent' bacteria was compared to the CFU of the 'seeded' bacteria. Likewise, the CFU of the 'invasive' bacteria was compared to the CFU of 'adherent' bacteria for each strain.

5.24.3 **Static biofilm assay for *N. meningitids***

Bacteria were grown over 8-10 h at 37 °C and 5% CO_2 on COS plates. Subsequently, the meningococci were resuspended in 5 ml of the biofilm medium (10% PPM^{+}, 50% $NDM^{+/-}$ and 40% 1x PBS) and were adjusted to an OD_{600} of 0.1. Hundert µl of the bacterial suspension was seeded per well in a 96-well microtiter plate and incubated at 37 °C, 5% CO_2 overnight. After 16 h the remaining medium was removed. To stain the adherent bacteria, 100 µl of 0.05% crystal violet was added for 10 minutes at room temperature. After two steps of washing with 200 µl 1x PBS per well, the crystal violet stain of the biofilm was dissolved with 100 µl 96% ethanol per well, incubated for 20 minutes at room temperature and quantified by measuring optical density at 595 nm in a spectrometer (Multiskan® EX, Thermo Scientific).

5.24.4 **Collection and processing of human specimens**

For the saliva and blood samples, donors were selected based on not having a history of vaccination against *N. meningitidis* serogroups A, B, C, W and Y, not having taken any antibiotics within 5 days prior sampling and not currently being carriers of meningococci. The human saliva samples were collected from the donors after stimulation with CRT paraffin. The collected saliva was centrifuged at 4000 rpm for 10 min and followed by filter sterilization using 0.2 µm filters. The human CSF samples were obtained from the routine diagnostic laboratory at the Institute for Hygiene and Microbiology of the University of Würzburg and tested for sterility and the absence of antibiotics as well as leucocytes according to established standard operating procedures. The CSF and saliva samples were pooled and stored at -20 °C. Prior to the experiment, the pooled CSF samples were gassed with CO_2 and pH was controlled to be in the physiologic range between pH 7.0 – 7.5. Heparinized human venous blood from three healthy donors (three males, aged between 30 and 50 years) was drawn fresh on the day of the experiment and was used within thirty minutes of collection.

5.24.5 ***Ex vivo* survival assays**

For the *ex vivo* survival assay bacterial strains were grown in PPM^+ medium to mid logarithmic phase (OD_{600nm} ~0.5 – 0.6). Afterwards, 1 ml of the culture was harvested by centrifugation and after washing with 1x PBS, the bacterial pellet was resuspended in 1 ml of 1x PBS. Ten microliter of this bacterial suspension corresponding to ~10^6 cfu/ml were inoculated into 1 ml of human saliva, blood or CSF and incubated at 37°C with shaking at 200 rpm. Hundert mircoliters were taken out after 30 minutes, 60 minutes and 120 minutes and serial dilutions were plated out on COS agar plates and the CFU estimated in duplicates. Whereas *ex vivo* infections using whole venous blood were performed individually, *ex vivo* infection experiments with human saliva and human CSF were performed using pooled saliva and pooled CSF samples as described above.

5.25 (p)ppGpp Extraction and Quantification

Strains were grown overnight at 37 °C and in 5% CO_2 on COS agar plates. The next day, bacterial cells from the third fraction were inoculated in PPM+ medium and grown at 37 °C and 200 rpm for 45'. Subsequently, bacterial cells were adjusted to an OD_{600} of 0.1 in 50 ml PPM^+ and grown at 37 °C and 200 rpm. The cells were collected by a centrifugation step at 4000 rpm for 10 minutes at 4 °C when the OD_{600} reached 0.5-0.6

for mid logarithmic phase (1.5 h) and <1.6 for late logarithmic phase (4-5 h). The pellets were frozen in liquid nitrogen and stored at -80 °C. The next day, the pellets were resuspended in 1.25 ml of ice-cold 2M formic acid, chilled on ice for 30 minutes and afterwards the samples were centrifuged at 4 °C and 4000 rpm for 10 minutes. The supernatant was filtered through a 0.2 µm filter and stored at -20 °C until analysis. The samples were sent on dry ice to Prof. Dr. Anke Becker (LOEWE Center for Synthetic Microbiology Marburg) for ppGpp analysis via High Performance Liquid Chromatography (HPLC). Each experiment was done in duplicate.

5.26 Computational analyses

For general data analysis and presentation Microsoft Excel 2013 was used. The Primer BLAST website (http://www.ncbi.nlm.nih.gov/tools/primer-blast/) of the National Center for Biotechnology Information (NCBI) was used for designing oligonucleotides. SnapGene 2.8 and Serial Cloner 2.6 were used to construct and visualize plasmids or DNA sequences, respectively. BioEdit 7.2.5 including CUSTALW was used for DNA sequence visualization, analysis and multiple sequence alignments. The NCBI BLAST website (http://blast.ncbi.nlm.nih.gov/Blast.cgi) of the National Center for Biotechnology Information (NCBI) was used for similarity searches against nucleotide and protein databases. Pfam 29.0 (http://pfam.xfam.org/) was used to assign protein domains and families. Operon predictions were based on the DOOR database [107] and promoter predictions were carried out using the online software tool BPROM from Softberry [108]. Artemis and the Artemis Comparison Tool (ACT) were used to visualize and compare genome sequences or retrieve information about gene localization. The microarray slides were analyzed using the GenePix Pro 7 software. Table 5.12 lists the programs used in this study.

Table 5.12 *Software programs used in this study*

Program	**Application**	***Developer/Source***
Excel 2013	Statistics and spreadsheet analysis	*Microsoft*
GenePix Pro 7	Microarray slides analysis	*Molecular Devices*
SnapGene 2.8	Plasmid construction	*GSL Biotech LLC*
Serial Cloner 2.6	DNA sequence analysis	*Serial Basic*
BioEdit 7.2.5	Sequence alignment and analysis	*Ibis Biosciences*, [109]
Artemis 16.0.0	Genome browsing	*Wellcome Trust Sanger Institute*, [21]
ACT 13.0.0	Pairwise comparison of two or more DNA sequences	*Wellcome Trust Sanger Institute*, [110]
PowerPoint 2013	Creating graphical figures or illustrations	*Microsoft*
Word 2013	Creating this work	*Microsoft*
BioCyc	Metabolic pathway construction	*Caspi et al.*, *2014* [111]
RNA fold	RNA secondary structure prediction	*Institute for Theoretical Chemistry*, [112]
BPROM	Promoter prediction	*Softberry*, [108]
'R' limma package	Microarray analysis	*R Core Team,* [102, 103]
Venn Diagram	Construction of venn diagrams	*Bioinformatics & Evolutionary Genomics*

6 Results

6.1 The stringent response in *N. meningitidis*

6.1.1 **Both strains express an almost identical RelA protein**

The meningococcal *relA* gene is predicted to encode a protein of 737 amino acids with a high similarity (42% amino acid identity) to the *E. coli* RelA protein. Pfam analysis detected four significant domain matches (Figure 6.1 A+B): An HD (PF13328, aa 40 to 201), a RelA/SpoT (PF04607, aa 260 to 371), a TGS (PF02824, aa 414 to 473) and an ACT (PF13291, aa 659 to 736) domain.

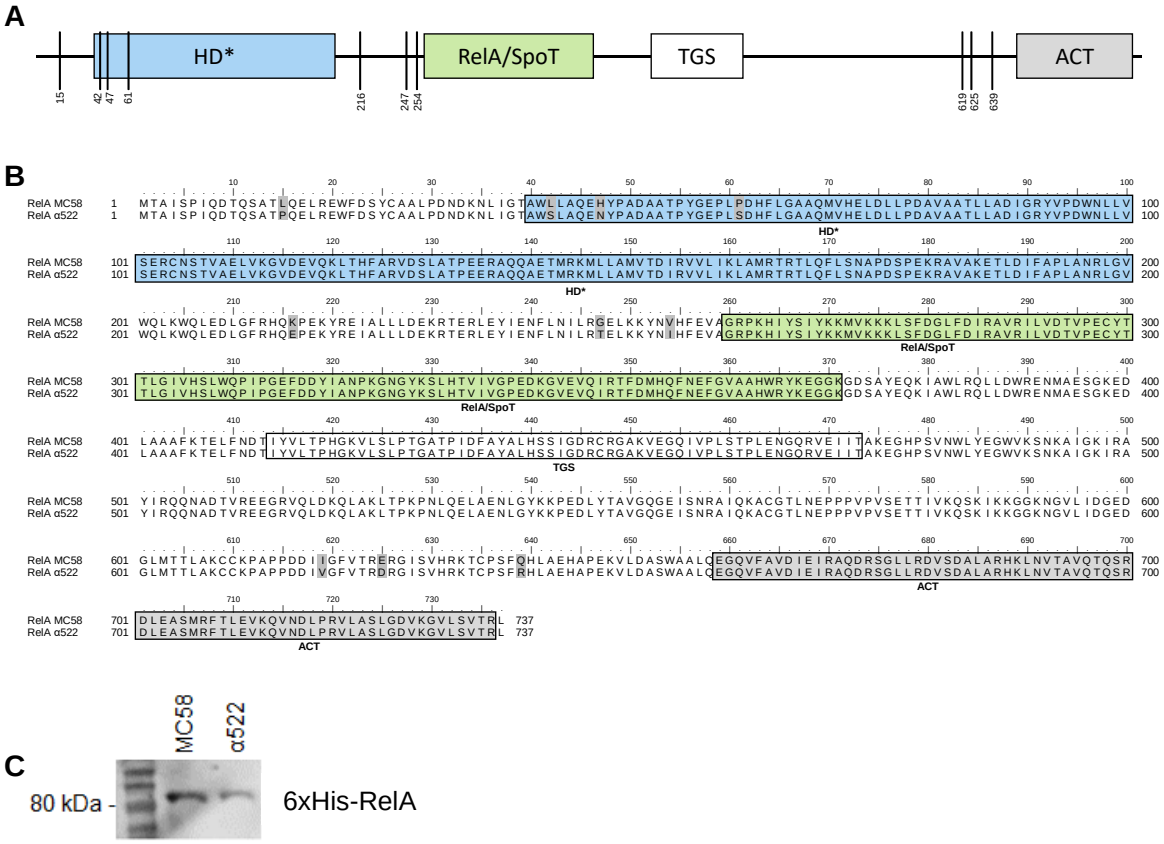

Figure 6.1 Sequence alignment of RelA, the predicted (p)ppGpp synthetase of MC58 and α522

A. Schematic representation of the meningococcal RelA domain structure (predicted by Pfam). Four functional regions have been predicted: the (p)ppGpp hydrolase domain (HD,*inactive), the (p)ppGpp synthetase domain (RelA/SpoT) and the TGS and ACT regulatory domains. Black vertical lines with residue numbers indicate mismatching amino acids of strain MC58 and strain α522.
B. Amino acid sequence alignment of strain MC58 and strain α522 RelA generated by CUSTALW, [109]. Colored boxes represent the predicted domains of RelA. Mismatches are highlighted in dark gray.
C. Western blot analysis of MC58 and α522 *relA* 6xHis-tagged protein lysates after 4 h of incubation in PPM$^+$.

The HD and RelA/SpoT domains together form the amino-terminal domain (NTD), whereas the TGS and ACT domains are both part of the carboxy-terminal domain (CTD) [113]. The HD domain named after the conserved catalytic residues histidine (H) and aspartate (D), contains the (p)ppGpp hydrolysis active site [114]. Notably, this metal dependent phosphohydrolase domain HD was shown to be inactive (indicated as * in Figure 6.1 A) in *E. coli* [88, 114, 115] Sequence analysis indicated that RelA of *N. meningitidis* might also not contain a catalytically active HD domain, since the predicted catalytic residues histidine and aspartate are not found within in this region (Figure 6.1 B). This suggests that, like in *E. coli*, meningococcal RelA is a monofunctional (p)ppGpp synthetase as it contains a RelA/SpoT domain. This region is found in RelA and SpoT proteins and contains the (p)ppGpp synthetase function. Pfam analysis further identified two other domains with putative regulatory function. The TGS domain, named after ThrRS, GTPase and SpoT, is a small domain which probably possess a beta-sheet structure and is a possible nucleotide-binding region [116]. The ACT (aspartokinase, chorismate mutase and TyrA) regulatory domain at the C-terminal end of the enzyme which presumably binds to amino acids and might controls its activity [88]. Although the exact molecular functions of the TGS and ACT domains remain unclear, it has been suggested that these domains regulate the enzymatic activities of the NTD [117].

The RelA amino acid sequence of MC58 and α522 share 99% identity, and CLUSTALW protein sequence alignment of MC58 and α522 RelA (Figure 6.1 B) identified only 10 mismatches. Three of them are inside the putative non-functional HD domain while the remaining mismatches are located between domains (Figure 6.1 A+B). To check if RelA is expressed in MC58 and α522, *relA* was flagged with a 6xHis-tag at the C-terminal end. Strains were grown in PPM^+ for approximately 4 h and protein lysates were analyzed with Western blot. As depicted in Figure 6.1 C, both strains express a RelA protein having the predicted size of 83 kDa in good agreement with the genome annotation.

6.1.2 **RelA is functional and the sole ppGpp synthase in *N. meningitidis***

In order to analyze the stringent response experimentally, *relA* single and *relAspoT* double mutants were constructed in the genetic background of *N. meningitidis* strain MC58 and α522. The deletion mutants were generated by replacing the entire coding sequence with a kanamycin or a chloramphenicol resistance cassette (chapter 5.13.1). The correct insertion of the resistance cassettes was confirmed by PCR and sequencing as well as by Southern blot analysis. Figure 6.2 depicts the results from PCR analysis (A+B) and Southern blot results (C+D).

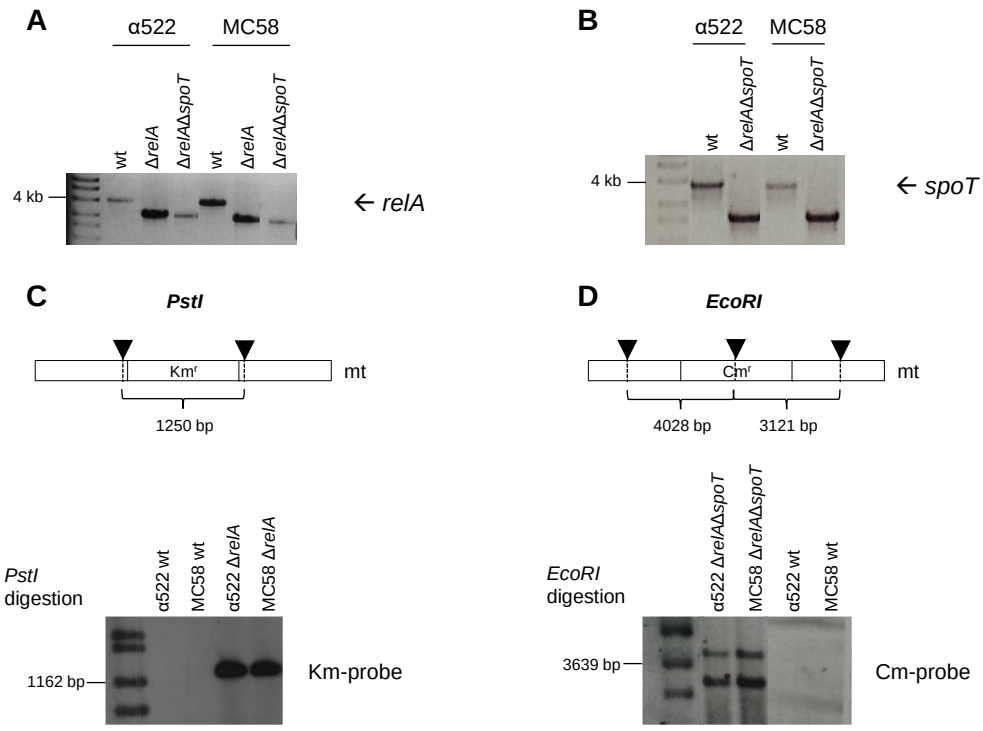

Figure 6.2 PCR and Southern blotting verification of knock-out mutants

Genomic DNA of wild-type and corresponding mutant strains were used as templates for PCR verification (A+B).
A. Each knock-out mutant produces a smaller band (~3000 bp) from the targeted *relA* gene than the wild-types (~4000 bp). The primers used for PCR amplification are listed in Table 4.28.
B. Each knock-out mutant produces a smaller band (~2200 bp) from the targeted *spoT* gene than the wild-types (~3600 bp). The primers used for PCR amplification are listed in Table 4.28.
C. Schematic representation of the *PstI* genomic DNA digestion at the *relA* locus and Southern blot analysis to verify the genotypes of α522Δ*relA*::Km^r and MC58Δ*relA*::Km^r. The genomic DNAs of the mutant and the wild-type strains were digested with *PstI* and then used for Southern blot hybridization with the kanamycin resistance gene as the probe. The size of the expected knock-out fragment is 1250 bp.
D. Schematic representation of the *EcoRI* genomic DNA digestion at the *spoT* locus and Southern blot analysis to verify the genotypes of α522Δ*relA*::Km^{r}Δ*spoT*::Cm^r and MC58Δ*relA*::Km^{r}Δ*spoT*::Cm^r. The genomic DNAs of the mutant and the wild-type strains were digested with *EcoRI* and then used for Southern blot hybridization with the chloramphenicol resistance gene as the probe. The size of the expected knock-out fragments are 4028 bp and 3121 bp.

To examine whether differences in the coding sequence between MC58 and α522 influence the catalytic activity of RelA ppGpp levels were assessed in wild-type, *relA* mutant as well as *relAspoT* double mutants in both strains during growth in PPM+ medium. The ppGpp production was analyzed *in vitro*, in the mid logarithmic and in the early late logarithmic growth phase (Figure 6.3).

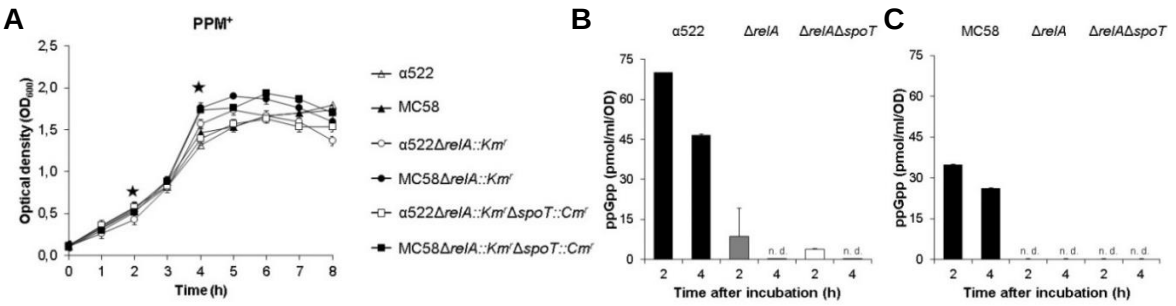

Figure 6.3 Analysis of *N. meningitidis relA* and *relAspoT* mutants for ppGpp production

A. Growth of wild-type, *relA* and *relAspoT* mutant strains grown in PPM+ medium at 37ºC over a time course of 8 h. Time points marked with an asterisk indicate times of sampling for ppGpp analysis presented in B and C.
B+C. ppGpp accumulation in wild-type strains, *relA* single and *relAspoT* double mutant strains grown at 37° C in PPM+ medium. ppGpp (pmol/ml/OD) values from one of three similar experiment are shown. n. d. = not detectable

As depicted in Figure 6.3 A, *relA* as well as *relAspoT* knock-out strains had no detectable growth defect in a rich medium (PPM^+) compared to the wild-type in both strains, indicating that in a rich growth medium ppGpp synthesis and the stringent response are dispensable for growth.

As measured by HPLC analysis, both wild-type *relA* alleles were also catalytically active with similar ppGpp levels in the mid compared to the late logarithmic growth phase, although the ppGpp levels seemed to be almost two-fold higher in both growth phases in strain α522 than in strain MC58 (Figure 6.3 B+C). Interestingly, ppGpp synthesis was almost completely abolished in the *relA* mutant strains, indicating that SpoT might have no catalytic active site for ppGpp production. Similar to *E. coli* (p)ppGpp^0 strains, the meningococcal *relAspoT* double mutants lacked all ppGpp synthesis.

In order to determine transcriptional differences between the wild-type strains MC58 and α522, bacteria were grown in PPM^+ and after 2 h and 4 h incubation at 37ºC samples were analyzed via qRT-PCR (Figure 6.4).

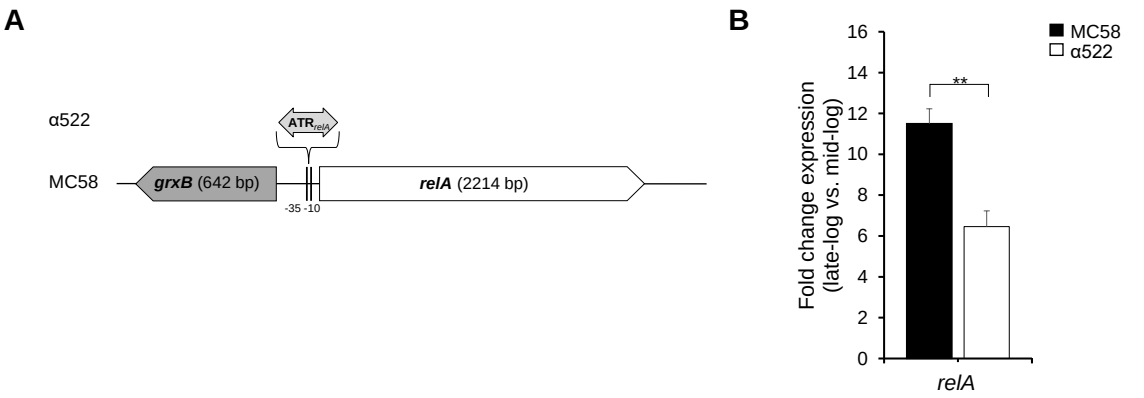

Figure 6.4 *relA* locus and expression differences between strain α522 and MC58

A. Schematic drawing of the *relA* locus in strain MC58 and α522. Sequence comparisons revealed that a MITE (ATR_{relA}) is integrated upstream of *relA* in strain α522. The promoter region of *relA* is indicated by two vertical black lines (-35, -10).
B. Transcription was analyzed by qRT-PCR after incubation in either mid logarithmic or late logarithmic growth phase. Bacteria were grown in rich medium (PPM+), at 37 °C. After approximately 2 h (mid logarithmic) and 4 h (late logarithmic) growth samples were analyzed. The results show the fold change in the mRNA levels of the *relA* gene in strains MC58 and α522. Expression levels were normalized to those of the *rpoC* gene. The fold change expression was calculated by dividing the mRNA levels from mid logarithmic bacteria to those from late logarithmic bacteria. The mean and standard deviation from three independent experiments are given (Welch's *t*-test, $**p<0.01$).

The transcription of *relA* is enhanced during the transition from the mid logarithmic to the late logarithmic growth phase (> 2-fold expression level differences late vs. mid logarithmic growth phase) and depends on the genetic background (about 2-fold difference, $p<0.01$, Welch´s two-sample t-test). In *N. meningitidis* MC58 and α522 the expression of *relA* was about 12- and 6-fold increased in late compared to mid logarithmic growth phase, respectively. These results suggest that *relA* transcription is growth phase dependent and might be differentially regulated in both genetic backgrounds.

6.1.3 SpoT is essential in *N. meningitidis*

In contrast to RelA, SpoT (and also DksA) have identical coding sequences and promoter regions in both strains. In contrast to RelA, SpoT can also hydrolyze (p)ppGpp to GTP and GDP, and was found to be essential in *E. coli* [118] and *N. gonorrhoeae* [119]. In line with these observations, *spoT* knock-out mutants could not be generated in MC58 as well as in α522. One presumable *spoT* 'knock-out' clone in MC58 had a deletion of 11 bp right upstream of the *relA* catalytic domain as revealed by sequencing of the *relA* gene (Figure 6.5 A).

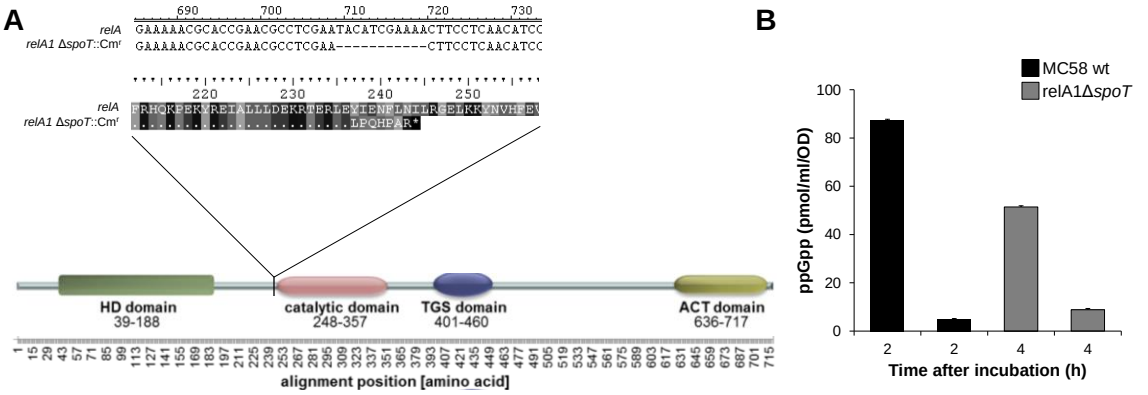

Figure 6.5 Analysis of *N. meningitidis* MC58 ***relA1ΔspoT*** mutant for ppGpp production

A. Sequence analysis of the 11 bp deletion in *relA* of the mutant strain MC58 ***relA1ΔspoT***. The position of a premature translational stop codon prior to the RelA catalytic domain in a Δ*spoT*::Cm^r mutant is indicated by a vertical line. The truncated RelA1 protein and the corresponding deletion leading to the frameshift in the Δ*spoT*::Cm^r mutant strain are indicated, each aligned with the corresponding MC58 wild-type sequences.
B. ppGpp accumulation in MC58 wild-type and in corresponding ***relA1ΔspoT*** mutant strain grown at 37 °C in PPM$^+$ medium. Samples were analyzed after 2 h and 4 h via HPLC. Values are averages of ppGpp (pmol/ml/OD) and standard deviation.

Consequently, the supposed knock-out mutant is functionally a double knock-out mutant of *relA* and *spoT*. This suggests that SpoT is essential for the hydrolyzation of (p)ppGpp as in *E. coli* and that too high levels of (p)ppGpp might be toxic for the meningococcal cell as was shown for *E. coli* [120]. This conclusion is supported by the observation that the ppGpp levels were drastically decreased in strain MC58*relA*1Δ*spoT* compared to the wild-type strain (Figure 6.5 B).

6.1.4 **RelA is likely required for amino acid biosynthesis**

In order to determine the functional role of the meningococcal RelA in response to amino acid starvation, wild-type, *relA and relAspoT* knock-out strains were grown in MMM with or without the addition of external amino acids (Figure 6.6 A+B).

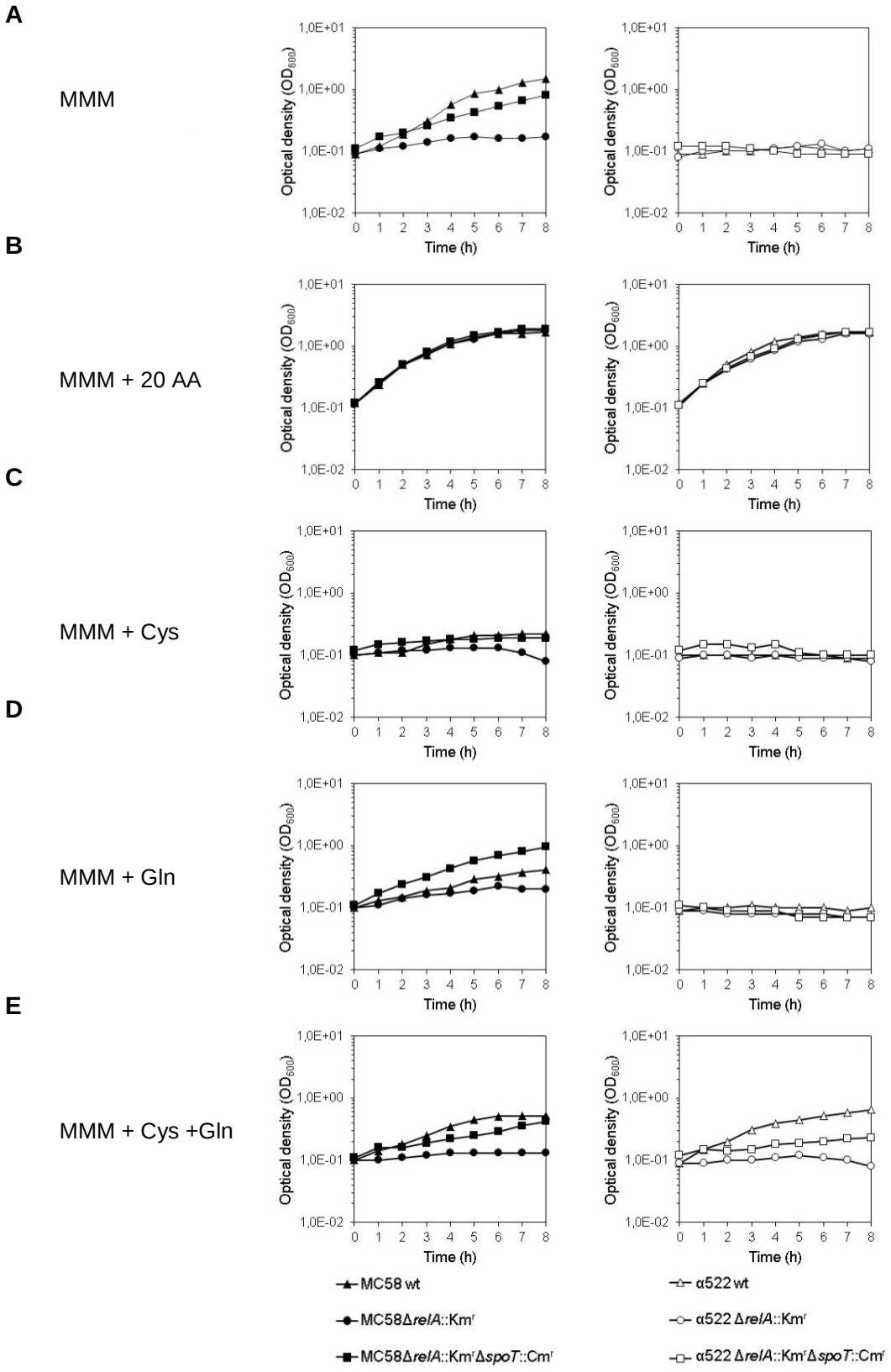

Figure 6.6 Amino acid dependent growth of wild-type and stringent response mutants

A-E. MC58 wild-type and *relA, relAspoT* mutant strains (on the left side) and strain α522 wild-type with corresponding *relA, relAspoT* mutant strains (on the right side) were grown in MMM (A), all 20 amino acids combined in MMM (B), MMM supplemented with 2.1 mM L-cysteine (C), MMM with 1 mM L-glutamine (D) and MMM with both amino acids (E). Over a time course of 8 h at 37 °C the optical density (OD_{600}) was determined every hour.

In MMM, the MC58 wt and the *relAspoT* mutant strains were able to grow, indicating that MC58 provides the entire set of genes necessary for amino acid biosynthesis. MC58 deficient in *relA* could not grow in MMM, indicating that *relA* is required for growth in MC58 in the absence of amino acids. Interestingly, the *relAspoT* double mutant regained the capacity to grow. This phenomenon is also described as the 'relaxed control' in *E. coli* [121]. In contrast to MC58, all strains of α522 were unable to multiply in MMM, suggesting that α522 per se has a growth defect in absence of amino acids and is impaired in the synthesis of at least one of them (Figure 6.6 A). When cultivated in MMM supplemented with 20 amino acids all mutants were able to grow like the respective wild-type, confirming that α522 has a defect in amino acid biosynthesis and that *relA* is involved in the adaption to amino acid starvation (Figure 6.6 B).

6.1.5 **Strain α522 differs from strain MC58 in amino acid metabolism**

In contrast to MC58 strain α522 was not able to grow in MMM but in MMM supplemented with 20 amino acids and in rich medium PPM^+ and former investigations showed that the requirement for cyst(e)ine is also known in other neisserial species [122]. Therefore, strain α522 was tested for its auxotrophy with different combinations of amino acids. Since previous experiments (data not shown) showed that cyst(e)ine must be supplemented in the medium for sufficient growth, cysteine was tested alone as well as in combination with the other 19 amino acids (Figure 6.7). Since MC58 and α522 were both able to grow in the chemically defined medium RPMI 1640 (data not shown), the concentrations of all amino acids, except L-glutamine, L-cysteine and L-alanine, were taken from the media formulation of the RPMI 1640 medium (*Thermo Fisher*, Table 4.25). The amino acid concentrations for L-glutamine and L-cysteine were taken according to the PolyVitex formulation (Table 4.16) and L-alanine according to the average overall amino acid concentration from the RPMI 1640 medium.

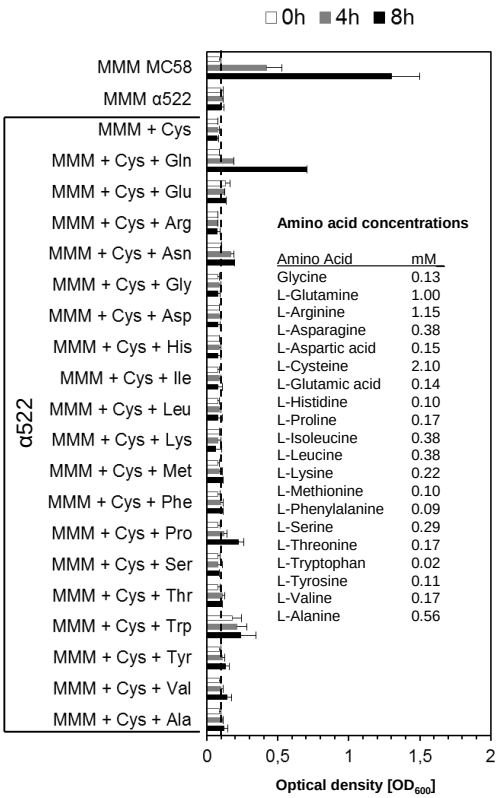

Figure 6.7 Growth of strain α522 in MMM supplemented with different combinations of amino acids

Bar plot depicting the optical density (OD600) at 0 h, 4 h and 8 h of growth in MMM supplemented with different combinations of amino acids as indicated on the ordinate. The insert gives the amino acid concentrations used in the growth experiments, and the error bars the standard error from three independent measurements. Strain MC58 was used as positive control as it is known to grow in MMM[95].

For the *in vitro* growth experiments strain α522 was incubated either in MMM or MMM supplemented with different combinations of amino acids and the optical density was measured at 0 h, 4 h and 8 h. As shown in Figure 6.7 supplementation of MMM with the combination of L-cysteine and L-glutamine restored growth of strain α522 comparable to MC58 in MMM. All other amino acid combinations could not restore the ability to grow in MMM, indicating that strain α522 has a defect in L-cysteine and or L-glutamine biosynthesis. Thus, the growth of the stringent response mutant strains was further characterized in MMM supplemented with glutamine and cysteine (Figure 6.6 C-E).

In both strains, the *relA* mutants were severely impaired in growth in the absence of all 20 proteinogenic amino acids (Figure 6.6 A). Surprisingly, L-cysteine had a growth-inhibitory effect in the MC58 wild-type as well as in the *relAspoT* mutant when compared to growth in MMM without amino acids (Figure 6.6 C). In contrast, the growth inhibitory effect of L-glutamine could only be observed in the wild-type but not in the *relAspoT* mutant (Figure 6.6 D). For the MC58 wild-type strain the growth-inhibitory effect of

L-cysteine could partially be restored by the presence of L-glutamine (Figure 6.6 E). Similar to the wild-type, the stringent response (*relA, relAspoT*) mutants in α522 were unable to grow in MMM and in MMM supplemented with either L-cysteine or L-glutamine alone (Figure 6.6 A+C+D). When the medium contained both L-glutamine and L-cysteine, the wild-type was able to grow and to a lesser extent also the *relAspoT* double mutant (Figure 6.6 E). As a control, all strains were able to grow in MMM supplemented with all 20 amino acids (Figure 6.6 B).

These data indicate that (i) α522 is auxotrophic for L-cysteine and L-glutamine, (ii) RelA is required for growth in the absence of external amino acids in strain MC58, and (iii) there is a complex regulatory interplay between the stringent response pathway and L-cysteine as well as L-glutamine metabolism.

6.1.6 Gene comparison of selected enzymes involved in cysteine and glutamine biosynthesis

The detailed bioinformatic analysis of putative proteins involved in cysteine and glutamine metabolism in *N. meningitidis* α522 and MC58 was based on the BioCyc Database Collection (biocyc.org, [111]). Genes important in the different biosynthetic pathways were selected, analyzed and similarities between both strains were assessed using BLASTP. Genome comparisons revealed that strain α522 encodes the same repertoire of enzymes as MC58 for the biosynthesis of L-cysteine and L-glutamine, but a more detailed analysis including also nucleotide sequence alignments of 100 bp upstream regions uncovered differences which might affect L-cysteine and L-glutamine biosynthesis. Figure 6.8 represents selected genes involved in cysteine and glutamine biosynthesis and shows similarity of the proteins in the respective pathways.

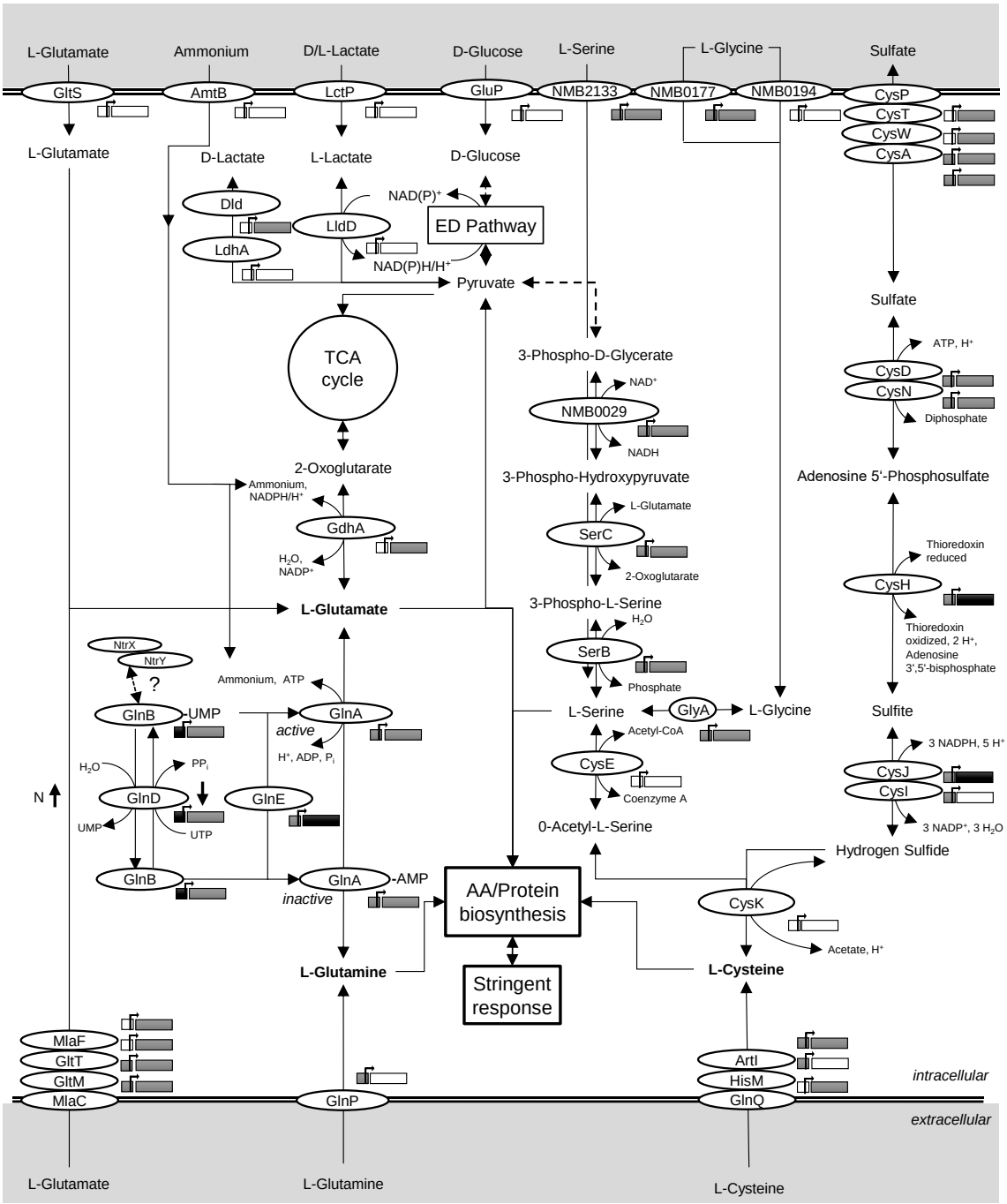

Figure 6.8 Putative metabolic pathways of L-cysteine and L-glutamine in *N. meningitidis*

Genes for the amino acid biosynthetic pathways (according to biocyc.org) of 21 amino acids were compared. Only biosynthetic pathways starting from an amino acid or a central pathway were analyzed and no regulatory or transporter/uptake genes were included. 'White' proteins indicate an BSRP of 1, 'grey' enzymes share a bit score between 0.957 - 1 and 'black' proteins have a bit score below 0.957. Hundred bp 5'-UTR of each protein were analyzed shown by the different colored boxes in front of each gene. A 'white' box indicates 100% identity, a 'grey' box indicates mismatches within the sequence (40%-99% sequence identity) and a 'black' box indicates no similarity (expected threshold of 10).

A total of 90 genes involved in the 21 amino acid biosynthetic pathways were found and compared on the basis of BLASTP bit scores. BLASTP bit score ratios (BSRP) were calculated using the MC58 coding sequence as query and either the best hit coding

sequence from α522 (best hit) or MC58 (self-hit) as subject sequences. To estimate the average sequence similarity between MC58 and α522, 1600 coding sequences annotated in MC58 were compared to α522. The comparison yielded an average of 0.957. Only glutamine- and cysteine biosynthetic pathways included genes with a BSRP below 0.957. All other amino acid biosynthetic pathways showed a BSRP above 0.957.

Closer analysis revealed several differences in the coding sequences and in the promoter regions of the proteins involved in the biosynthesis of cysteine between both strains. The biosynthetic pathway of L-cysteine starts with the uptake of extracellular sulfate into the cell by proteins of the *cysTWA* operon and *cysP*. Figure 6.9 compares the schematic organization of the *cysTWA* locus of MC58 and α522.

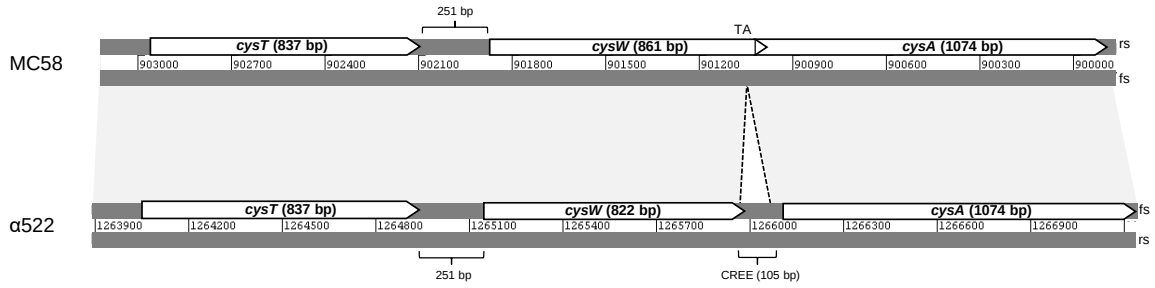

Figure 6.9 Schematic organization of the *cysTWA* locus in MC58 and α522

Depicted is the comparison of the genomic organization of the *cysTWA* locus in strains MC58 and α522, using ACT (Artemis Comparsion Tool from *Sanger,* [110]). The coding sequences of *cysT* from both strains share a high amino acid identity of 99%, cysW 99% (only the first 273 residues) and cysA 98% identity. In MC58 the termination codon of *cysW* is overlapping (4 bp) with the next ORF from *cysA*. In α522 an integration of a CREE (105 bp) next to the end of *cysW* (the TA indicates as the insertion region) leads to a stop codon and shortens the protein by 13 amino acids. Abbreviations: fs, forward strand; rs, reverse strand.

Whereas *cysT* and *cysA* have a high amino acid identity of 99% and 98%, *cysW* is varying. In contrast to strain α522 the termination codon of *cysW* in strain MC58 is overlapping (4 bp) with *cysA.* In strain α522 a CREE (105 bp in length) was integrated at the 3'-end of *cysW,* which leads to a stop codon and shortens the protein by 13 amino acids. Thus the *cysW* gene of MC58 encodes for a protein of 286 amino acids the $CysW_{α522}$ protein consists only of 273 residues.

To test whether the neisserial *cysWA* is transcribed in one transcription unit or if the insertion of the CREE element in strain α522 functions as a terminator [123], RT-PCR experiments were performed (Figure 6.10).

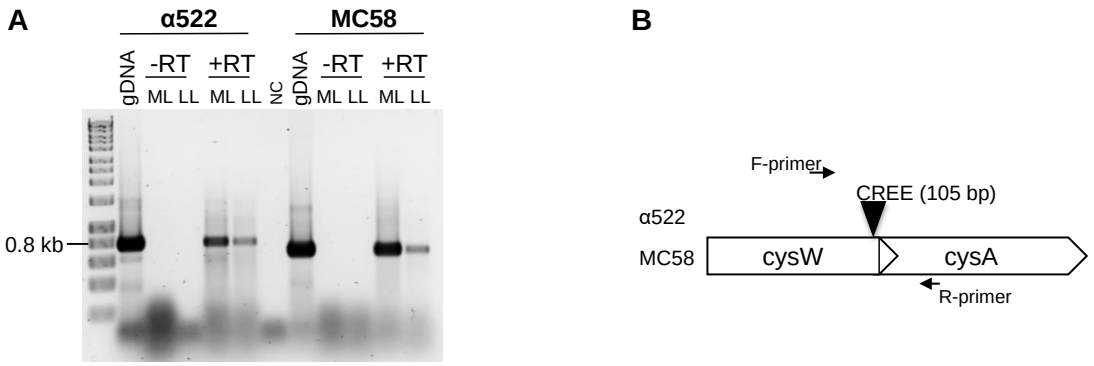

Figure 6.10 CysWA consist of one transcription unit

A. Results observed from RT-PCR experiments. Bacteria were grown in PPM$^+$. RNA samples from mid (ML) and late logarithmic (LL) growth phase were isolated and transcribed. RNA (-RT), cDNA (+RT) and genomic (g)DNA were used as templates in PCR with primers for a putative *cysWA* amplicon. Abbreviations: NC, negative control.
B. Schematic representation of the RT-PCR experiment from A. Note that the illustration is not to scale. The expected PCR product is in MC58 600 bp and in α522 700 bp in length.

The RT-PCR results revealed that in both strains the genes *cysWA* appear to be transcribed as an operon in mid and also in late logarithmic growth phase (Figure 6.10 A). The integration of the CREE at the end of *cysW* in strain α522 did not lead to a transcription termination [123], since the PCR product included parts of *cysW* and *cysA* (Figure 6.10 B). However, the translational coupling of *cysA* and *cysW* might be different in both strains. It cannot be excluded that the smaller *cysW* protein of in strain α522 might be functionally impaired due to the insertion of the CREE and might affect the transport of sulfate into the cell.

The uptake of sulfate is followed by its reduction. The *cysGHDNJI* operon includes genes important for the reduction of sulfate to sulfide [124], which is an essential step for the acquisition of sulfur and the biosynthesis of cysteine. Genome wide comparisons already demonstrated that in contrast to α522 MC58 has a duplication of the *cysGHDNJI* operon [19].

Moreover, the analysis revealed that *cysH* coding for a phosphoadenosine phosphosulfate reductase (PAPS) is among the least conserved genes within the amino acid biosynthetic genes and with a BSRP below the average BSRP (0.957). $CysH_{\alpha522}$ shares only 91% amino acid identity with $CysH_{MC58}$. Twelve of 25 amino acid mismatches were found inside the PAPS domain (PF01507) (Figure 6.11), which could affect the transformation from adenosine 5'-phosphosulfate to sulfite.

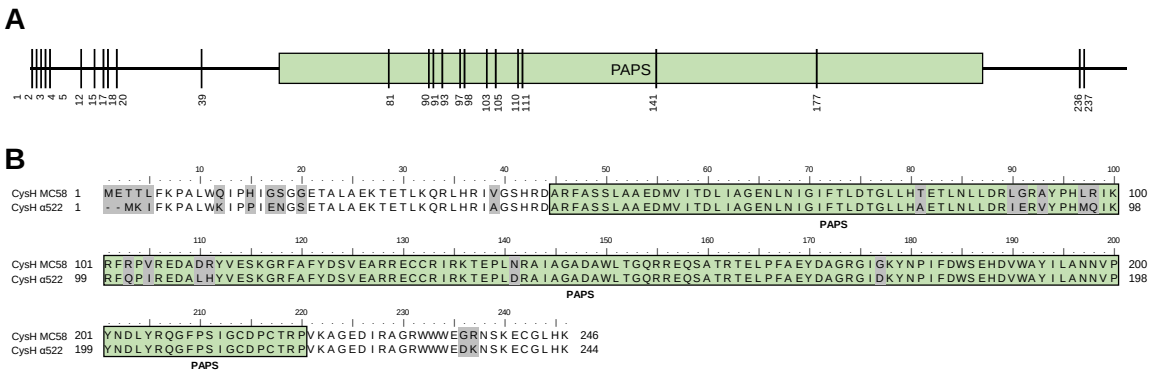

Figure 6.11 Sequence alignment of CysH from MC58 and α522

A. Schematic representation of the CysH domain structure (predicted by Pfam). One functional region, a 'PAPS' domain (PF01507) has been predicted. Black vertical lines with residue numbers indicate a mismatching amino acid of strain MC58 and strain α522.
B. Amino acid sequence alignment of strain MC58 and strain α522 CysH generated by CUSTALW, [109]. Colored boxes represent the predicted domain (from A) of CysH. Mismatches are highlighted in gray.

Also CysJ is among the least conserved genes within the amino acid biosynthetic genes and with a BSRP below the average BSRP (0.957). $CysJ_{α522}$ shares only 95% amino acid identity with $CysJ_{MC58}$. Twenty-seven of 31 amino acid mismatches were found in the predicted domains. Five mismatches were located within the flavodoxin domain (PF00258), 13 in the FAD binding domain (PF00667) and 6 in the oxidoreductase NAD-binding domain (PF00175) (Figure 6.12), potentially affecting the reduction of sulfate to sulfide.

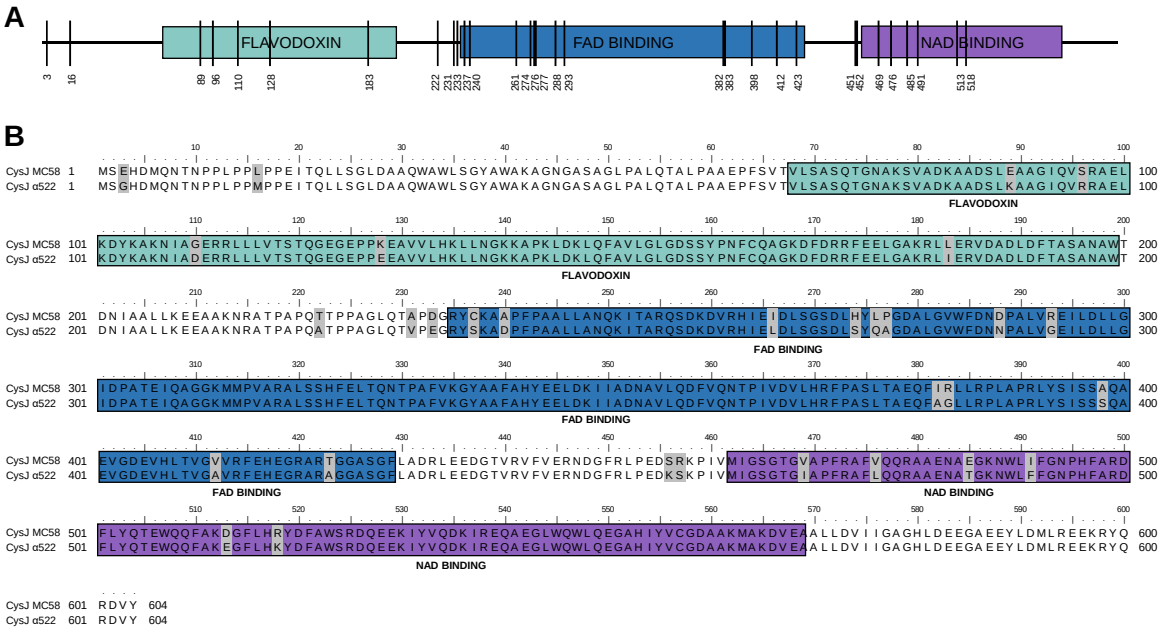

Figure 6.12 Sequence alignment of CysJ from MC58 and α522

A. Schematic representation of the CysJ domain structure (predicted by Pfam). Three functional regions have been predicted: a 'FLAVODOXIN' domain (PF00258), a 'FAD BINDING' (PF00667) domain and a 'NAD BINDING' domain (PF001755). Black vertical lines with residue numbers indicate a mismatching amino acid of strain MC58 and strain α522.
B. Amino acid sequence alignment of strain MC58 and strain α522 CysJ generated by CUSTALW, [109]. Colored boxes represent the predicted domains (from A) of CysJ. Mismatches are highlighted in gray.

The analysis of the genes of 21 amino acid biosynthetic pathways also suggested potential differences in the biosynthetic pathway of glutamine. The genetic comparisons of the genes involved in glutamine biosynthesis revealed that *glnE* coding for a glutamine synthetase adenylyltransferase/glutamine synthetase deadenylylase was also among the least conserved proteins within the amino acid biosynthetic genes and with a BSRP below the average BSRP (0.957), and $GlnE_{\alpha522}$ shared only 94% amino acid identity with $GlnE_{MC58}$. The amino acid sequence alignment from both GlnE coding sequences revealed 51 mismatching amino acids between strain MC58 and the L-glutamine auxotrophic strain α522 (Figure 6.13).

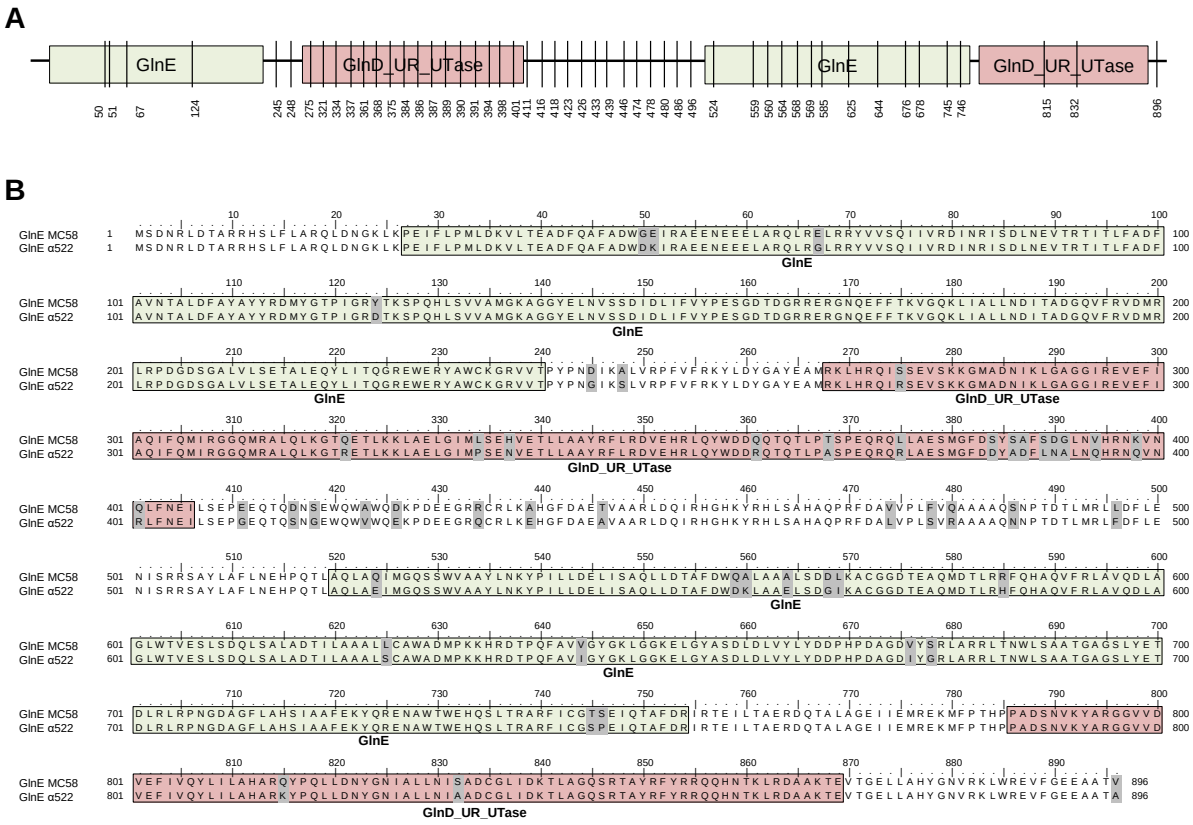

Figure 6.13 Sequence alignment of GlnE from MC58 and α522

A. Schematic representation of the GlnE domain structure (predicted by Pfam). Two functional regions have been predicted: a 'GlnE' domain (PF03710) and a 'GlnD_UR_UTase' (PF08335) domain. Black vertical lines with residue numbers indicate a mismatching amino acid of strain MC58 and strain α522.
B. Amino acid sequence alignment of strain MC58 and strain α522 GlnE. Colored boxes represent the predicted domains (from A) of GlnE. Mismatches are highlighted in gray.

Pfam searches found two different domains within the protein sequence: two glutamate-ammonia ligase adenylyltransferase domains 'GlnE' (PF03710) and two GlnD PII-uridylyltransferase domains 'GlnD_UR_UTase' (PF08335) (Figure 6.13 A). Seventeen mismatches were located within the two GlnE domains (from residues 27 to 240 and from 520 to 754), 18 within the two GlnD_UR_UTase domains (from residues 268 to 406 and from 786 to 869) and 16 mismatches were found between the domains (Figure 6.13 B).

In *E. coli*, *glnE* encodes a bifunctional protein with both glutamine adenylyltransferase and glutamine deadenylase activity. The catalytic activity of the glutamine synthetase (*glnA*) is regulated by its adenylylation status which is completed via GlnE. Unadenylylated GlnA remains active whereas adenylylated GlnA inactivates the catalytic site [125] (Figure 6.8). Moreover, the regulation of GlnA is subjected to a complex network in which different enzymes are involved. GlnB, also called PII protein, plays a

key role in the regulation of nitrogen assimilation by controlling the activity of glutamine synthetase [126]. Sequence alignments of the 5'-UTR upstream of *glnB* revealed that the promoter region is entirely different in both strains (Figure 6.14).

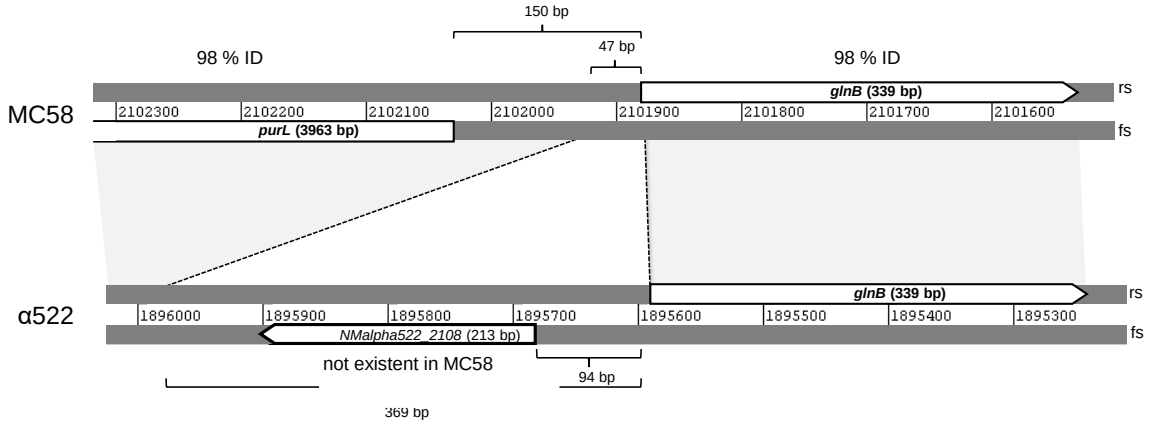

Figure 6.14 Organization of the *glnB* locus in MC58 and α522

The coding sequence of GlnB from both strains share a high amino acid identity of 98%, but strain MC58 and α522 differ in the 5'UTR of *glnB*. Upstream of *glnB* in α522, within the putative promoter region, a 71 aa hypotetical protein (*Nmalpha522_2108*, absent in MC58) is integrated. Abbreviations: fs, forward strand; rs, reverse strand, ID, identity.

In MC58, the *nadA* gene was inserted in the intergenic region between *purL* and *glnB*, suggesting that the regulatory network of nitrogen assimilation is altered in strain α522 or rather different in both strains.

Taken together, the results of the phenotypic and genomic comparison indicate that the strains differ in the biosynthesis of L-cysteine and L-glutamine and/or its regulation, which might in part be explained by genetic differences in CysH, CysJ, GlnE and/or GlnB. These might in turn to some extent explain the different phenotypes of the stingent response mutants in both genetic backgrounds.

However, a more detailed biochemical and genetic analysis of the L-cysteine and L-glutamine metabolism in both strains was beyond the scope of this work.

6.1.7 **Global gene expression during stringent response**

It is known that (p)ppGpp is required for stringent induction [82] and in particular under amino acid deplete conditions. To further characterize the transcription patterns during stringent response, MC58 wild-type and the MC58 *relA* deficient strain were grown aerobically in rich medium (GCBL^{++}) at 37 °C. Growth was determined by measuring the optical density at 600 nm for both strains, and they showed almost identical growth (Figure 6.15).

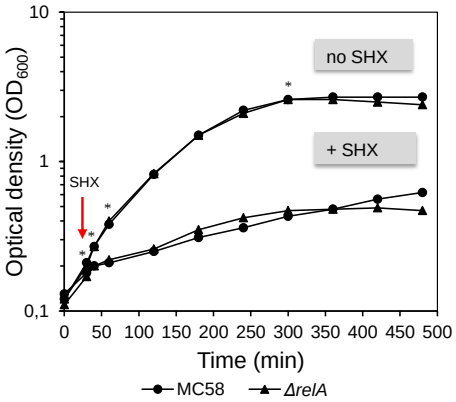

Figure 6.15 Growth during an SHX-mediated stringent response

Growth curves for strain MC58 and strain MC58*ΔrelA* with and without treatment with 100 µg/ml SHX, by determining the optical density at 600 nm. At an optical density of ~0.2, samples for time point 'zero' (0 min) were taken and SHX was added (indicated by the arrow). After 10, 30 and 240 minutes expression profiles were determined (indicated with asterisks) for both strains with and without treatment of SHX. One representative of three experiments is shown.

At an optical density of ~0.2 and approximately 30 min after incubation, cultures were treated with 100 µg/ml SHX, a serine analogue that inhibits serine tRNA synthetase and thus mimics serine starvation [127, 128]. The optical density of both strains stopped increasing almost immediately following SHX addition, and remained nearly constant over the next 1-2 h. To analyze the expression profile, samples were taken just prior to SHX addition (time zero, indicated by the red arrow), and after 10, 30 and 240 minutes after treatment (indicated with asterisks) with and without exposure of SHX (Figure 6.15). Total RNA was transcribed into cDNA, labeled and hybridized to the microarray slides. Normalized data for three replicates were averaged, and genes with an adjusted *p*-value of <0.05 were regarded as significantly differentially expressed. Differentially expressed genes were further grouped according to the clusters of orthologous groups (COGs) functional classification scheme [104]. Three different comparisons at the designated time points were performed. Comparison 1 compared changes in the expression profile of MC58 wild-type and the *relA* mutant strain, to find genes that were positively or negatively regulated by RelA, independent of SHX. Comparison 2 analyzed the SHX-mediated stringent response in a native genetic background by comparing the MC58 wild-type strain to the SHX treated wild-type strain. And finally, comparison 3 compared the expression profiles of the *relA* mutant strain to the mutant strain treated with SHX.

At first, volcano plots were created to represent the whole microarray data (Figure 6.16).

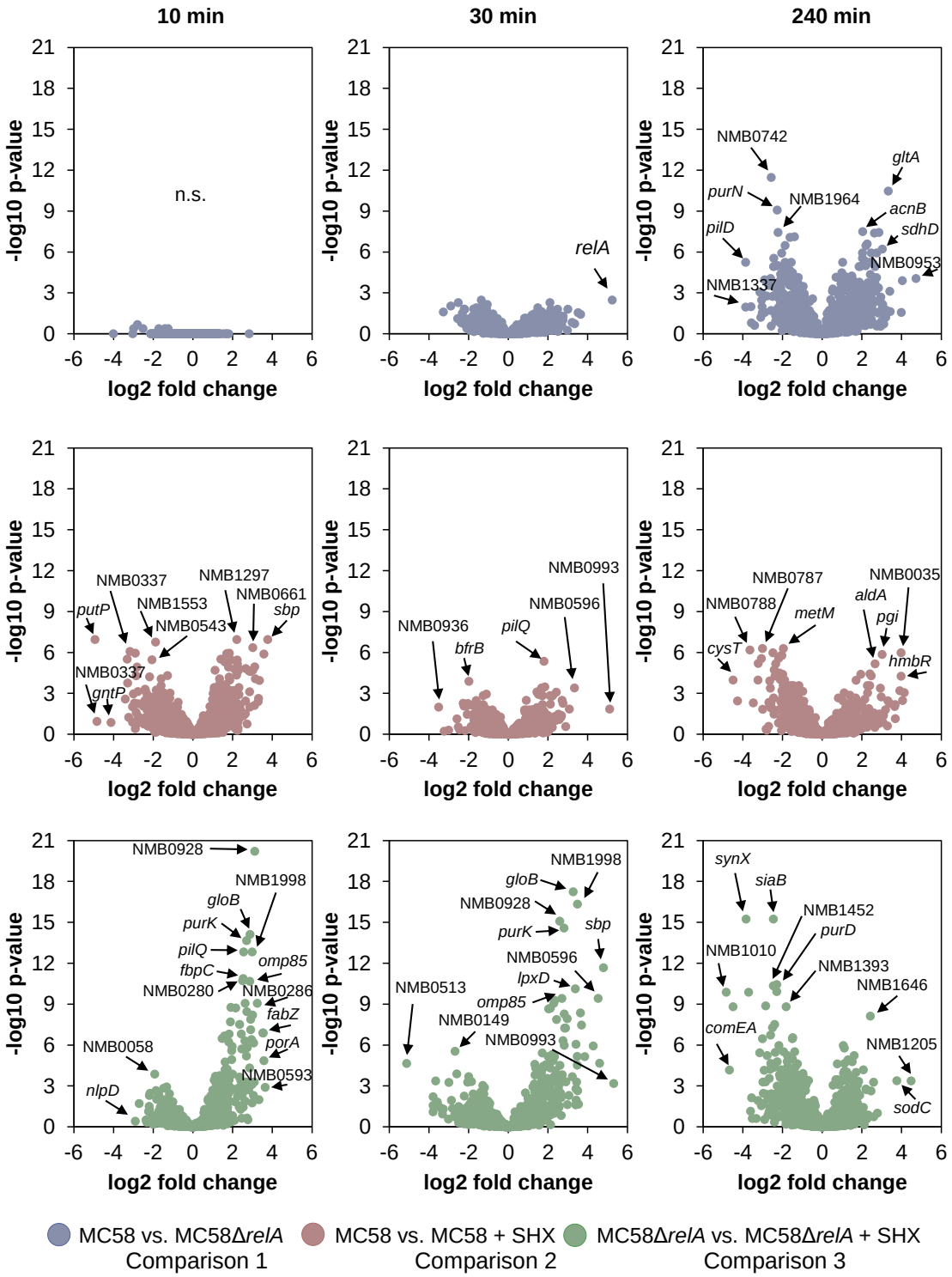

Figure 6.16 Vulcano plot representation of microarray data

Gene expression profiles of comparison 1 (MC58 vs. MC58Δ*relA*) (blue), 2 (MC58 vs. MC58 + SHX) (red) and 3 (MC58Δ*relA* vs. MC58Δ*relA* + SHX) (green) at time points 10 min, 30 min and 240 min. Gene expression profiles were plotted according to the $\log_2$ fold change (X axis) and -log 10 adjusted *p*-value (Y axis). Selected genes with conspicuous expression differences were marked with arrows.

The volcano plots visualize the results of the microarray data with depicted genes belonging to each comparison at time point 10 min, 30 min and 240 min after SHX

addition (Figure 6.16). Comparison 1 showed no significantly regulated genes (log 2-fold change >1, -log10 adj. *p*-value >1.3) at time point 10 min between MC58 and MC58Δ*relA*. At time point 30 min the vulcano plot shows a small number of signifcantly differently expressed genes, and almost the same number of up- and down- regulated genes. At time point 240 min the volcano plot shows large numbers of differently expressed genes and nearly the same number in both directions.

MC58 compared to MC58 treated with SHX (comparsion 2) showed significant changes in global gene expression already within 10 minutes after SHX addition. Similar numbers of genes were up- and down-regulated. Thirty minutes after SHX addition, the transcription differences were less pronounced compared to time point 10 min. Two hundert forty minutes after the SHX addition the results clearly show again a large number of significantly differently expressed genes with about the same number in both directions.

The addition of SHX resulted mostly in an upregulation in the MC58 strain defective in RelA compared to the untreated mutant at 10 and 30 minutes (comparison 3). Two hundred forty minutes later the transcriptional differences were more balanced with numerous genes that were particulary higher expressed under SHX treated conditions.

Taken together, the transcriptional differences between *relA* mutant and wild-type strains as well as between SHX treated and un-treated strains varied largely over time, and also the sets of genes with the highest expression level differences varied over time and between the comparison (Figure 6.16).

In order to get a more comprehensive overview of the expression profile, histograms of the number of differentially expressed genes and Venn diagrams of the three comparisons are given in Figure 6.17.

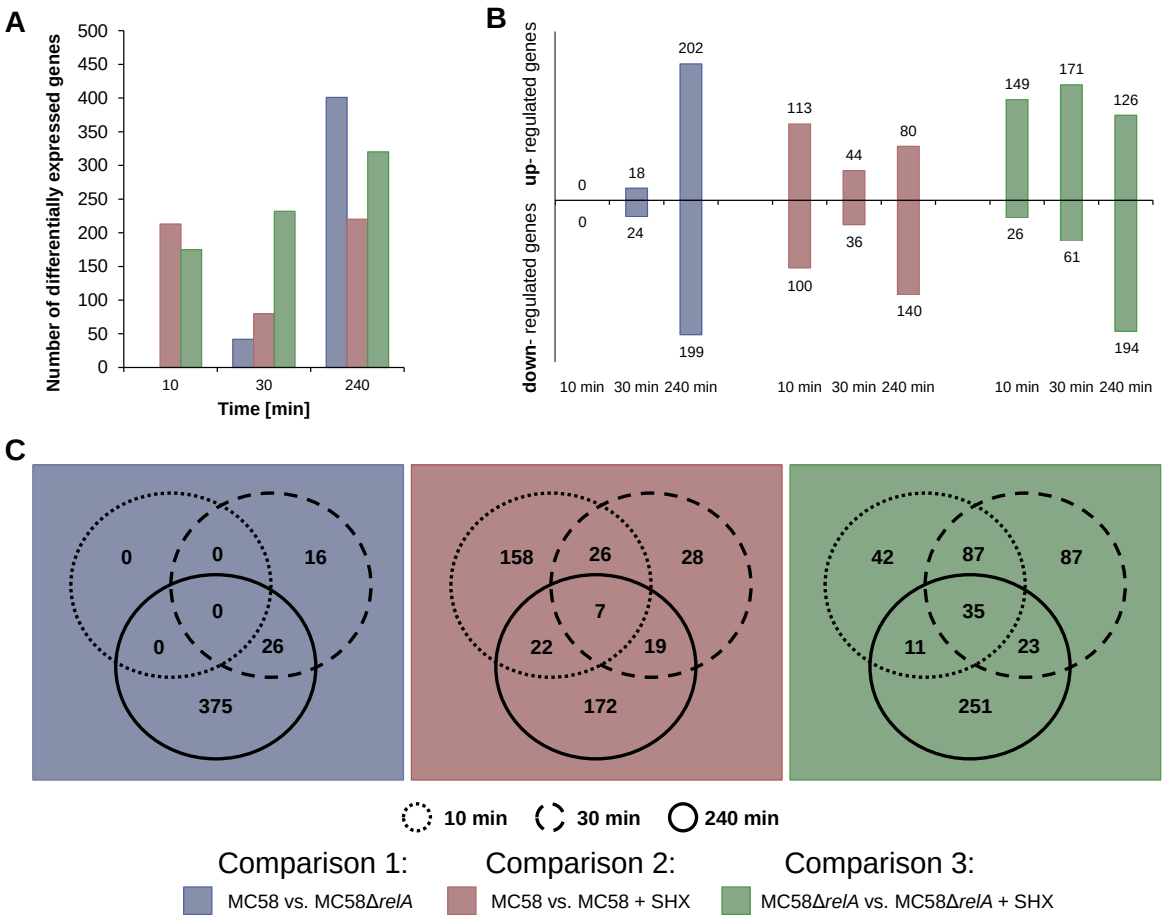

Figure 6.17 Expression profile overview

Overview of differentially expressed genes (adj. *p*-value <0.05) from comparison 1 (MC58 vs. MC58 *relA)*, comparison 2 (MC58 vs. MC58 + SHX) and comparison 3 (MC58Δ*relA* vs. MC58 Δ*relA* + SHX) over a time course of 10, 30 and 240 min after 'SHX' addition.
A. Histogram showing all differentially expressed genes.
B. Differentially up- and down- regulated genes.
C. Venn diagrams of overlapping differentially expressed gene sets over the time course.

Comparison 1 (MC58 vs. MC58Δ*relA*) showed a steady increase of differentially regulated genes over the time course (Figure 6.17 A). As already shown in the volcano plots, comparison 1 showed no differentially expressed genes at time point 0 min (data not shown) and at 10 min, indicating that RelA is dispensable at this time points. Twenty minutes later MC58 wild-type strain showed a small number of differentially expressed genes compared to MC58Δ*relA*. Forty-two genes were differentially regulated and about half were up- and down regulated, respectively (Figure 6.17 B). At time point 240 min, comparison 1 showed the largest number of significantly differentially expressed genes, and 199 were down- and 202 were up- regulated (Figure 6.17 B). More than a half of the genes from 30 min were also found at 240 min, and the highest number of differentially expressed genes was found at 240 min, indicating that RelA is important during late logarithmic growth phase (Figure 6.17 C).

Comparison 2 (MC58 vs. MC58 + SHX) showed first an increase, then a decrease and again an increase in the number of differentially regulated genes during the time course (Figure 6.17 A). Already after 10 min, the addition of SHX resulted in a rapid change in the expression profile. The comparison yielded around 200 differentially expressed genes. Around 100 genes were up- and nearly the same amount was down- regulated. Twenty minutes later, the effect of SHX was decreased. Only around 40 genes were up- or down- regulated. In the late the logarithmic growth phase 240 min after SHX addition, 140 genes were down- regulated and 80 were up- regulated, thereby showing again an increase in the number of differentially expressed genes (Figure 6.17 B). Taken together, 10 min after SHX addition there was a huge number of differentially expressed genes between MC58 and MC58 challenged with SHX, indicating that SHX treatment resulted in rapid and extensive transcriptional reprogramming. However, only a small number of differentially expressed genes were overlapping with time point 30 and 240 min after SHX addition (Figure 6.17 C). Interestingly, the highest number of differentially expressed genes were found 240 min after SHX addition, suggesting late logarithmic effects.

In contrast to comparison 2, comparison 3 (MC58Δ*relA* vs. MC58Δ*relA* + SHX) showed a steady increase in the number of differentially expressed genes. Nevertheless, the addition of SHX also resulted in a large change in the expression profile already 10 minutes after SHX addition. Around 200 genes were differentially expressed and the majority of the genes were up- regulated (149) and only a few were down regulated (26). The same was seen 30 min after SHX addition, 171 genes which were up- regulated and 61 genes that were down- regulated (Figure 6.17 B). Two hundred forty min after SHX addition the comparison showed further an increased number of differentially expressed genes. One hundred ninety-four genes were down- and 126 genes were up- regulated in MC58Δ*relA* compared to MC58Δ*relA* challenged with SHX.

Therefore, the RelA mutant showed also a fast reaction to SHX treatment with a huge number of genes (87) that were differentially expressed at time point 10 and 30 min, indicating a ‘longer’ reaction to SHX. Two hundred forty min after SHX addition, the highest number of differentially expressed genes was found, with only a few genes also differentially expressed at 10 and 30 min, suggesting late logarithmic effects.

In summary, in this experimental setup RelA is important in the late logarithmic growth phase were nutrients get depleted. The SHX response results in rapid transcription changes whereas at later time points in the late logarithmic growth phase leads to other transcriptional responses. This together indicates a bi-phasic response of RelA, in

early-middle growth phase a SHX-mediated stringent response and in late logarithmic growth phase a nutrient starvation-mediated stringent response.

To further find overlapping genes between the different comparisons, Venn diagrams were created to find RelA and SHX depended genes during the time course (Figure 6.18).

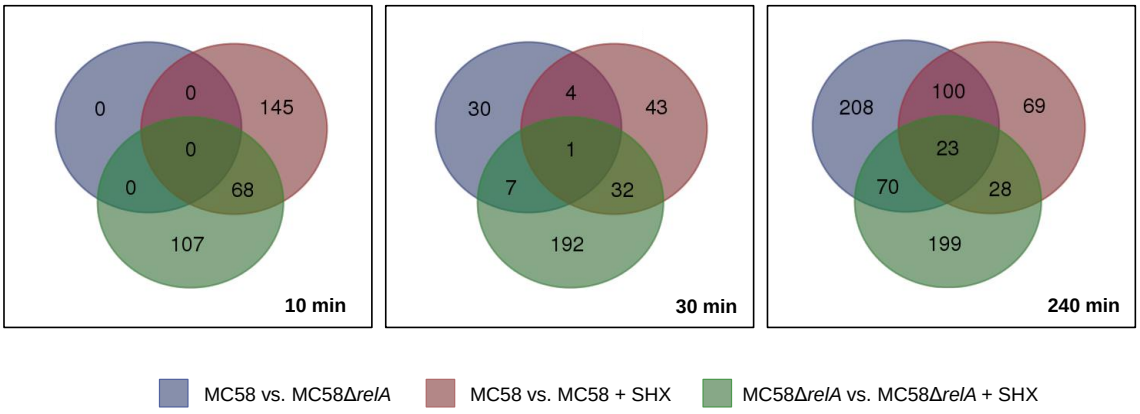

Figure 6.18 Expression profile overview of the three different comparisons

Venn diagrams of overlapping differentially expressed gene (adj. *p*-value <0.05) sets from the three different comparisons: Comparison 1 (MC58 vs. MC58 *relA)*, comparison 2 (MC58 vs. MC58 + SHX) and comparison 3 (MC58Δ*relA* vs. MC58 Δ*relA* + SHX) over a time course of 10, 30 and 240 min after 'SHX' addition.

Ten minutes after SHX addition there were 68 overlapping genes between comparison 2 and 3, with 13 genes (largest group) coding for cell wall/membrane/envelope biogenesis (COG M) functions. Interestingly, in both non-overlapping gene sets the largest fraction (23 and 15 genes, respectively) code for amino acid transport and metabolism functions.

Thirty minutes after SHX addition only very few genes of comparison 1 were shared with the SHX treated comparisons. This indicates that the deletion of *relA* caused transcriptomic changes that were partially independent of SHX treatment and vice versa.

As described above, 240 min after SHX addition mostly late logarithmic effects were seen. Large numbers of differentially expressed genes were shared between the comparisons.

Comparison 1 (MC58 compared to MC58Δ*relA*) showed the highest number of differentially expressed genes, but almost the half of the genes were shared with the comparison 2 or 3, suggesting again a large number of genes that were not responsive to SHX treatment but probably to other nutrient limitations in the late logarithmic growth phase. Around half of the differentially expressed genes were not shared with the

SHX-treated samples of comparison 2 and 3, again indicating that a large number of genes were affected by *relA* deletion but not SHX treatment.

Of note, a comparably large group of genes (199) were only found to be differently regulated in comparison 3, suggesting that the deletion of *relA* and the addition of SHX caused transcriptional changes not caused by either factor in isolation.

In summary, the transcriptional response to SHX treatment is rather fast whereas of late time points, the limitation of important nutrients causes transcriptional changes requiring RelA.

Table 6.1 gives an overview of the COG categories that are affected by differential expression in the three comparisons. Based on these transcritomic comparisons COG enrichment analyses were performed to identify biological processes that might be particularly affected by the deletion of *relA* and for the addition of SHX.

Table 6.1 *COG gene enrichment analysis*

		Comparison 1: MC58 vs. MC58Δ*relA* [a]									Comparison 2: MC58 vs. MC58 + SHX [a]									Comparison 3: MC58Δ*relA* vs. MC58Δ*relA* + SHX [a] [b]								
		10 min			30 min			240 min			10 min			30 min			240 min			10 min			30 min			240 min		
COG		OR (95%-CI)[b]	P[c]	FDR[d]	OR (95%-CI)[b]	P[c]	FDR[d]	OR (95%-CI)[b]	P[c]	FDR[d]	OR (95%-CI)[b]	P[c]	FDR[d]	OR (95%-CI)[b]	P[c]	FDR[d]	OR (95%-CI)[b]	P[c]	FDR[d]	OR (95%-CI)[b]	P[c]	FDR[d]	OR (95%-CI)[b]	P[c]	FDR[d]	OR (95%-CI)[b]	P[c]	FDR[d]
INFORMATION STORAGE AND PROCESSING	A	0 (0-Inf)	1,00	1,00	0 (0-230,75)	1,00	1,00	Inf (0,72-Inf)	0,04	0,20	0 (0-43,13)	1,00	1,00	0 (0-125,86)	1,00	1,00	0 (0-42,93)	1,00	1,00	0 (0-53,89)	1,00	1,00	0 (0-40,01)	1,00	1,00	0 (0-26,25)	1,00	1,00
	B	0 (0-Inf)	1,00	1,00	0 (0-1631,89)	1,00	1,00	0 (0-149,73)	1,00	1,00	0 (0-313,99)	1,00	1,00	0 (0-904,46)	1,00	1,00	0 (0-312,48)	1,00	1,00	0 (0-391,5)	1,00	1,00	0 (0-291,33)	1,00	1,00	0 (0-191,47)	1,00	1,00
	J	0 (0-Inf)	1,00	1,00	0,85 (0,17-2,7)	1,00	1,00	1,25 (0,82-1,86)	0,25	0,56	0,61 (0,291,15)	0,14	0,67	1,14 (0,44-2,52)	0,67	1,00	1,91 (1,19-2,99)	0,00	0,11	0,46 (0,18-1)	0,05	0,22	0,56 (0,27-1,06)	0,07	0,27	1,06 (0,66-1,65)	0,82	0,99
	K	0 (0-Inf)	1,00	1,00	0,65 (0,02-3,95)	1,00	1,00	0,94 (0,47-1,77)	1,00	1,00	0,25 (0,03-0,94)	0,04	0,25	0 (0-1,34)	0,11	0,53	1,64 (0,76-3,23)	0,16	0,76	1,21 (0,46-2,7)	0,66	1,00	1,35 (0,61-2,73)	0,43	0,87	1,34 (0,68-2,49)	0,32	0,59
	L	0 (0-Inf)	1,00	1,00	0 (0-1,15)	0,07	0,14	0,42 (0,22-0,75)	0,00	**0,03**	1,08 (0,59-1,88)	0,78	1,00	0,51 (0,1-1,59)	0,37	1,00	0,77 (0,38-1,42)	0,48	0,96	0,88 (0,42-1,67)	0,88	1,00	1,16 (0,65-1,95)	0,58	0,87	0,64 (0,35-1,1)	0,12	0,33
METABOLISM	E	0 (0-Inf)	1,00	1,00	2,49 (0,93-5,76)	0,04	0,17	1,43 (0,94-2,14)	0,08	0,28	1,87 (1,13-2,98)	0,01	0,09	1,07 (0,37-2,49)	0,82	1,00	1,05 (0,57-1,82)	0,89	1,00	1,45 (0,8-2,48)	0,17	0,40	1,05 (0,58-1,79)	0,89	1,00	1,45 (0,92-2,23)	0,08	0,32
	F	0 (0-Inf)	1,00	1,00	1,9 (0,22-7,68)	0,30	1,00	1,96 (0,99-3,72)	0,04	0,18	0,73 (0,19-2,04)	0,81	1,00	1,59 (0,31-5,11)	0,44	1,00	1,39 (0,52-3,17)	0,48	0,89	2,4 (1-5,13)	0,03	0,21	1,76 (0,74-3,75)	0,17	0,40	1,3 (0,57-2,7)	0,44	0,70
	G	0 (0-Inf)	1,00	1,00	1,56 (0,18-6,22)	0,38	1,00	1,23 (0,62-2,32)	0,51	0,94	1,11 (0,42-2,51)	0,83	1,00	0,84 (0,1-3,26)	1,00	1,00	0,59 (0,15-1,62)	0,40	0,87	1,17 (0,41-2,78)	0,64	1,00	1,03 (0,39-2,32)	0,84	1,00	1,75 (0,89-3,25)	0,07	0,36
	H	0 (0-Inf)	1,00	1,00	0,52 (0,01-3,13)	1,00	1,00	1,17 (0,65-2)	0,58	0,82	1,27 (0,6-2,45)	0,47	1,00	1,22 (0,32-3,36)	0,57	1,00	0,51 (0,16-1,27)	0,21	0,70	0,79 (0,28-1,84)	0,70	0,93	0,37 (0,1-1,01)	0,05	0,32	1,11 (0,58-1,99)	0,76	0,96
	I	0 (0-Inf)	1,00	1,00	1,95 (0,22-7,86)	0,29	0,77	0,79 (0,31-1,72)	0,72	0,86	0,96 (0,29-2,46)	1,00	1,00	0,51 (0,01-3,04)	1,00	1,00	1,67 (0,67-3,69)	0,23	0,62	1,21 (0,37-3,1)	0,61	1,00	1,1 (0,38-2,64)	0,82	1,00	1,52 (0,69-3,09)	0,24	0,52
	P	0 (0-Inf)	1,00	1,00	1,09 (0,13-4,3)	0,71	1,00	0,8 (0,41-1,45)	0,57	0,86	1,01 (0,44-2,07)	1,00	1,00	3,16 (1,34-6,66)	0,00	0,06	1,89 (0,98-3,41)	0,04	0,35	2,2 (1,12-4,05)	0,02	0,18	1,9 (1,01-3,4)	0,03	0,39	0,68 (0,31-1,35)	0,36	0,62
CELLULAR PROCESSESS AND SIGNALING	C	0 (0-Inf)	1,00	1,00	1,68 (0,43-4,73)	0,31	1,00	1,95 (1,25-2,99)	0,00	**0,02**	1,52 (0,83-2,62)	0,16	0,63	1,13 (0,35-2,83)	0,80	1,00	1,08 (0,55-1,98)	0,76	1,00	1,93 (1,05-3,35)	0,02	0,19	1,5 (0,84-2,57)	0,13	0,34	1,65 (1,01-2,62)	0,04	0,21
	D	0 (0-Inf)	1,00	1,00	1,66 (0,04-10,59)	0,47	1,00	0,67 (0,17-1,96)	0,63	0,84	0,31 (0,01-1,9)	0,35	0,94	0,9 (0,02-5,64)	1,00	1,00	1,85 (0,54-5,07)	0,21	0,64	2,33 (0,68-6,4)	0,09	0,24	2,17 (0,71-5,63)	0,12	0,36	0,85 (0,21-2,52)	1,00	1,00
	M	0 (0-Inf)	1,00	1,00	1,48 (0,38-4,18)	0,36	0,66	1,03 (0,63-1,63)	0,91	0,99	2,07 (1,24-3,35)	0,00	**0,05**	3,09 (1,53-5,85)	0,00	**0,03**	1,41 (0,79-2,4)	0,18	0,74	1,68 (0,92-2,9)	0,07	0,25	1,7 (1-2,78)	0,04	0,33	1,49 (0,92-2,33)	0,08	0,28
	N	0 (0-Inf)	1,00	1,00	1,54 (0,04-9,76)	0,49	0,84	1,23 (0,44-3)	0,64	0,81	1,3 (0,33-3,81)	0,55	1,00	0,84 (0,02-5,2)	1,00	1,00	0,28 (0,01-1,74)	0,36	0,87	1,63 (0,41-4,79)	0,33	0,65	0,55 (0,06-2,22)	0,57	0,97	1,9 (0,72-4,5)	0,13	0,32
	O	0 (0-Inf)	1,00	1,00	2,01 (0,39-6,54)	0,21	0,33	1,6 (0,89-2,77)	0,09	0,28	0,76 (0,27-1,79)	0,70	1,00	0 (0-1,28)	0,11	0,45	1,06 (0,43-2,26)	0,85	1,00	0,29 (0,03-1,12)	0,08	0,25	0,84 (0,32-1,87)	0,85	1,00	1,38 (0,72-2,52)	0,26	0,51
	Q	0 (0-Inf)	1,00	1,00	0 (0-9,44)	1,00	1,00	1,79 (0,55-5,07)	0,25	0,61	0,45 (0,01-2,86)	0,71	1,00	1,31 (0,03-8,5)	0,55	1,00	0,45 (0,01-2,84)	0,71	1,00	1,19 (0,13-5,08)	0,69	0,97	0,41 (0,01-2,65)	0,72	1,00	1,32 (0,32-4,17)	0,55	0,82
	T	0 (0-Inf)	1,00	1,00	2,84 (0,32-11,77)	0,17	0,21	0,68 (0,2-1,81)	0,52	0,89	0,81 (0,16-2,63)	1,00	1,00	0 (0-2,8)	0,64	1,00	0,8 (0,16-2,61)	1,00	1,00	1,01 (0,2-3,3)	1,00	1,00	1,04 (0,26-2,99)	1,00	1,00	2,51 (1,09-5,45)	0,02	0,14
	U	0 (0-Inf)	1,00	1,00	0,6 (0,01-3,6)	1,00	1,00	1,29 (0,71-2,27)	0,37	0,75	1,48 (0,69-2,9)	0,25	0,85	2,22 (0,76-5,32)	0,07	0,56	1,16 (0,5-2,38)	0,70	1,00	1,46 (0,63-3,03)	0,29	0,64	1,22 (0,55-2,44)	0,58	0,92	1,09 (0,54-2,03)	0,75	1,00
	V	0 (0-Inf)	1,00	1,00	0 (0-10,02)	1,00	1,00	0 (0-0,87)	0,03	0,21	1,63 (0,3-5,81)	0,44	1,00	1,39 (0,03-9,07)	0,53	1,00	1,01 (0,11-4,32)	1,00	1,00	0,59 (0,01-3,82)	1,00	1,00	1,51 (0,28-5,38)	0,46	0,85	0,61 (0,07-2,63)	0,75	1,00
	W	0 (0-Inf)	1,00	1,00	0 (0-1631,89)	1,00	1,00	Inf (0,72-Inf)	0,21	0,55	0 (0-313,99)	1,00	1,00	0 (0-904,46)	1,00	1,00	0 (0-312,48)	1,00	1,00	0 (0-391,5)	1,00	1,00	Inf (0,19-Inf)	0,12	0,40	0 (0-191,47)	1,00	1,00
POORLY CHARAC-TERIZED	R	0 (0-Inf)	1,00	1,00	0,53 (0,06-2,08)	0,58	0,77	0,86 (0,55-1,32)	0,54	0,86	1,27 (0,75-2,08)	0,35	1,00	0,29 (0,03-1,09)	0,09	0,53	0,59 (0,28-1,1)	0,11	0,67	0,45 (0,18-0,97)	0,04	0,20	0,55 (0,26-1,02)	0,05	0,26	0,66 (0,38-1,09)	0,12	0,36
	S	0 (0-Inf)	1,00	1,00	2,48 (0,98-5,48)	0,03	**0,03**	1,07 (0,7-1,59)	0,76	0,87	1,08 (0,62-1,8)	0,79	1,00	0,73 (0,23-1,82)	0,68	1,00	0,87 (0,48 -1,5)	0,70	1,00	1,12 (0,61-1,93)	0,67	1,00	1,27 (0,76-2,03)	0,31	0,68	0,44 (0,23-0,78)	0,00	0,07

[a]Comparison of significantly (adj. *p*-value<0.05) versus non-significantly (adj. *p*-value>0.05) expressed genes to identify COG categories that are affected by differential expression in general.

[b]Odds ratio (OR) (with 95%-CI) based on Fisher's exact test. Values greater than 1 indicate that significantly differentially expressed genes are enriched for genes from the corresponding COG functional class.

[c]*p*-values from Fisher's exact test.

[d]False discovery rate based on *p*-values from Fisher's exact test and the Holm-Bonferroni multiple testing correction. Values with a FDR <0.05 are highlighted in red.

[e]A: RNA processing and modification; B: Chromatin Structure and dynamics; J: Tranlsation; K: Transcription; L: Replication and repair; E: Amino Acid metabolis and transport; F: Nucleotide metabolism and transport; G: Carbohydrate metabolism and transport; H: Coenzyme metabolis; I: Lipid metabolism; P: Inorganic ion transport and metabolism, C: Energy production and conversion; D: Cell cycle control and mitosis; M: Cell wall/membrane/envelop biogenesis; N: Cell motility; O: Post-translational modification; Q: Secondary Structure; T: Signal Transduction; U: Intracellular trafficing and secretion; Y: Nuclear structure; Z: Cytoskeleton; R: General Functional Prediction only; S: Function Unknown ; X: Not in COG.

Closer analyses of the data by using COG enrichment analyses revealed no overrepresented COG classes at time point 10 and 30 min within comparison 1. However, after 240 min genes for energy production and conversion (COG C) as well as genes involved in replication, recombination and repair (COG L) were overrepresented among the differently expressed genes. In COG class C, 34 of 36 genes were notably upregulated (Table 6.2).

Table 6.2 *Differently expressed genes (FDR <0.05) for energy production and conversion (COG C) after 240 min incubation in comparison 1*

Locus[a]	Gene name[b]	logFC[c]	Product[d]	Role[d]
NMB0123	-	-1.13	Putative ferredoxin	Electron carrier
NMB0543	-	1.56	Putative L-lactate permease	-
NMB0581	-	-1.62	Putative electron transfer flavoprotein-ubiquinone oxidoreductase	-
NMB0631	-	2.75	Putative phosphate acetyltransferase	-
NMB1436	-	0.70	Conserved hypothetical protein	-
NMB1712	-	2.82	L-lactate permease-like protein	-
NMB1342	*aceF*	1.03	Dihydrolipoyllysine-residue acetyltransferase	-
NMB1572	*acnB*	2.05	Bifunctional aconitate hydratase 2/2-methylisocitrate dehydratase	Tricarboxylic acid cycle
NMB1968	*aldA*	1.68	Aldehyde dehydrogenase A	-
NMB1938	*atpF*	0.84	ATP synthase B chain	ATP proton motive force interconversion
NMB0997	*dld*	1.86	D-lactate dehydrogenase	Aerobic respiration
NMB1723	*fixP*	1.54	Cytochrome c oxidase polypeptide III	-
NMB1458	*fumC*	2.95	Fumarate hydratase	Tricarboxylic acid cycle
NMB0954	*gltA*	3.33	Type II citrate synthase	Tricarboxylic acid cycle
NMB2060	*gpsA*	0.73	Glycerol-3-phosphate dehydrogenase	-
NMB0029	*hprA*	1.46	Putative D-3-phosphoglycerate dehydrogenase	Serine
NMB1031	*leuB*	0.64	3-isopropylmalate dehydrogenase	Leucine
NMB0568	*nqrB*	1.78	Na(+)-translocating NADH-quinone reductase subunit B	-
NMB0567	*nqrC*	0.86	Na(+)-translocating NADH-quinone reductase subunit C	-
NMB0241	*nuoA*	1.78	NADH-quinone oxidoreductase chain A	Aerobic respiration
NMB0244	*nuoD*	2.46	NADH dehydrogenase subunit D	Aerobic respiration
NMB0245	*nuoE*	1.75	NADH-quinone oxidoreductase chain E	Aerobic respiration
NMB0246	*nuoF*	1.91	NADH-quinone oxidoreductase chain F	Aerobic respiration
NMB0249	*nuoG*	1.08	NADH-quinone oxidoreductase chain G	Aerobic respiration
NMB0250	*nuoH*	2.98	NADH dehydrogenase I subunit H	Aerobic respiration
NMB0251	*nuoI*	1.67	NADH-quinone oxidoreductase chain I	Aerobic respiration

Locus[a]	Gene name[b]	logFC[c]	Product[d]	Role[d]
NMB0257	*nuoL*	1.96	NADH-quinone oxidoreductase chain L	Aerobic respiration
NMB2052	*petB*	1.56	Cytochrome b	Aerobic respiration
NMB0980	*pntA*	1.16	NAD(P) transhydrogenase subunit alpha	-
NMB0978	*pntB*	1.89	NAD(P) transhydrogenase subunit beta	-
NMB2061	*ppc*	2.43	Phosphoenolpyruvate carboxylase	-
NMB0431	*pprC*	2.99	2-methylcitrate synthase	Propionate degradation
NMB0950	*sdhA*	2.47	Succinate dehydrogenase. flavoprotein subunit	Tricarboxylic acid cycle
NMB0951	*sdhB*	1.70	Succinate dehydrogenase iron-sulfur protein	Tricarboxylic acid cycle
NMB0948	*sdhC*	3.98	Succinate dehydrogenase. cytochrome b556 subunit	Tricarboxylic acid cycle
NMB0949	*sdhD*	2.86	Succinate dehydrogenase. hydrophobic membrane anchor protein	Tricarboxylic acid cycle

[a,b]According to gene annotations from ref [19]

[c]Up- regulation is indicated in green. Red highlights down- regulation

[d]Accorrding to Biocyc [111] and Microscope [57]

Most of the up- regulated genes were involved in the tricarboxylic acid (TCA) cycle and the aerobic respiration. Many enzymes of the TCA cycle, including *gltA*, encoding for a citrate synthase, *sdhB*, which encodes for a succinate dehydrogenase and *fumC*, encoding for a fumarate hydratase which is negatively controlled by Fur [58, 129], appear to be positively regulated by RelA. As already described in the introduction, *fur* encodes for a ferric uptake regulation protein, which can act as a repressor as well as an activator for putative virulence genes *in vivo* and *in vitro* [58]. Moreover, nearly all subunits of the NADH ubiquinone reductase (H^+-translocating) were upregulated. This enzyme is involved in the aerobic respiration process by building up a proton gradient and accompanying membrane potential, which leads to the synthesis of ATP. The gene cluster (*nuoABCDE**)*** encoding for a large part of the NADH ubiquinone reductase is also controlled by Fur (activates and represses) [58, 129], suggesting a regulatory cross-talk between iron metabolism and the stringent response.

The other COG class L comprises genes important for replication, recombination and repair. In this group, 14 genes were differentially expressed, 9 genes were down- and 5 genes were up-regulated (Table 6.3).

Table 6.3 *Differently expressed genes (FDR <0.05) for replication, recombination and repair (COG L), after 240 min incubation in comparison 1*

Locus[a]	Gene name[b]	logFC[c]	Product[d]	Role[d]
NMB1337	-	-3.85	Conserved hypothetical protein	-
NMB1420	-	-2.35	DNA-binding protein Fis	-
NMB1368	-	-2.04	ATP-dependent RNA helicase	-
NMB0057	-	-1.03	RNA modification	-
NMB1873	-	-0.82	DNA polymerase	-
NMB1553	-	1.33	Truncated ISNme1 transposase	-
NMB1539	-	1.39	ISNme1 transposase	-
NMB0919	-	1.48	ISNme1 transposase	-
NMB1601	-	1.54	ISNme1 transposase	-
NMB1384	*gyrA*	1.47	DNA gyrase subunit A	DNA bending. supercoiling. inversion
NMB0642	*ntpA*	-2.12	dATP pyrophosphohydrolase	-
NMB0851	*rdgC*	-1.23	Recombination associated protein RdgC	-
NMB1673	*tag*	-1.10	DNA-3-methyladenine glycosylase I	DNA repair
NMB0399	*xthA*	-1.33	Exodeoxyribonuclease III	-

[a,b]According to gene annotations from ref [19]

[c]Up- regulation is indicated in green. Red highlights down- regulation

[d]Accorrding to Biocyc [111] and Microscope [57]

A large group of transposases were up- regulated, which all are *IS1106* transposase. These IS elements were probably under the positive control of RelA. IS-mediated DNA rearrangements potentially play an adaptive role by giving plasticity to the bacterial genome under conditions of nutritional limitations [130].

Moreover, most of the down-regulated genes in the COG class L include many DNA and RNA associated enzymes. DNA associated proteins such as a DNA polymerase (NMB1873), a Fis protein (NMB1420) and an exodeoxyribonuclease III (NMB0399) are downregulated, indicating that replication might be down-regulated. Fis proteins are important DNA-associated enzymes which play a role in affecting the bacterial chromosome structure and the initiation of DNA replication [131]. Also genes in RNA modification, for instance NMB0057 and NMB1368, were down regulated. NMB1368, encoding for a ATP-dependent RNA helicase, was two-fold down regulated. Helicases catalyze the unwinding of double-stranded nucleic acids and thus are involved in processes such as DNA replication, recombination, as well as RNA transcription and splicing [132].

Of note, comparison 1 showed also significant overrepresentation of COG class X at time point 30 and 240 min, indicating that a large number of uncharacterized genes might possibly be subject to RelA-mediated regulation.

In the second comparison analyzing the effect of SHX on the transcriptional profile of MC58 wild-type strain, genes coding for cell wall/membrane/envelope functions (COG M) were overrepresented among the differentially expressed genes 10 min after SHX addition. Table 6.4 lists all differentially expressed genes belonging to this group.

Table 6.4 *Differently expressed genes (FDR <0.05) for cell wall/membrane/envelope biosynthesis (COG M) 10 min after SHX addition in comparison 2*

Locus[a]	Gene name[b]	logFC[c]	Product[d]	Role[d]
NMB1957	-	-2.79	Putative acetyltransferase	
NMB2004	-	-1.91	Conserved hypothetical membrane protein	
NMB2001	-	-0.89	Conserved hypothetical membrane-associated protein	
NMB0280	-	1.16	Organic solvent tolerance protein	Other stresses (mechanical. nutritional. oxidative)
NMB1961	-	1.27	Putative VacJ-like protein	-
NMB1998	-	1.93	Autotransporter MspA	-
NMB0181	-	2.21	Periplasmic chaperone Skp	Chaperoning. folding
NMB1297	-	2.22	Membrane-bound lytic murein transglycosylase D	-
NMB1693	-	2.42	Putative AsmA-like protein	-
NMB0596	-	3.59	Conserved hypothetical integral membrane protein	-
NMB1651	*alr*	-1.44	Alanine racemase	-
NMB0456	*amiC*	1.30	N-acetylmuramoyl-L-alanine amidase AmiC	Cell division
NMB0638	*galU*	0.99	UTP--glucose-1-phosphate uridylyltransferase	-
NMB1985	*hap*	1.39	Autotransporter App	Virulence associated
NMB0700	*iga*	1.87	IgA-specific serine endopeptidase	-
NMB0622	*lolA*	-1.58	Outer-membrane lipoprotein carrier protein	-
NMB0178	*lpxA*	2.33	UDP-N-acetylglucosamine acyltransferase	Lipid A
NMB0180	*lpxD*	2.31	UDP-3-O-[3-hydroxymyristoyl] glucosamine N-acyltransferase	Lipid A
NMB0420	*murD*	1.85	UDP-N-acetylmuramoyl-L-alanyl-D-glutamate synthetase	Peptidoglycan (murein)
NMB0416	*murF*	1.06	UDP-MurNAc-pentapeptide synthetase	Peptidoglycan (murein)
NMB0182	*omp85*	1.47	Outer-membrane protein assembly factor Omp85	-
NMB1705	*rfaK*	1.52	Alpha 1.2 N-acetylglucosamine transferase	-

Locus[a]	Gene name[b]	logFC[c]	Product[d]	Role[d]
NMB0069	*siaB*	1.03	N-acylneuraminate cytidylyltransferase	-
NMB0068	*siaC*	2.68	Sialic acid synthase	-

[a,b]According to gene annotations from ref [19]

[c]Up- regulation is indicated in green. Red highlights down- regulation

[d]Accorrding to Biocyc [111] and Microscope [57]

Genes in COG class M were mainly upregulated. For example, genes for the biosynthesis of lipid A (*lpxA*, *lpxD*) and the peptidoglycan biosynthesis (*murD*, *murF*), which are both components of the gram negative bacterial cell wall were upregulated. Moreover, *siaB* and *siaC* encoding for capsule biosynthesis proteins, were also in the group of upregulated genes.

Additionally, also stress-related genes such as NMB0280, encoding for an organic solvent tolerance protein, and NMB0181 coding for a chaperone (Skp) were upregulated. In the group of the downregulated genes were mostly poorly characterized membrane-associated proteins of unknown function.

Thirty minutes after SHX addition, COG class M was still significantly overrepresented, although with a lower number of differentially regulated genes (Table 6.5).

Table 6.5 *Differently expressed genes (FDR <0.05) for cell wall/membrane/envelope biosynthesis (COG M) 30 min after SHX addition in comparison 2*

Locus[a]	Gene name[b]	logFC[c]	Product[d]	Role[d]
NMB0464	-	-1.45	Putative phospholipase A1	-
NMB2001	-	-1.04	Conserved hypothetical membrane-associated protein	-
NMB0548	-	-1.01	Putative membrane fusion protein	-
NMB1297	-	1.51	Putative membrane-bound lytic murein transglycosylase D	-
NMB1998	-	1.67	Autotransporter MspA	-
NMB0181	-	1.72	Periplasmic chaperone Skp (OmpH)	Chaperoning. folding
NMB0596	-	3.33	Conserved hypothetical integral membrane protein	-
NMB0638	*galU*	0.87	UTP--glucose-1-phosphate uridylyltransferase	-
NMB0190	*gidB*	-1.37	Methyltransferase GidB	Cell division
NMB0700	*iga*	1.71	IgA-specific serine endopeptidase	-
NMB0420	*murD*	2.10	UDP-N-acetylmuramoylalanine--D-glutamate ligase	Peptidoglycan (murein)
NMB0416	*murF*	1.64	UDP-N-acetylmuramoyl-tripeptide--D-alanyl-D-alanine ligase	Peptidoglycan (murein)

Locus[a]	Gene name[b]	logFC[c]	Product[d]	Role[d]
NMB0182	*omp85*	1.84	Outer-membrane protein assembly factor Omp85	-

[a,b]According to gene annotations from ref [19]

[c]Up- regulation is indicated in green. Red highlights down- regulation

[d]Accorrding to Biocyc [111] and Microscope [57]

Of the 13 differently regulated genes in this class 4 were down- and 9 were up-regulated. Nearly all of them were already differentially expressed 10 minutes after SHX addition, but the general size of this class has decreased.

Of note, comparison 2 and 3 also showed significant overrepresentation of COG class X at time point 10 min, indicating that poorly characterized as well as many so far hypothetical proteins might be subject to the regulation by the stringent response and in particular RelA.

Finally, the obsered microarray data were assessed via qRT-PCR expression analysis of selected stringent response genes using the same samples as for the microarray experiments. Figure 6.19 depicts the results and shows the expression of the stringent response genes *relA*, *spoT*, *dksA* and *grxB* located next to *relA* in both strains.

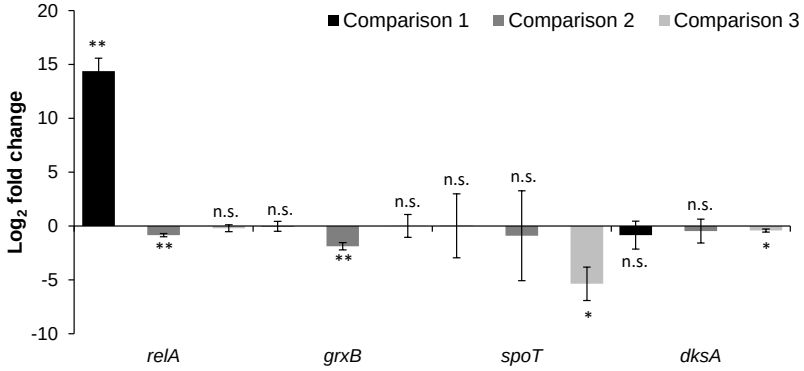

Figure 6.19 qRT-PCR validation of microarray data

Log_2 fold change expression values (qRT-PCR) between MC58 and MC58Δ*relA* (comparison 1), MC58 and MC58 treated with SHX (comparison 2) and MC58Δ*relA* and MC58Δ*relA* treated with SHX (comarison 3). Positive value of log_2 fold change indicates up regulation in the first condition, negative value of log_2 fold change indicates down regulation in the first condition. The mean and standard deviation from three independent experiments are presented. (Student's t-test, *p<0.05, **p<0.01, n.s. = not significant)

As a control, *relA* was nearly 15-fold up- regulated in the wild-type compared to the mutant strain in comparison 1 at 30 min, as expected. In line with the microarray data the other response genes as well *grxB* showed no significant expression differences.

Also in comparison 2 *spoT* and *dksA* showed no significant gene expression differences whereas the exposure to SHX lead to a slightly down- regulation of *relA and grxB* in the wild-type. This indicates that SHX might affect upregulation of *relA* and *grxB*.

In comparison 3 no significant expression differences were detected for *grxB* and as expected, no expression differences were found for *relA*. A slightly down regulation of *spoT* and *dksA* was observed, indicating that SHX might affect upregulation of both genes. However, this was only detected in the *relA* deficient strain and not in the wild-type compared to SHX treated strains.

Table 6.6 lists in addition the log_2 fold changes for the stringent response genes obtained by microarray hybridization.

Table 6.6 *Log_2 fold changes with according p-values from microarray hybridizations*

Condition	*relA*	P_{relA}	*grxB*	P_{grxB}	*spoT*	P_{spoT}	*dksA*	P_{dksA}
1	6,97	0,00	0,67	0,18	0,60	0,27	-0,79	0,03
2	-0,18	0,88	-0,81	0,10	1,36	0,01	-0,16	0,64
3	-1,27	0,34	0,56	0,26	0,72	0,19	0,25	0,47

Overall, the qRT-PCR results (Figure 6.19) confirmed the results of the microarray. Comparison of the expression levels of the four stringent response genes revealed a good correlation between the microarray and the corresponding qRT-PCR data (n = 3 measurements, Person's adjusted $R^2 = 0.7591$, $p_{Pearson} < 10^{-4}$).

6.1.8 Static biofilm formation is nutrient dependent and enhanced in *relAspoT* double mutant

Meningococci have been shown to form biofilms on abiotic and biotic surfaces [94, 133]. To examine the role of the stringent response in biofilm formation under static conditions, biofilm formation was assessed in a polystyrene microtiter plate as described in 5.24.3 using a semi-defined medium (10% PPM^+, 50% $NDM^{+/-}$, 40% 1x PBS) with the wild-type and the corresponding stringent response mutants (Figure 6.20).

To further investigate the impact of nutrient supply on biofilm formation, the same biofilm medium was also tested without adding PolyVitex. The addition of PolyVitex increases the concentration of e.g., cysteine, glutamine, thiamine, and vitamin B12 (chapter 4.5.1). The biofilm experiments revealed that the carriage strain α522 has a significantly higher biofilm production compared to the hyperinvasive strain MC58 in the biofilm medium supplemented with PolyVitex (Figure 6.20 A). Without the addition of PolyVitex the biofilm medium showed no significant difference between both strains. However, the addition of PolyVitex increased the biofilm formation in both strains and to a similar extent, although the difference was statistically significant only in strain α522 (Figure 6.20 A).

Under nutrient rich conditions biofilm formation slightly impaired in the *relA* knock-out strain compared to the respective wild-type strain in both genetic backgrounds, although this difference was statistically significant only in α522 (Figure 6.20 B). In contrast, the *relAspoT* double knock-outs showed increased biofilm formation in both strains.

Interestingly, under nutrient poor conditions there were at best only small differences in biofilm formation between the wild-type and the mutant strains in both genetic backgrounds, whereas the addition of PolyVitex resulted in a higher biofilm formation specifically in the MC58 *relAspoT* mutant strain (Figure 6.20 B).

The results indicate that genes of the stringent response affect biofilm formation and that the impact of the stringent response on biofilm formation seems not to be dependent on the genetic background.

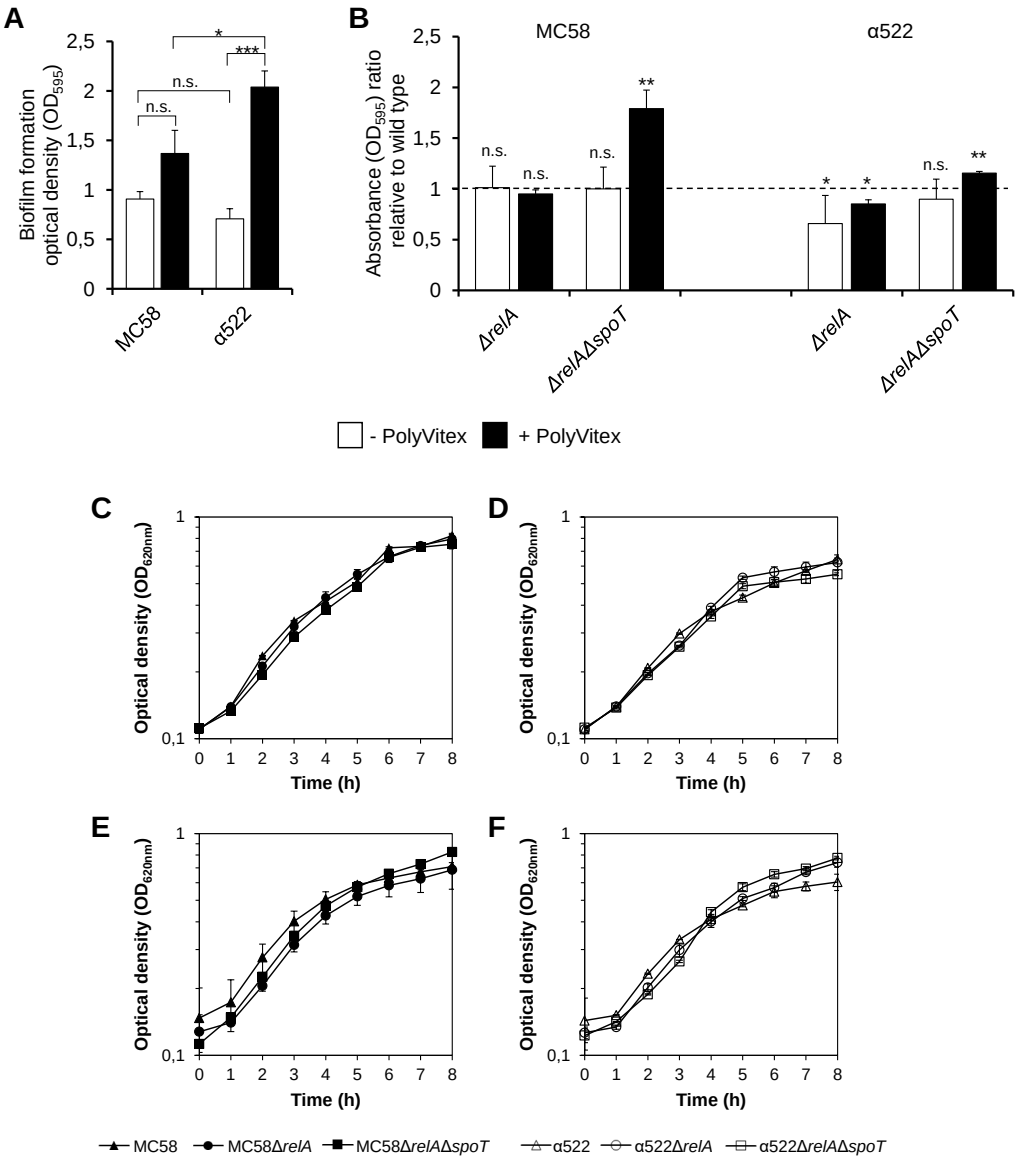

Figure 6.20 Biofilm formation and the effect of PolyVitex under static conditions

The strains were cultured in a semi-defined medium (10% PPM, 50% NDM and 40% 1x PBS) with or without the addition of PolyVitex at 37 °C/5% CO_2 and static biofilm formation was determined after 16 h incubation. Biofilms were performed in 96-well microtiter plates and for quantification the biofilms were stained with crystal violet and OD_{595} was determined.

A. Comparison of MC58 and α522 wild-type strains. The average optical density (OD_{595}) ratio from three independent experiments with standard deviation is shown. (Welch's t-test, *p<0.05,***p<0.001, n.s = not significant).

B. Biofilm formation was compared between the wild-type and stringent response mutant strains. The data represent the means and standard deviations of at least three independent experiments, and values are given as relative to the corresponding parental strain, which was set at 1.0, calculated as the optical density (OD_{595}) ratio of mutant compared to wild-type strains. (Welch´s test, *p<0.05, **p<0.01, n.s = not significant).

C+D. Growth control in biofilm medium with PolyVitex of MC58 wt, α522 wt and their corresponding *relA* and *relAspoT* knock-out strains.

E+F. Growth control in biofilm medium without PolyVitex of MC58 wt, α522 wt and their corresponding *relA* and *relAspoT* knock-out strains.

Of note, this effect was independent of the bacterial growth properties since the wild-type and the respective mutant strains displayed similar growth phenotypes in both strains in the medium used for the biofilm assay (Figure 6.20 C-F).

Together, this indicates that biofilm formation is condition- and strain-dependent and the stringent response is important to control biofilm formation in both strains.

6.1.9 **RelA is essential for cell invasion**

A central step in developing IMD is the ability of the bacteria to adhere to human cells and occasionally also invade the cell [4, 5].

Accordingly, nasopharyngeal cell lines were used to assess the adhesion and invasion of the wild-type and the *relA* mutant strains. Detroit cells were cultivated in EMEM^{+++} (Table 4.24) and were infected with the meningococcal strains. After 4 hours of incubation the amount of the bacteria were determined as described in 5.24.2 (Figure 6.21).

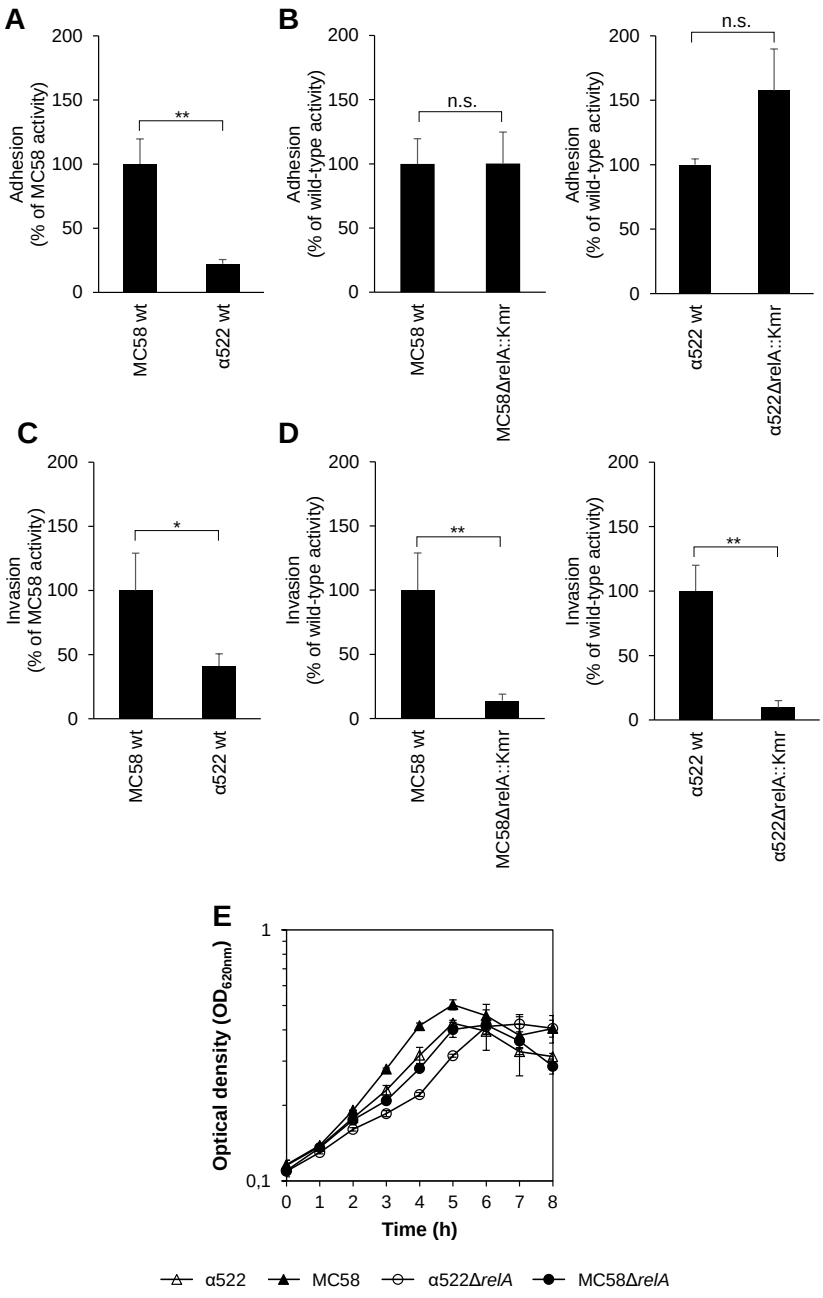

Figure 6.21 Cell invasion assay

A+B. Cell adhesion assays. Strain MC58, strain α522 and their respective *relA* mutant strains were tested for the adhesion to the epithelial cell line Detroit in EMEM^{+++}. One representative experiment of at least two or three experiments is shown.
C+D. Cell invasion assays. Strain MC58, strain α522 and their respective *relA* mutant strains were tested for the invasion into the epithelial cell line Detroit in EMEM+++. One representative experiment of at least two or three experiments is shown.
E. Growth control of wild-type strain MC58, α522 and their respective *relA* mutant strains in EMEM^{+++} medium at 37ºC over a time course of 8 h. One representative of three experiments is shown.

As shown in Figure 6.21 A and C, strain MC58 had a significantly higher adhesion as well as invasion rate than α522 while having the same growth rate in the medium used for the adhesion and invasion assays (Figure 6.21 E). In both strains, deletion of *relA*

resulted in a significantly decreased invasion rate while not significantly affecting adhesion (Figure 6.21 B+D) or growth in the cell culture medium (Figure 6.21 E). Together, these results suggest that the stringent response and *relA* are required for intracellular survival in both strains.

6.1.10 **Phenotypic chractarization of the strigent response in an *ex vivo* infection model**

Previous investigations revealed that *relA* is differently regulated in MC58 and α522 (chapter 6.1.2) and that the expression of stress response and metabolic genes differ among both strains especially in human blood [134]. Since differentally expressed genes might contribute to the survival of *N. meningitidis*, an *ex vivo* infetion model was used in order to simulate the *in vivo* conditions during carriage and invasive disease, respectively, and the impact of *relA* and *relAspoT* deletions on *ex vivo* growth was assessed in both strains (Figure 6.22).

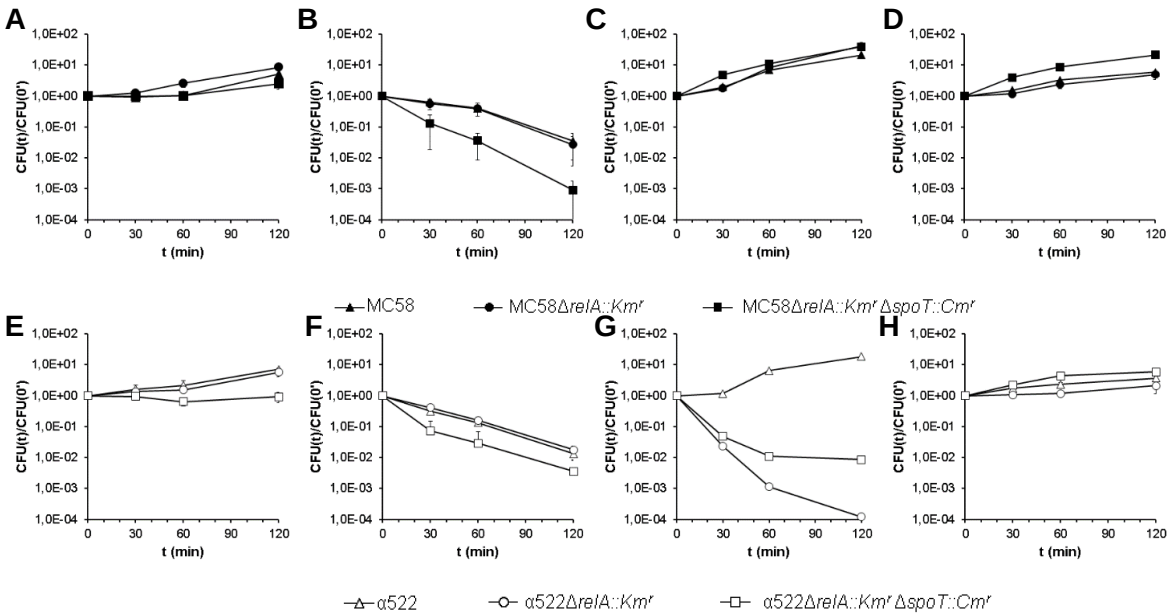

Figure 6.22 Growth and survival of MC58 and α522 wild-type strains and deletion mutants in an *ex vivo* infection model

Deletion mutants in strain MC58 (A-D) and in strain α522 (E-H) were tested for survival using an *ex vivo* infection model over a time course of 120 minutes. Values are averages of normalized CFU/ml of three independent experiments with standard deviation. For human whole blood (C+G), the median of three donors is shown. Strains were grown in PPM+ medium (A+E), human saliva (B+F), and human CSF (D+H).

Three independent experiments with the wild-type and mutant strains were performed in saliva, human whole blood and CSF for two hours at 37 °C and samples were taken at 0 h, 0.5 h, 1 h and 2 h for CFU determination. As a control, the bacteria were also grown in PPM$^+$ broth at 37 °C. The growth of the mutants in PPM$^+$ was comparable to the

respective wild-type strains, which suggests that the stringent response is dispensable for growth in rich medium (Figure 6.22 A+E).

In saliva (Figure 6.22 B+F), all wild-type and mutant strains were unable to grow. Human saliva is poor in nutrients and contains antimicrobial peptides [135, 136] which might explain to the some extent why even the wild-type strains were unable to grow in this condition.

To mimic conditions during invasive disease when *N. meningitidis* has to survive in the bloodstream, the MC58 and α522 wild-type and mutant strains were incubated in human whole blood from three different donors (Figure 6.22 C+G). Whereas both wild-type strains were able to grow almost equally well in human blood, the *relA* and the double knock-out *relAspoT* showed different results in both strains. *N. meningitidis* α522 deficient in RelA and RelA/SpoT were impaired in human whole blood whereas in the genetic background of strain MC58 the growth was not affected. This indicates that the differerent regulation of *relA* might play an important role and/or that the two strains have fundamental differences in their metabolism, as shown in chapter 6.1.6.

Finally, when the bacteria cross the blood-brain barrier they have to survive in CSF. Accordingly, bacteria were inoculated into human CSF and the CFU was determined in the same experimental condtions as before. As shown in Figure 6.22 D and H, the wild-type and mutants strains showed nearly the same growth phenotype in both strains which was comparable to the growth in rich medium.

Together, these data indicate that *relA* is required for *ex vivo* survival in a strain- and condition- dependent manner. In particular, RelA is essential only for survival in human whole blood and only in strain α522.

6.2 The effect of an intergenic insertion sequence on stringent response

6.2.1 Characterization of the *relA* locus in strain α522 and MC58

The results in chapter 6.1.2 and previous results from transcriptome comparisons of the invasive meningococcal serogroup B strain MC58 and serogroup B carriage strain α522 revealed that *relA* was upregulated in the hyperinvasive strain MC58 compared to α522 especially in blood [134]. To find hints why *relA* is differentially expressed in both strains, the *relA* locus of the two strains was compared in more detail.

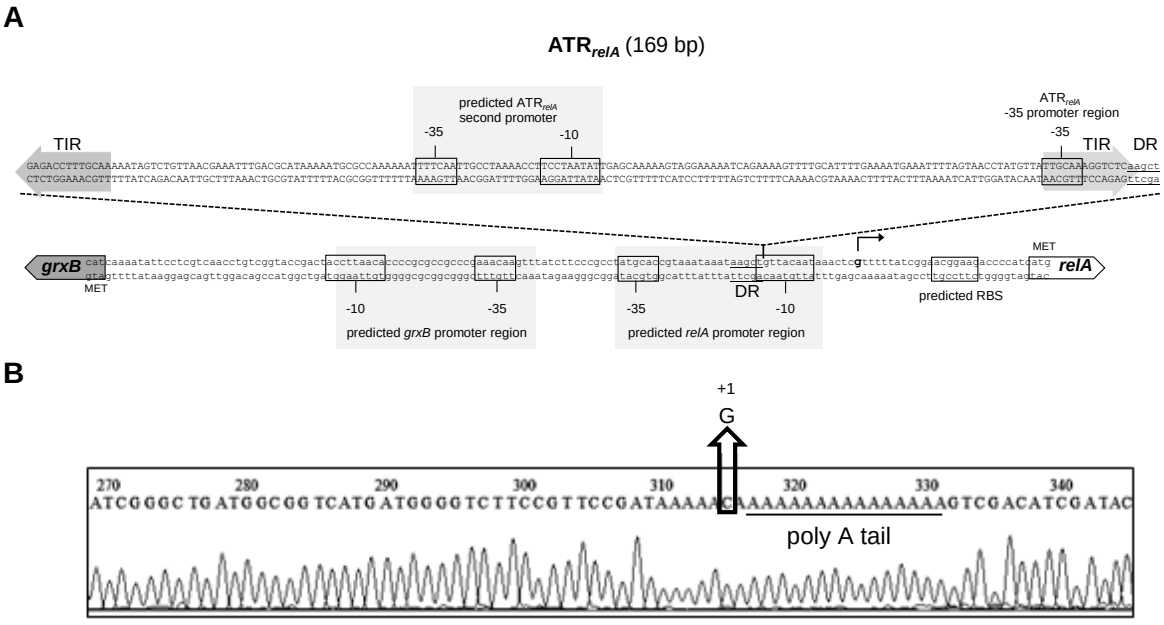

Figure 6.23 Organization of the *relA* – *grxB* locus in MC58 and α522

A. Detailed representation of the *relA* locus in strain MC58 compared to the *relA* locus in strain α522. Promoter regions of *relA* and *grxB* were predicted by using BPROM (prediction of bacterial promoters, [108]). In strain α522 a 169 bp ATR$_{relA}$ is placed between the -35 and the -10 boxes upstream of *relA*. TIRs were determined, DR (aagct) and a second promoter was predicted in the ATR.
B. Results from 5′-RACE PCR experiments. The last base upstream of the A tail corresponds to the first nucleotide transcribed. The transcriptional initiation nucleotide (G) on the reverse-complement strand is indicated by an arrow in the chromatogram.

As depicted in Figure 6.23, in strain α522 a 169 bp ATR$_{relA}$ is placed between the -35 and the -10 boxes upstream of *relA* as obtained by 5' RACE and computational operon prediction. The integration of ATR thus changes the promoter region of *relA* in stain α522 compared to MC58 (Figure 6.23 A). Moreover, a second promoter was predicted in ATR$_{relA}$, which may contain other binding sites for alternative regulators (Figure 6.23 A), although exactly the same transcription start site was determined in strain α522 (data not shown) as in strain MC58 (Figure 6.23 B) via 5' RACE. Interestingly, and in contrast to the *relA* locus, the *spoT* as well as the *dksA* loci were identical in both strains.

Together, these data indicate that ATR_{relA} might affect the regulation of *relA* (and *grxB*) expression in a strain-dependent manner.

6.2.2 **Characterization of an AT-rich repeat**

Genome sequence comparisons revealed that ATRs appear in both strain distributed over the entire chromosome. ATR sequence searches uncovered 13 ATRs in strain MC58 and 11 ATRs found in strain α522. The results from sequence alignments of all ATRs found in strain MC58 and α522 are presented in Figure 6.24.

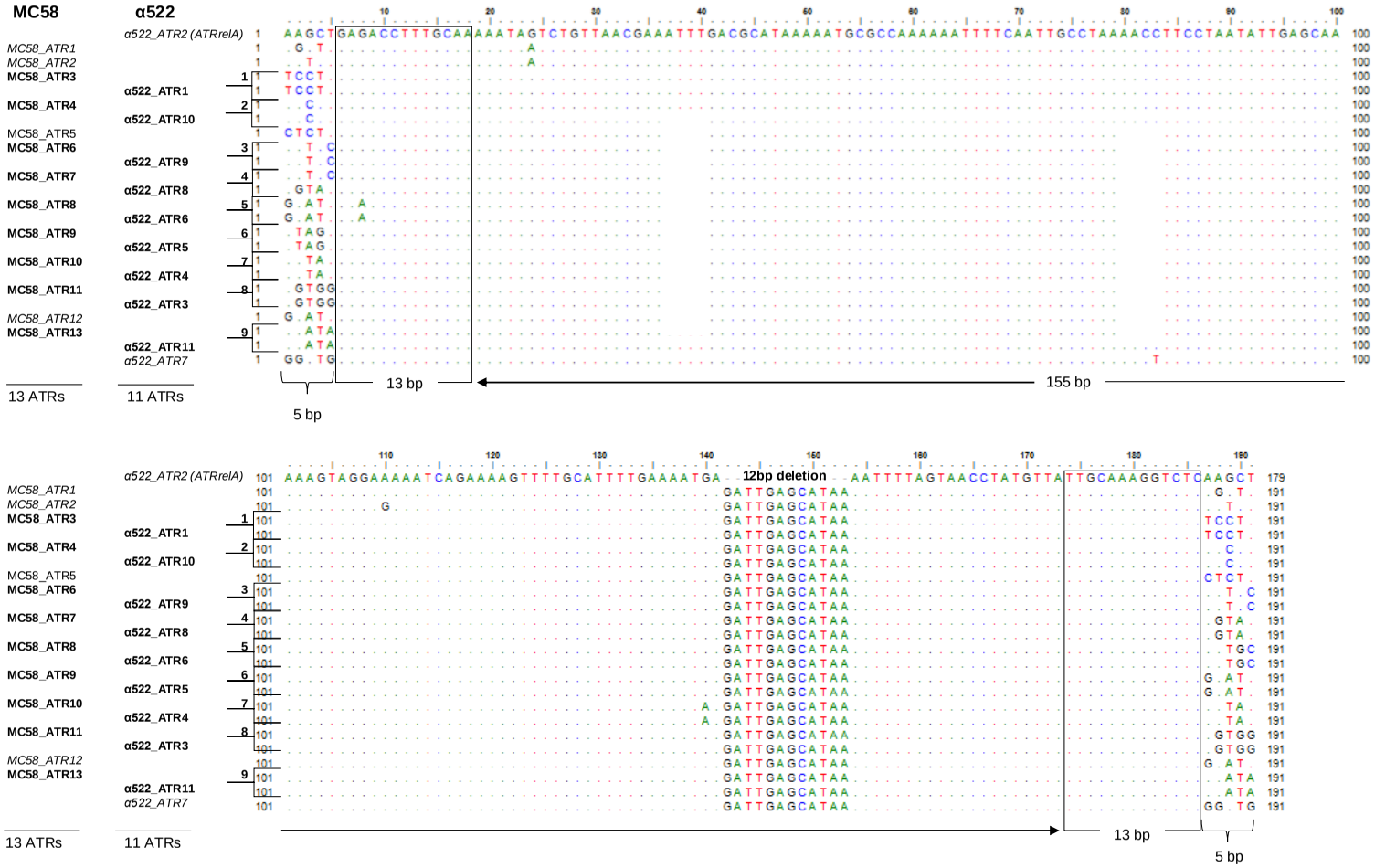

Figure 6.24 ATR sequence alignment

ATR nucleotide sequence alignment of strain MC58 and α522. ATRs were counted and numbered from 1 to 13 in strain MC58 or from 1 to 11 in α522 in order of their appearance in the corresponding chromosome starting at bp 0. As labeled on the left side of the legend, ATRs marked in bold indicate presence in both strains. ATRs that occur only in one of the two strains are printed in italics. Numbered and half open boxes illustrate 9 almost identical ATRs. Five bp variable nucleotides framing the ATR constitute DR. In the big boxes the putative 13 bp TIRs are indicated. The 'core' sequence of an ATR shows a conserved length of 155 bp, with the exception of ATR$_{relA}$ having a length of 143 bp due to the deletion of 12 nucleotides as indicated in the figure.

Nine ATRs were almost identical in both strains and located at the same loci. MC58 has additionally 4 ATRs which were absent in strain α522. Conversely, strain α522 has 2 ATRs which were absent in strain MC58. In contrast to all the other ATR copies, ATR_{relA} has a 12 bp deletion spanning the nucleotides –GATTGAGCATAA- (Figure 6.24). Sequence analysis indicate that the ATRs contain no ORF longer than 33 amino acids and do not code for any known transposase in particular. Furthermore, each ATR has a GC content of 30% and almost every of them was found in intergenic regions. Whereas the TIRs were highly conserved the DRs showed a high sequence variability among the ATR copies. However, the sequence at 5'-DR was almost always the same as at the 3'-DR.

All ATRs from strain MC58 and strain α522, described in Figure 6.24, were further analyzed for their putative integration site specifity (Figure 6.25).

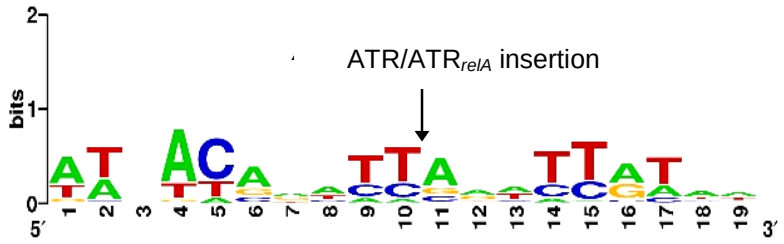

Figure 6.25 ATR/ATR_{relA} integration site

Pictogram representing the frequency of each nucleotide at the ATR/ATR_{relA} insertion sites in *N. meningitidis*. Nineteen bp long sequences surrounding the 'ATRs' from strain MC58 and strain α522 (described in Figure 6.24) were analyzed and created by WebLogo [137, 138].

The results from the sequence analysis revealed that the insertion site is not highly conserved with only a small tendency for the bases 5'-TTA-3'.

To further characterize the ATRs found in the fully sequenced chromosome of MC58, all 13 ATRs were analyzed with respect to their location relative to the neighboring coding sequences, by using different tools for genomic analysis (Table 6.7).

Table 6.7 *Chromosomal organization of 13 ATRs in strain MC58*

ATR-Location[a]	Schematic organization and orientation of ATR integration[b]	Locus[a]	(Flanking) Genes[a]	Product[a]	ATR in strain α522[c]
106.670..106.860		NMB0096 NMB0097 NMB0098	- - -	Hypothetical protein Putative secretion protein, degenerate ATP-binding protein, authentic frameshift	absent
224.480..224.670		NMB0217 NMB0218	*rpoN* *pglA*	Putative RNA Polymerase sigma-54 factor RpoN Glycosyltransferase	absent
315.901..316.091		NMB0305 NMB0306 NMB0307	- - *aroG*	Hypothetical protein Hypothetical protein Aldolase	present
542.403..542.593		NMB0517 NMB0518 NMB0519 NMB0520	- - - -	Hypothetical protein Hypothetical protein Hypothetical protein Hypothetical protein	present
634.606..634.796	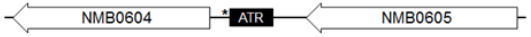	NMB0604 NMB0605	- -	Alcohol dehydrogenase Histone deacetylase	absent
713.267..713.457		NMB0687	*era*	GTP-binding protein	present
773.303..773.493		NMB0740 NMB0741	*recN* -	DNA repair protein RecN Conserved hypothetical protein	present
1.427.707..1.427.897		NMB1398 NMB1399	*sodC* -	Cu-Zn-superoxide dismutase *IS1106* transposase	present
1.466.687..1.466.875	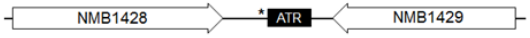	NMB1428 NMB1429	- -	Putative aminopeptidase Outer membrane protein PorA	present

ATR-Location[a]	Schematic organization and orientation of ATR integration[b]	Locus[a]	(Flanking) Genes[a]	Product[a]	ATR in strain α522[c]
1.797.541..1.797.731	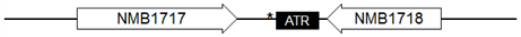	NMB1717 NMB1718	*mtrR* -	trancscriptional regulator MtrR Hypothetical protein	present
1.811.112..1.811.302		NMB1727 NMB1728	- *exbD*	Conserved hypothetical protein Biopolymer transport protein	present
2.081.762..2.081.952		NMB1982 NMB1983	*polA* -	DNA polymerase I Hypothetical protein	absent
2.260.048..2.260.238	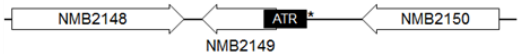	NMB2148 NMB2149 NMB2150	- - -	Transposase, IS30 Hypothetical protein Conserved hypothetical protein	present

[a]According to accession no. AE002098 and determined by using Artemis.

[b]The asterisk indicates the putative direction from ATR*relA*, orientated in wild-type (α522) direction to *relA* (the schematic representation is not to scale).

[c]Comparative analysis performed by using Artemis comparison tool.

Adjacent genes can be orientated and transcribed in three possible directions, collinear (→→), convergent (→←) and divergent (←→) [139]. In MC58 46.2% of all 13 ATRs are located in intergenic regions that are flanked by convergently (→←) transcribed genes, 23% are inserted between collinear (→→) genes and 0% are placed between divergently (←→) transcribed genes (Table 6.7).

The genome of MC58 consists of 1.798.767 bp coding sequences and 473.593 bp non-coding sequences. According to the proportion of coding and non-coding sequences in the genome, one would expect mainly intragenic insertions, if the distribution of the ATRs over the chromosome was entirely random. However, the 13 ATRs from MC58 are significantly enriched for ATR within intergenic regions (Fisher's exact test, OR = 6.85, $p<0.05$). Moreover, the large part (1517 genes) of 2063 genes is orientated collinearly in the chromosome. However, the majority of the ATRs are inserted significantly between convergently orientated genes (Fisher's exact test, OR = 1.33, $p<0.05$). Interestingly, none of the MC58 ATRs was placed between divergently transcribed genes, as it is the case for ATR_{relA} in strain α522.

This indicates that the location in potential promoter regions might be under negative selection possibly due to adverse effects on the expression of neighboring genes.

The ATRs are located next to important genes, for instance *mtrR* (NMB1717), *era* (NMB0687) and *sodC* (NMB1398). MtrR is a transcriptional regulator, Era is involved many cellular processes and SodC encodes for superoxide dismutase, which is important in the reduction of superoxide (O_2) radicals.

Together this indicates that this group of MITEs are not randomly distributed. They might alter transcription when they are integrated upstream of the gene or are potentially protecting mRNAs for degradation when they are integrated downstream of the relevant gene.

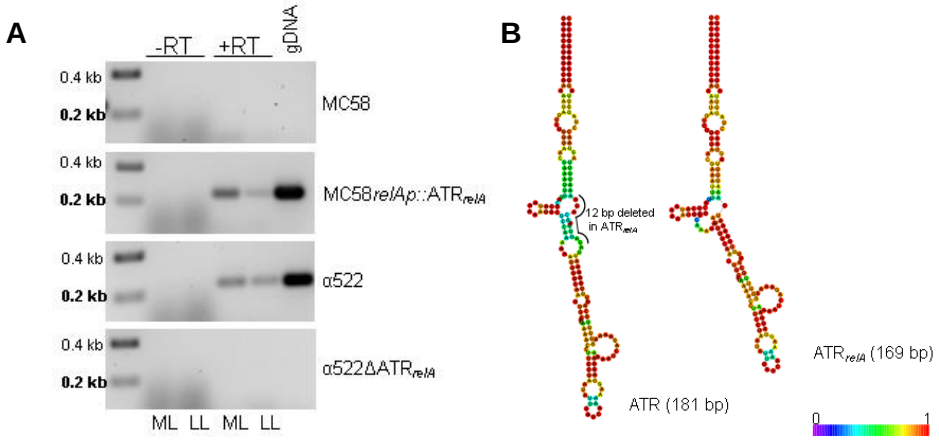

Figure 6.26 Characterization of ATR_{relA}

A. Results observed from RT-PCR experiments for ATR_{relA}. RNA was isolated from strain MC58, α522 and corresponding ATR knock-in/knock out mutants grown in PPM^{+}. RNA was isolated and transcribed from samples of the mid and late logarithmic growth phase. RNA (-RT), cDNA (+RT) and genomic (g)DNA were used as templates in PCR with primers for a putative ATR amplicon.
B. Secondary structure of ATR and ATR_{relA} predicted by RNAfold, [112]. Drawings show the minimum free energy (MFE) structure encoding base-pair probabilities.

Further RT-PCR experiments showed that ATR_{relA} is transcribed (Figure 6.26 A). Whereas in MC58 wild-type and the α522ΔATR_{relA} mutant strain no amplicon could be detected, transcription of ATR_{relA} was detectable in mid and late logarithmic growth phase in the α522 wild-type strain and the MC58 ATR_{relA} knock-in strain MC58*relAp*::ATR_{relA} (Figure 6.26 A). When transcribed into RNA, ATRs could form strong secondary structure as depicted in Figure 6.26 B. Taken together, these findings are again typical features of MITEs and suggest that ATR_{relA} would possibly also act in trans, for example on the regulation of other genes.

6.2.3 **ATR$_{relA}$ has no *in trans* effect on *ex vivo* survival**

Since ATR$_{relA}$ is also transcribed (Figure 6.26 A) it might encode a functional RNA and thus have also a *trans* effect on meningococcal fitness. To test for possible *trans* effects strains were constructed by cloning an ATR$_{relA}$ in two different orientations downstream of a *porA* promoter into plasmid pAP1 (Figure 6.27 A). As demonstrated by Northern blot ATR$_{relA}$ was transcribed by the *porA* promoter in both orientations in α522 and α522ΔATR$_{relA}$ strains (Figure 6.27 B) complemented with the plasmids pLK14 and pLK13, respectively, after 2 h of incubation.

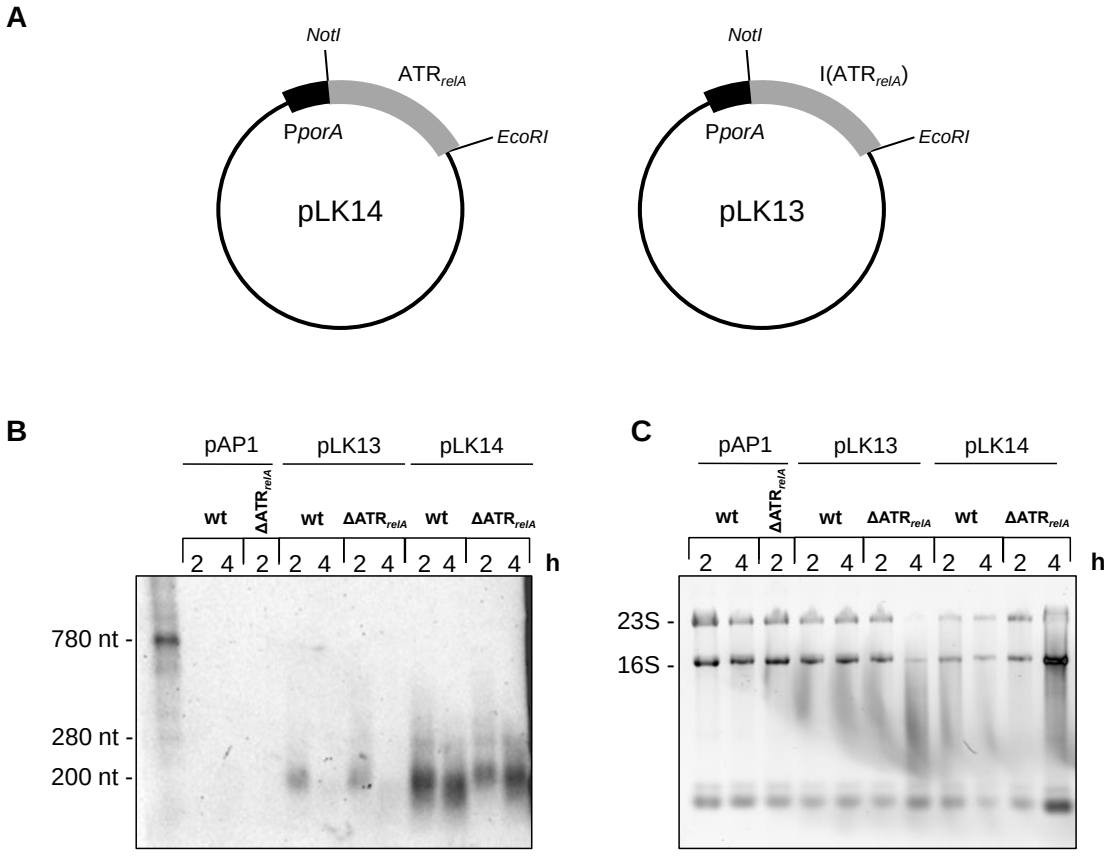

Figure 6.27 Northern blot analysis of ATR$_{relA}$

A. pAP1 ATR$_{relA}$ plasmid constructs.
B. Wild-type strain α522 and α522ΔATR$_{relA}$ harboring either pAP1, pLK13 or pLK14 were grown in PPM^{+} medium and after 2 h and 4 h of incubation, RNA was isolated and analyzed for ATR$_{relA}$ transcripts by Northern blot. One of three similar experiments is shown.
C. RNA control gel of the samples used for the Northern blot (B). Intact 23S and 16S are indicated.

In order to test for putative *in trans* effects of ATR$_{relA}$ on fitness of strain α522, α522ΔATR$_{relA}$ harboring pAP1 used as a control, α522ΔATR$_{relA}$ mutant harboring either pAP1, pLK13 or pLK14 were tested in the *ex vivo* infection model (Figure 6.28).

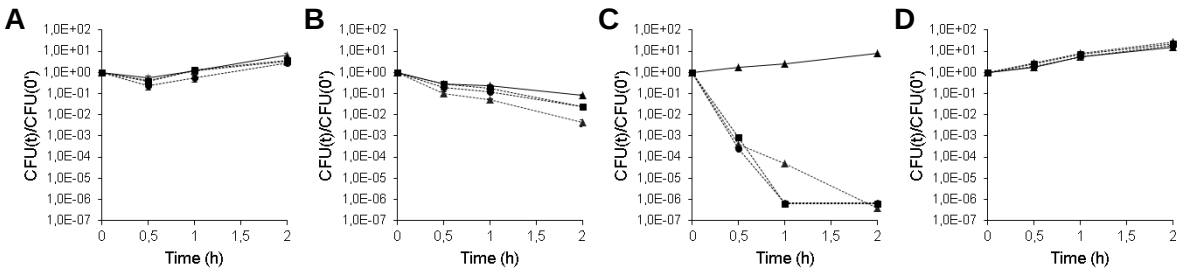

Figure 6.28 Survival of α522 wild-type strains and ATR$_{relA}$ complementing mutant strains in an *ex vivo* infection model

Strain α522 harboring pAP1, α522ΔATR$_{relA}$ mutant harboring pAP1, pLK13 (*porAp*::I(ATR$_{relA}$)) or pLK14 (*porAp*::ATR$_{relA}$) were tested for survival using an *ex vivo* infection model over a time course of 120 minutes. Values are averages of normalized CFU/ml of three independent experiments with standard deviation, except for the *ex vivo* model in human whole blood (C), where the median of three donors is shown.
A. Growth control in PPM$^+$ medium.
B. Human saliva.
C. Human whole.
D. Human CSF.

Mutant strain α522ΔATR$_{relA}$ possessing pAP1, pLK13 or pLK14 showed comparable growth to the wild-type strain α522 pAP1 in rich medium (PPM$^+$) and human CSF (Figure 6.28 A+D), and all strains were killed by human saliva (Figure 6.28 B). As expected the control strain α522ΔATR$_{relA}$ possessing pAP1 was unable to grow in human whole blood in contrast to the α522 pAP1 wild-type strain (Figure 6.28 C). However, the growth defect of α522ΔATR$_{relA}$ could not be complemented by either pLK13 nor by pLK14, indicating that ATR$_{relA}$ has likely no *in trans* effect on meningococcal *ex vivo* fitness.

6.2.4 ***In cis* effect of ATR on the transcription of *relA* and *grxB***

Due to the differences in the *relA* promoter region between both serogroup B meningococci as described above, *relA* and also *grxB* transcription was determined in MC58, MC58*relAp::*ATR$_{relA}$, α522 and α522ΔATR$_{relA}$ in order to assess possible polar effects of ATR$_{relA}$ on *grxB* and *relA* expression. Strains were grown in PPM$^+$ at 37 ºC/5% CO_2 to mid and late logarithmic growth phase. RNA was isolated, transcribed into cDNA and used for qRT-PCR experiments (Figure 6.29).

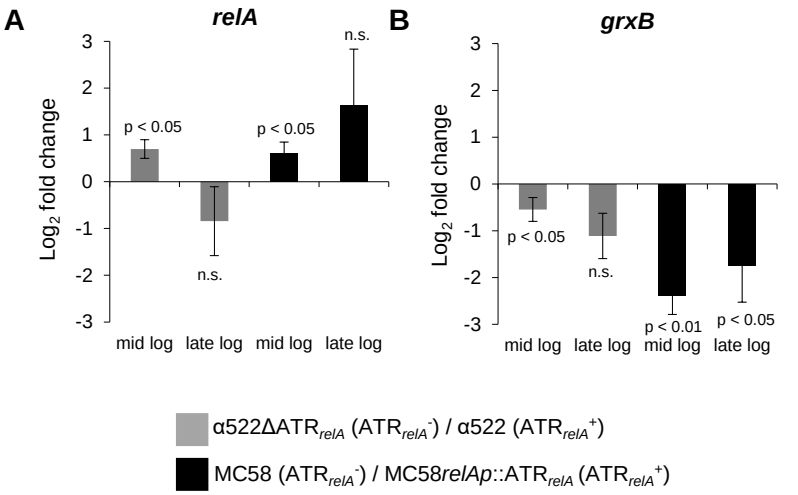

Figure 6.29 Polar effect of ATR on the transcription of *relA* and *grxB*

Transcription was analyzed by qRT-PCR after incubation in PPM+ in either mid logarithmic or late logarithmic growth phase. Bacteria were grown in PPM+ at 37 °C for approximately 2 h (mid log) and 4 h (late log). Expression levels were normalized to those of *rpoC* gene. Fold change was calculated by dividing the mRNA levels from ATR_{relA}^- bacteria to those from ATR_{relA}^+ bacteria. The mean and standard deviation from three independent experiments are presented.
A. Log_2 fold change in the mRNA levels of *relA* in the ATR_{relA}^- strains compared to the ATR_{relA}^+ strains in both genetic backgrounds (Student's t-test, $p<0.05$, n.s. = not significant).
B. Log_2 fold change in the mRNA levels of *grxB* in the ATR_{relA}^- strains compared to the ATR_{relA}^+ strains in both genetic backgrounds (Student's t-test, $p<0.05$, $p<0.01$, n.s. = not significant).

The qRT-PCR experiments revealed that upregulation of *relA* in the mid logarithmic growth phase was significantly higher in the strains harboring an ATR_{relA} in the promoter region of *relA* in both genetic backgrounds. However, in late logarithmic growth phase ATR_{relA} seems to have contrary effects on the expression of *relA*. Whereas in strain α522 ATR_{relA} leads to a down regulation of *relA*, ATR_{relA} in strain MC58 caused upregulation of relA expression (Figure 6.29 A) compared to the respective ATR_{relA}-negative strain, although in both cases the effects were not statistically significant.

In contrast to *relA* in both genetic backgrounds ATR_{relA} led to a downregulation in mid and late logarithmic growth phase of *grxB* expression (Figure 6.29 B).

Overall, the impact of ATR_{relA} was slightly dependent on the genetic background and the growth phase, and ATR_{relA} has an *in cis* effect on the expression of *relA* and *grxB* in a growth phase depended manner.

6.2.5 Epistatic effect of ATR$_{relA}$ on *ex vivo* survival in blood

In order to further test the effect of ATR$_{relA}$ on *ex vivo* fitness wild-type and ATR$_{relA}$ mutant strains were challenged *ex vivo* with human saliva, blood and CSF, respectively, over a time course of 120 minutes and the CFUs were determined (Figure 6.30).

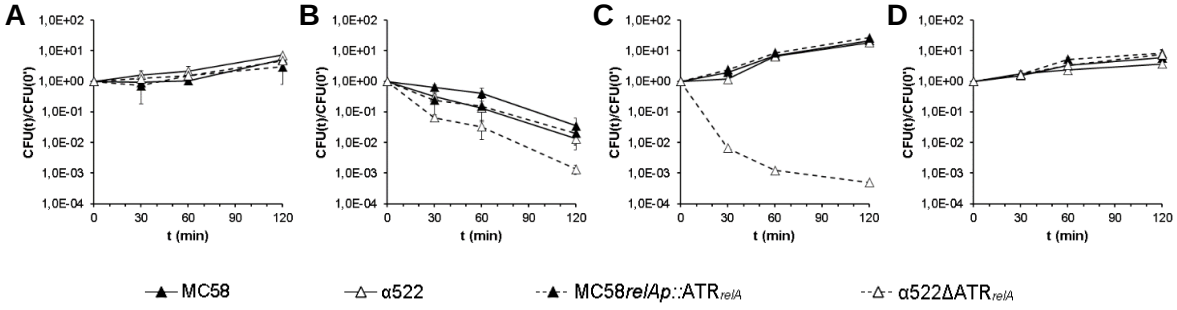

Figure 6.30 *S*urvival of MC58 and α522 wild-type strains and ATR$_{relA}$ mutant strains in an *ex vivo* infection model

ATR$_{relA}$ deletion and insertion mutants in MC58 and α522 were tested for survival over a time course of 120 minutes. Values are averages of normalized CFU/ml of three independent experiments with standard deviation, except for human whole blood (C), where the median of three donors is shown.
A. Growth control in PPM$^+$.
B. Human saliva.
C. Human whole blood.
D. Human CSF.

To exclude a general growth defect strains were incubated in PPM$^+$ medium. MC58*relAp::*ATR$_{relA}$ and a522ΔATR$_{relA}$ showed comparable growth to their corresponding wild-types (Figure 6.30 A). Likewise, all strains were again killed by human saliva (Figure 6.30 B). Furthermore, the deletion of ATR$_{relA}$ in α522 had the same *ex vivo* phenotype as the *relA* deficient strain and was unable to grow in human blood (Figure 6.30 C+D), suggesting that due to the insertion of ATR$_{relA}$ the binding sites for transcription regulators might differ and contribute to the observed condition-dependent effect of ATR$_{relA}$ on the *ex vivo* fitness. The wild-type strains and MC58*relAp::*ATR$_{relA}$ were both able to grow in human blood and CSF, indicating that the insertion of ATR$_{relA}$ in the *relA* upstream region of strain MC58 has not affected the *ex vivo* fitness in MC58 (Figure 6.30 C+D). Further support of a condition dependent effect of ATR$_{relA}$ on meningococcal fitness was the growth in human CSF of the α522 ATR mutant strain (Figure 6.30 D).

These results indicate that ATR$_{relA}$ exerts a polar effect on *relA* which is dependent on the condition and the genetic background and is therefore epistatic.

6.2.6 **Putative function of ATR$_{relA}$ in minimal growth conditions**

In chapter 6.1.4 and in chapter 6.1.5 it was demonstrated that RelA is involved in amino acid biosynthesis in both strains. To further check the condition-dependent effect of ATR$_{relA}$ on meningococcal fitness, MC58 as well as α522 wild-type and their corresponding ATR$_{relA}$ insertion or ATR$_{relA}$ deletion strains were grown in MMM with different combinations of L-glutamine and L-cysteine (Figure 6.31) as described before (chapter 6.1.5).

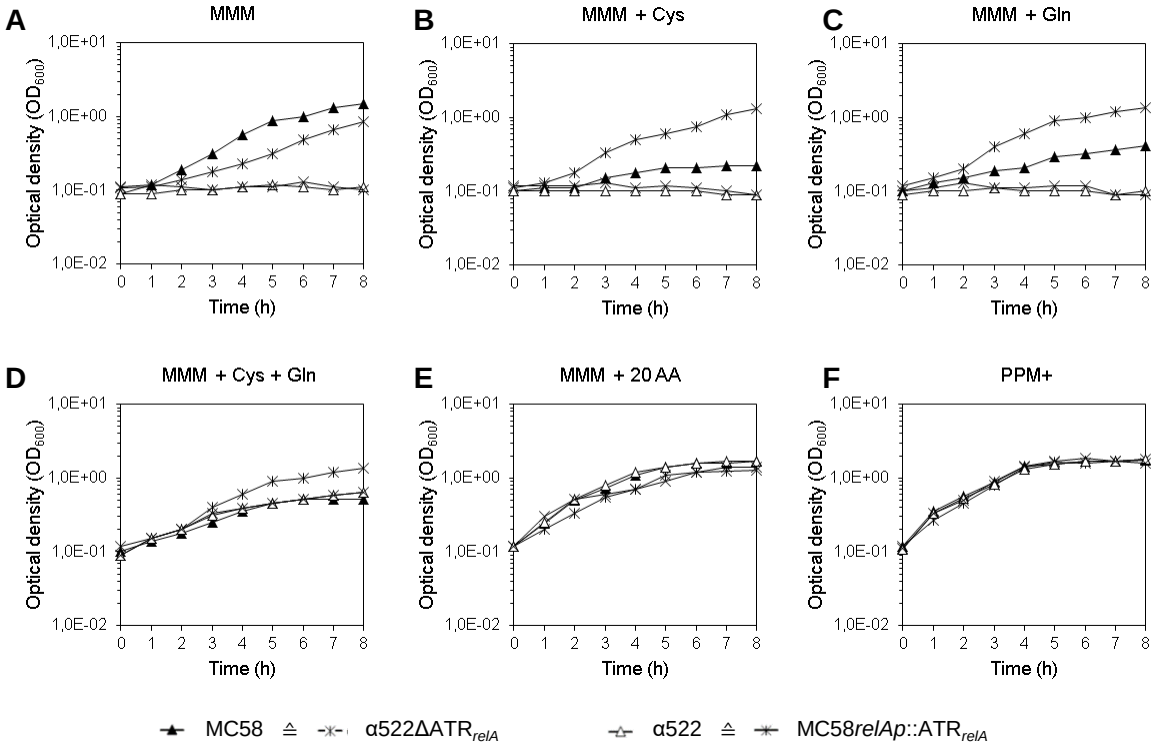

Figure 6.31 Impact of ATR$_{relA}$ on meningococcal growth *in vitro*

In vitro growth experiment of MC58, α522 wild-type and corresponding ATR$_{relA}$ mutant strains grown in MMM supplemented with different combinations of L-cysteine and L-glutamine. Strains were grown over a time course of 8 h at 37 °C and the optical density (OD_{600}) was determined every hour. For each panel one of two similar experiments is shown:
A. Growth in MMM.
B. Growth in MMM supplemented with L-cysteine (Cys).
C. Growth in MMM supplemented with L-glutamine (Gln).
D. Growth in MMM supplemented with L-cysteine (Cys) and L-glutamine (Gln).
E. Growth control in MMM supplemented with 20 amino acids.
F. Growth control in PPM^{+}.

Surprisingly, as depicted in Figure 6.31 strain MC58*relA*p::ATR$_{relA}$ showed improved growth in MMM supplemented with either L-cysteine or L- glutamine alone or when supplemented with both amino acids together than the wild-type strain (Figure 6.31 B+C, D). This suggests that ATR$_{relA}$ might affect the binding of transcription regulators linked to L-cysteine and/or L-glutamine metabolism to the *relA* promoter. In strain α522 no differences between wild-type and the ATR$_{relA}$ deletion mutant were observed, possibly

due to the general L-glutamine and L-cysteine auxotrophy (Figure 6.31 D). Together, these results confirm that the impact of ATR_{relA} on meningococcal fitness depends on the presence L-glutamine and L-cysteine of and on the genetic background of the strain.

7 Discussion

Recent studies have shown that the stringent response contributes to bacterial virulence [88]. Unfortunately, nothing is known about the stringent control in meningococci. Therefore, this study used an invasive meningococcal serogroup B strain MC58 as well as a carriage meningococcal serogroup B strain α522 to analyze the contribution of the stringent response to meningococcal fitness under *in vivo* mimicking conditions in a strain- dependent manner. In addition, differences in transcriptional regulation of *relA* were analyzed using *in silico* comparisons, qRT-PCR and *in vitro* experiments.

Finally, this study analyzed in detail the differences in the amino acid biosynthesis between both meningococcal strains, described the physiology of the stringent response and in particular RelA, and assessed the functions of a non-coding MITE, like ATR_{relA}.

7.1 Defects in amino acid biosynthesis in strain α522 (Cys/Gln auxotrophy)

Growth and fitness of a bacterial cells depend on the availability of environmental nutrients. It is known that some *Neisseria* species have an absolute requirement for L-cysteine [122]. *In vitro* growth experiments revealed that strain α522 exhibits an auxotrophy for L-cysteine and also for L-glutamine (chapter 6.1.5) which might have a direct effect on the pathogenicity of the strain due to the dependence of nutrients supplied by the host.

Sulfate and L-serine are required for the biosynthesis of L-cysteine. L-serine is converted via serine O-acetyltransferase (*cysE*, NMB0560) to O-acetyl-L-serine and cysteine synthase (*cysK*, NMB0763) catalyzes O-acetyl-L-serine with H_2S (hydrogen sulfide) to L-cysteine and acetate. Hydrogen sulfide is catalyzed by the reduction of sulfate and sulfate must be extracellularly taken into the cell. In *E. coli*, the sulfate and thiosulfate uptake is enabled by a periplasmic transport system: *cysU* (formerly kown as *cysT*), *cysW*, *cysA*, *cysP* and *sbp* [140]. *Sbp* encodes the gene for a sulfate-binding protein (SBP) and *cysP* encodes the gene for a thiosulfate-binding protein, although *cysP* is not essential to the cell [141]. Single *cysP* and *sbp* mutants are able to utilize both sulfate and thiosulfate but the inactivation of both genes leads to cysteine auxotrophy [142]. In the genome of strain MC58 and strain α522 only one putative SBP (NMB1017) was found, suggesting that this protein might bind sulfate and thiosulfate. The neisserial SBP shares 48% amino acid identity with *E. coli* SBP, whereas CysP from *E. coli* shares 47% identity to the *sbp* gene product from the meningococcus.

Besides the two different periplasmic binding proteins *sbp* and *cysP*, the sulfate-thiosulfate transport system of *E. coli* consists of two inner membrane proteins, *cysT* and *cysW*, which might assemble to a channel in the membrane and *cysA* encodes for the ATP-binding component [143]. The genomes of the meningococcal serogroup B strains harbor also a locus with *cysT*, *cysW* and *cysA* genes. Whereas CysT and CysA from strain MC58 and α522 share around 47-49% identity to the proteins from *E. coli*, $CysW_{MC58}$ shows with 60% ($CysW_{α522}$ 54%) a high identity to the amino acid sequence from *E. coli cysW*.

A closer and detailed description of the *cysTWA* locus further revealed crucial differences between strain MC58 and strain α522. Genome comparisons showed that in contrast to MC58, strain α522 has a CREE inserted between the genes *cysWA* (Figure 6.9), which might affect the ability to take up sulfate. The insertion of the CREE leads to a stop codon in strain α522 and shortens the length of CysW compared to CysW of MC58 by 13 residues. Additionally, in MC58 and also in *E. coli*, but not in strain α522, the end of *cysW* and the start of *cysA* are overlapping, suggesting that translational processing could play an important role [144].

Also in *E. coli* insertion elements were found along the sequence, the so-called repetitive extragenic palindromic (REP) sequences, which build up several stem-and-loop structures, but these elements were only located in untranslated regions [143]. Such elements might protect the mRNA transcript from degradation [144].

More differences between strain MC58 and α522 were found for genes important for sulfate assimilation. In contrast to strain α522, MC58 has a duplication of six the genes (*cysGHDNJI*) within the chromosome [19]. Each belongs to one transcription unit according to $DOOR^2$ [107]. These proteins encoded by *cysG*, *cysH*, *cysD*, *cysN*, *cysJ* and *cysI* are expected to give the bacterial cell the ability to assimilate sulfate by reducing sulfate into hydrogen sulfide.

CysN (subunit 1) together with CysD (subunit 2) encode for a sulfate adenylyltransferase which is responsible for the activation of sulfate by adding an ATP to yield adenosine 5'-phosphosulfate (APS) and PPi (diphosphate). Whereas in *E. coli* the second reaction is catalyzed through *cysC*, encoding for an APS kinase, to give 3'-phosphoadenylsulfate (PAPS), this enzyme seems to be lacking in *Neisseria*. Whereas the other genes of the *cysGHDNJI* cluster share 48-69% identity to those of *E. coli*, CysH shares only 27% identity with the *E. coli* orthologue remarkably. Furthermore, neisserial CysH is predicted to catalyze APS to PAPS and reduces PAPS to sulfite [124]. With CysJ (alpha subunit) and CysI (beta subunit), sulfite is reduced to hyrdogen sulfide.

CysG has an indirect function, due to the biosynthesis of siroheme, which is an cofactor of CysI in *E. coli* [140]. Gene comparisons of strain MC58 and α522 revealed that *cysG*, *cysH* and *cysJ* are the most divers within the *cysGHDNJI* gene cluster. NCBI BLASTP searches revealed that CysH and CysG from strain α522 were also found in other *Neisseria* species with an identity of 99%-100%, but CysJ was only found from 95% and less in other species. However, whereas CysJ of MC58 shares very high identity (99%) with CysJ from other *Neisseria* species, CysJ from α522 has less than 95% identity with CysJ from other *Neisseria*.

Moreover, in strain α522 a 155 bp CREE is integrated 289 bp upstream of *cysG*. This insertion leads to a repeated promoter region, which might have an effect on the transcription of the large operon *cysGHDNJI*.

Together, this might indicate that strain α522 is unable to reduce sulfate to sulfide and it appears to be not the only meningococcal strain with this defect. Le Faou 1984 showed that some *N. meningitidis* and all *N. gonorrhoeae* strains were unable to use sulfate as the sole source of sulfur and required cysteine for growth, suggesting that sulfate reduction is defective in these strains [145]. This corresponds to the statement from Rusnionk *et al.* 2009, who described that in *N. gonorrhoeae* an in-frame 3.4 kbp deletion has occurred between *cysG* and *cysN*, which leads to the inability to reduce sulfate into hydrogen sulfide [124]. However, the cysteine auxotrophy of *N. gonorrhoeae* can be dissolved with 2 mM thiosulfate, but not with sulfate or sulfite [145]. Le Faou also demonstrated that the inability to grow with sulfate as single source for sulfur was correlated to the deficit in sulfite-reducing activity [145]. This perfectly fits to the results with the exception that strain α522 was unable to grow in the presence of sulfate or thiosulfate, suggesting that the carriage strain has additionally a defect in the sulfate/thiosulfate uptake transporter. Also the increase of thiosulfate from 0.4 mM to 2 mM did not achieve growth of strain α522 in meningococcal minimal medium (data not shown).

Further investigations should experimentally clarify the reasons for the L-cysteine auxotrophy in strain α522, and the question arises whether the sulfur metabolism might be critical for meningococcal survival in the host.

In addition to the cysteine auxotrophy, strain α522 is also defective in its glutamine biosynthetic pathway. A genome-wide comparison of genes involved in amino acid biosynthetic pathways (Figure 6.8) revealed differences in particular in *glnE* which is involved in the glutamine and nitrogen metabolism.

In *E. coli* GlnE is involved in the activation of GlnA, which catalyzes the reaction from L-glutamate and ammonia to L-glutamine:

ATP + L-glutamate + NH_4 <=> ADP + phosphate + L-glutamine (EC 6.3.1.2) [146]

The activation of GlnA is coupled to a complex cascade (Figure 6.8) of protein-protein interactions. First *glnD*, coding for an uridylylation as well as for a de-uridylylation regulatory protein, might sense cellular nitrogen concentrations to GlnB [126]. *GlnB* encodes for the so-called PII regulatory protein which is a key player in controlling nitrogen metabolism. GlnB interacts with GlnE by triggering its de-adenylylation or adenylylation activity. GlnB-UMP stimulates the de-adenylylation reaction of GlnE, resulting in the activation of glutamine synthethase, and in the reverse reaction de-uridylylated GlnB stimulates the adenylyltransferase activity of GlnE which leads to the addition of AMP to glutamine synthetase and thus to the reduction in glutamine synthetase activity [147].

The amino acid sequence alignment from both *GlnE* coding sequences revealed 51 mismatching amino acids (Figure 6.13 B) between strain MC58 and the L-glutamine auxotrophic strain α522. Moreover, a BLASTP search revealed that only GlnE from of α522 but not from any other meningococcal strain shows a high sequence identity of 98% with GlnE from *N. lactamica*. In addition, comparisons of the GlnE protein sequence of α522 with GlnE sequences from other meningococcal strains (α153, α275, α710, MC58, α14, Z2491, α704) revealed around 93-95% identity, indicating that strain α522 shares a higher sequence identity to GlnE from *N. lactamica* than to the closer related strains from the same species.

Another genetic difference between MC58 and α522 that might impact L-glutamine biosynthesis in strain α522 are the differences in the *glnB* locus. As described, GlnB is one of the initial proteins for the regulation of glutamine biosynthesis and is also involved in nitrogen regulation in bacteria [148]. Sequence alignments of the coding region of GlnB from both strains revealed that they share a high amino acid identity of 98%, but strain MC58 and α522 totally differ in the 5'UTR of *glnB*. Genome comparisons found a 71 aa hypotetical protein (*Nmalpha522_2108*) integrated upstream of *glnB* in α522, within putative promoter region (Figure 6.14).

Genbank database similarity searches with the 400 bp 5' UTR sequence of *glnB* from strain α522 and strain MC58 revealed that both 'variants' occur frequently within *Neisseriaceae*. For the MC58 upstream region 19 matches were found (best hits with a threshold of 10).

One (*N. meningitidis* LNP21362) is identical, 12 share 99% identity, including e.g. *N. meningitidis* WUE2594, 8013, α14, FAM18 and 6 share 97% identity to the glnB 5'-UTR found in *N. gonorrhoeae* strains (e.g., FA19, MS11, FA1090). The 400 bp upstream *glnB* region of strain α522 was found only 10 times (best hits with a threshold of 10) with 97-98% identity, including for instance, *N. lactamica* 020-06, *N. meningitidis* α710, Z2491 and H44/76. Interestingly, the sequence comparison showed that within these ten strains the first 56 bp are always lacking which contains the whole putative MC58-type *glnB* promoter region. These genetic differences might lead to varying binding sites for regulators and/or alternative sigma factors, which in turn suggests that these strains might differ in their nitrogen metabolism.

Taken together, differences in the *glnE* gene and in the *glnB* promoter region could contribute to differences in the nitrogen and/or L-glutamine metabolism between strain MC58 and α522.

7.2 Physiology of the stringent response in *N. meningitidis*

If amino acids like L-cysteine and L-glutamine are getting limited, the stringent response is important in *E. coli* to signal such stresses and to adjust the metabolism of the cell [113, 149].

This study found similarities as well as differences in the physiology of the stringent response between *N. meningitidis* and *E. coli*. ppGpp analysis (chapter 6.1.2, 6.1.3) revealed that neisserial RelA is monofunctional and the only ppGpp synthetase. Additionally, in *E. coli,* a *relAspoT* double mutant, often annotated as $ppGpp^0$ bacteria, lacks all synthetase activity [118]. The same was demonstrated for the neisserial *relAspoT* double mutants, which are lacking all ppGpp synthetase activity (Figure 6.3).

Another similarity to *E. coli* is that SpoT is essential in both meningococcal strains (chapter 6.1.3). All transformation efforts failed to generate a SpoT single knock out. In addition, in strain MC58 a genetic compensation occurred near the active site in *relA* in a *spoT* deletion strain, resulting in a double knock-out phenotype. The same observation was described in gonococci [119], which can tolerate *spoT* insertional mutants only nearby but not located in the putative hydrolase domain, and insertions integrated in the hydrolase domain could only be transformed into a *relA* deficient strain [119]. Together, this indicates that SpoT is essential for the degradation of too high levels of (p)ppGpp in the cell and thus prevents toxicity.

In contrast to the neisserial SpoT, SpoT is a bifunctional enzyme in *E. coli*. SpoT$_{E.\ coli}$ possesses a (p)ppGpp hydrolase activity as well as a synthetase activity [150, 151]. SpoT of strain MC58 and α522 seem to be monofunctional. ppGpp analysis (chapter 6.1.3) revealed that ppGpp synthesis is catalyzed only by the RelA protein in *N. meningitidis.* The neisserial SpoT harbors an inactive ppGpp synthetase domain which was also confirmed by multiple sequence alignment analysis. Figure 7.1 depicts a multiple sequence alignment of the (p)ppGpp hydrolase and synthetase domains of RelA, SpoT and Rel proteins of different bacterial species and shows the putative functional motifs along with their consensus sequences and the experimentally tested functionality or non-functionality of the protein.

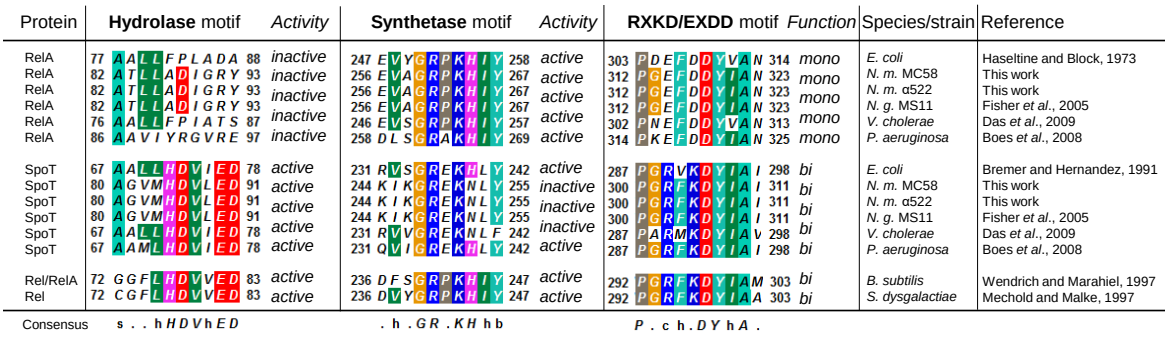

Figure 7.1 Multiple alignment of the conserved motifs in RelA/SpoT and Rel enzymes

Multiple alignment was created by using Clustal W. The alignment is splitted into three blocks for RelA, SpoT and Rel, respectively. Protein names are given in the left-hand column and the source-organism on the right. Conserved residues are shown in white on a colored background. Abbreviations in the consensus sequence stand for 's', small residues (A, C, D, G, N, P, S, T and V), 'h', hydrophobic residues (A, C, F, I, L, M, V, W and Y), 'b', big residues (F, I, L, M, V, K, R, E and Q) and 'c' for charged residues (D, E, R, K and H). 'X' or '.' stands for any amino acid. The HD motif was specified according to Aravind and Koonin *et al*., 1998 [114]. The synthetase motif was found within the conserved domain, PF04607. The *RXKD* and *EXDD* motif was based on the work of Sajish and Kalayil *et al*., 2009 [152].

The multiple sequence alignments revealed that an active HD motif (hHDVhED) was only found in SpoT and Rel proteins, whereas RelA proteins did not contain a functional HD motif. Consequently, *E. coli*, all tested *Neisseria* species and strains, *V. cholera*, *P. aeruginosa*, *B. subtilis* and *Streptococcus dysgalactiae* possess SpoT but not RelA with a functional (p)ppGpp hydrolase motif (hHDVhED).

The cross-strain multiple sequence alignments gave also further evidence of the synthetase active motif in (p)ppGpp producing enzymes. In *N. gonorrhoeae* it was shown that RelA alone is essential for (p)ppGpp production when the organism encounters nutritional stress [119].

Also in *V. cholerae* SpoT was unable to produce (p)ppGpp [153]. Conversely *E. coli*, *P. aeruginosa* [154], *B. subtilis* [155] and *Streptococcus equisimilis* [156] contain a (p)ppGpp producing SpoT or Rel enzyme, respectively. The GRXKH motif (active) was found in RelA, SpoT and Rel proteins which possess functional active (p)ppGpp synthetase. SpoT proteins who carry a GREKN motif (inactive) within their RelA/SpoT domain were unable to synthesize (p)ppGpp (Figure 7.1).

In addition, Hogg *et al.* 2004 characterized the functionality of the bifunctional Rel protein in *S. dysgalactiae* in more detail [157]. They described the absolutely conserved residues throughout the mono- and bifunctional Rel and SpoT homologs. They found the missense point mutations that lead to defective synthetase activities. Almost all of these missense point mutations were found in the synthetase domain of the SpoT proteins from *N. meningitidis* MC58/α522, *N. gonorrhoeae*, and *V. cholerae*.

Based on the work of Sajish *et al.* from 2009, the *RXKD* motif was found in 'bifunctional' RelA/SpoT homologues and *EXDD* motif in monofunctional proteins [152].

Together, this *in silico* analysis confirmed that SpoT synthetase of *N. meningitidis*, *N. gonorrhoeae*, and *V. cholerae* might be inactive.

To further analyze the physiology of the stringent response, the role of RelA under amino acid limiting conditions was tested by *in vitro* growth experiments in MMM. The growth experiments revealed that RelA is in both strains is required for growth in the absence of amino acids. In contrast to the wild-types, RelA deficient strains were unable to grow in MMM (Figure 6.6 A and Figure 6.6 E), with the difference that strain α522 has a general auxotrophy for cysteine and glutamine. In *E. coli* a *relA* deficient strain shows a growth resumption delay during transition from rich to minimal medium for around five hours, indicating the important role of RelA to regulate amino acid biosynthesis [158].

Taken together, RelA and thus (p)ppGpp is essential to signaling amino acid limiting conditions, probably for the biosynthesis of amino acids and to overcome such starvation conditions.

Furthermore, the addition of two amino acids to the MMM, cysteine and glutamine, showed a growth inhibitory effect in MC58. Especially cysteine exerted a strong growth inhibitory effect in the wild-type strain MC58 (Figure 6.6 C). This indicates that cysteine (and glutamine) somehow induces a starvation effect. In *E. coli* it is known that cysteine can induce an amino acid starvation effect, but the mechanism is still unclear [159].

Interestingly, the addition of cysteine and glutamine could not restore the growth defect in the RelA deficient strains. Only the supplementation of all 20 amino acids repaired the growth defect, suggesting that cysteine and glutamine are not enough to dispense the stringent response. Further investigations should analyze which amino acids exactly are sufficient to abstain RelA.

To analyze the global effect of the stringent response on gene expression in strain MC58 microarray experiments were performed in *relA* deletion and wild-type strains as well as in response to SHX. The observations will be discussed and compared to the model organism *E. coli*, although a RelA deficient *E. coli* strain cannot be compared to a meningococcal strain deficient in RelA, since SpoT is not able to produce ppGpp in *Neisseria* as discussed above.

The comparison of the transcription patterns of the MC58 wild-type and the mutant strain MC58Δ*relA* yielded an extremely complex pattern of gene expression and showed no significant differences in the COG classes of the encoded proteins around time points 30 and 40 minutes corresponding to mid logarithmic growth phase. At time point 60 minutes, only minor differences were observed, overrepresented classes were COG class S (unknown function) and X (not in COG), suggesting that there are many genes probably subject to stringent response regulation that are still uncharacterized in *Neisseria*. After 300 minutes of growth, when the bacteria come in to the early stationary phase, functional differences were more pronounced. This fits to the assumption that the stringent response, and in particular RelA, is important when nutrients get limited and the bacteria enter starvation conditions. Unfortunately, until now there is only little data existing that examined the transcriptional profile in terms of the stringent response in late logarithmic growth phase. Most of the genes for the TCA and the aerobic respiration were upregulated in the wild-type compared to the RelA deficient strain, indicating that (p)ppGpp is necessary to induce the stringent response. In an *E. coli* (p)ppGpp^0 strain is was also shown that the TCA cycle was down-regulated in response to isoleucine-starvation [82]. One would assume that SHX addition would lead to the same results as in the stringent response gene expression pattern. However, our data indicate that SHX mediated stringent response is somewhat different to the stringent response in late logarithmic growth phase. Significantly enriched COG classes were observable only at 10 and 30 minutes after SHX addition. This fits to the general knowledge that the SHX mediated stringent response is mounted immediately after exposure to SHX [81, 160]. Probably, after around 300 minutes of growth, SHX has no impact anymore. Ten and 30 minutes after SHX addition COG class M was significantly enriched among the differently expressed genes. This analysis revealed that mostly stress-related and cell membrane

associated pathways were upregulated which is also described in *E. coli* [81]. This confirms that the addition of SHX leads to the activation of the stringent response as described in the literature but the stringent response in late logarithmic growth phase differs from the SHX-mediated stringent control. The last condition compared the expression patterns of the RelA deficient strain with the RelA deficient strain exposed to SHX. Here, no enriched COG classes were found, which suggests that due to the lack of *relA* the expression profiles resulted in an unspecific response to overcome SHX.

7.3 The contribution of the stringent response to meningococcal carriage and invasive disease

In asymptomatic carrier state, meningococci colonize the nasopharynx without causing any adverse symptoms. Here the bacteria have to adhere to the mucosal surface and to survive in human saliva. The *ex vivo* survival experiments revealed that neither the wild-types nor the mutant strains were able to growth in human saliva. Gordon described already in 1916 an anti-meningococcal effect of human saliva [161], and a carriage study in 2003 compared meningococcal isolation rates in swabs of saliva (front of mouth), tonsils, and nasopharynx. Of the 258 participants, 32.2% were identified as carrying *N. meningitidis* in the nasopharynx, whereas tonsillar carriage was 19.4% and only one (0.4%) of the 258 saliva swab specimens was positive in saliva [162].

Together, this indicates that saliva has an anti-menigococcal property, and in this experimental setup no information about the virulence of a strain can be obtained.

Biofilm formation, which enhances resistance to antibiotics and provides some protection against the human immune system [163], increases also the stability to mechanical stress and might thus provide an advantage in nutrient poor conditions [164]. Here, the stringent response probably plays an important role. In *E. coli* it was shown that a *relAspoT* mutant has enhanced biofilm formation in rich medium and showed decreased biofilm formation in minimal medium compared to the wild-type. Surprisingly, the *relA* single mutant showed no differences compared to the wild-type strain [165]. A study with *Bordetella pertussis* described that in a defined medium that lacked casamino acids, iron, cysteine, ascorbic acid, nicotinamide, glutathione, magnesium and calcium (p)ppGpp^0 mutants showed a decreased biofilm formation compared to the wild-type [166]. Moreover, in *V. cholerae* biofilm formation is regulated by stringent response genes, and (p)ppGpp^0 mutants showed decreased production of biofilm in rich medium (LB) [167].

In this study, biofilm formation was tested in a semi-defined medium (10% PPM^{+}, 50% $NDM^{+/-}$ and 40% 1x PBS) in two variants, one with the addition of PolyVitex and one without the addition of PolyVitex. Both wild-type strains, but mainly strain α522 showed an enhanced biofilm formation in the nutrient rich medium compared to strain MC58, indicating that a nutrient rich environment triggers biofilm formation. Neil and Apicella discussed that the presence of meningococci in microcolonies on tonsillar tissue might indicate that a biofilm phenotype may be important for carriage [163]. The carrier strain α522 showed a significantly higher biofilm production than the hyperinvasive strain MC58 (Figure 6.20 A). The *relA* deficient mutants showed different results compared to their wild-types (Figure 6.20 B). Decreased biofilm formation (in both media) was only seen in the carriage, not in the invasive strain, suggesting that *relA*, and thus (p)ppGpp, is necessary for biofilm production in α522. Similar to *E. coli* [165], in both strains biofilm formation was enhanced in the *relAspoT* double mutant compared to the wild-type strains particular in nutrient rich conditions, but not in nutrient poor conditions (Figure 6.20 B). This indicates that the stringent response is involved in biofilm formation in a condition- dependent manner. Of course, the question remains whether biofilm formation on abiotic surfaces is similar to the colonization of bacteria on epithelial cells [168].

Even more so than in their propensity to form biofilms cell culture experiments revealed a general difference between the carriage and the invasive strain in their interaction with human cells (Figure 6.21). Both, adhesion and invasion rates were lower in strain α522 than in strain MC58. One explanation could be that some of the putative virulence genes which are present in strain MC58 are missing in strain α522. For example the carriage strain α522 lacks parts of the islands of horizontal transfer B and C, which encode for a two component secretion system involved in host cell interaction and adhesion [169]. Whereas the adhesion in the *relA* mutants was not affected, the invasion rate was significantly lower compared to the wild-types, indicating that RelA contributes to bacterial virulence. In other commensal or pathogenic bacteria it is suspected that (p)ppGpp plays a crucial role in host interaction [113]. For example, a *Salmonella enterica* serovar Gallinarum *relAspoT* double mutant, which lacks all (p)ppGpp synthesis, showed a strikingly reduced level of invasion (>90%) into human epithelial type 2 (HEp-2) cells [170], and also a *Campylobacter jejuni* strain defective in *spoT* showed decreased ability to colonize the host gut [171].

Taken together, the stringent response is likely to have an important role *in vivo* for colonization of the host and probably also for invasion when causing IMD.

When the bacteria penetrate the nasopharyngeal mucosa, they have to survive within the bloodstream. For the meningococcus, growth in blood appears to be an easy game since the carriage strain α522 and invasive strain MC58 were both able to grow in human whole blood (chapter 6.1.10). This indicates hat carriage and invasive strains cannot per se be distinguished in this *ex vivo* condition. However, there are differences in the expression profile of both strains, specifically in blood [134]. For instance, the expression of *relA* was significantly higher in the invasive strain MC58 compared to α522 in blood [134]. Even more surprising was the finding that the survival of strain α522 was *relA*-dependent, and also the α522 *relAspoT* mutant was unable to grow in human whole blood (Figure 6.22). This indicates that differences in the genetic background and transcription regulation of the strain contribute to differences in the *ex vivo* survival in blood.

When the bacteria resist the host defenses and replicate within the bloodstream, they can reach the CSF. For the survival in CSF the stringent response genes were not essential and all mutants showed growth comparable to the wild-type strains as fast as in rich medium. However, to reach the subarachnoid space and to replicate in CSF the bacteria have to penetrate the blood-brain barrier. For this step they have to get through endothelial cells. Further investigations should therefore examine differences between carriage and invasive strains and the role of the stringent response in the invasion into endothelial cells [172].

Overall, the question arises whether RelA is a potential virulence factor. As a definition, a virulence gene is a gene whose loss specifically impairs virulence but not viability in rich media and which should be associated with pathogenic but not with non-pathogenic strains of a species [173, 174]. This extensive characterization of the stringent response in the *ex vivo* survival model in two different serogroup B meningococci revealed different results with respect to the function of RelA in varying environmental conditions.

In both strains RelA is not essential in nutrient rich conditions. Also in both strains biofilm formation was slightly decreased in the *relA* mutant compared to the wild-type strain (chapter 6.1.8) as well as the invasion into human epithelial cells (chapter 6.1.9). However, for the survival in human whole blood *relA* appears to be essential only for the carriage strain (chapter 6.1.10), indicating that the results cannot be transferred over the entire species. Therefore, RelA can only be considered as a virulence factor in a strain dependent manner and the application of RelA as potential drug target must therefore be evaluated critically [175].

7.4 Epistatic effects of ATR

The regulation of *relA* appears to be different between the carriage strain α522 and the hyperinvasive strain MC58, and genome-wide comparisons revealed that an ATR is integrated in the promoter region of *relA* only in strain α522. As described in chapter 6.2.2, the ATR element in the *relA* promoter region has hallmark characteristics of MITEs in other microorganisms.

MITEs are widely distributed within bacteria, plants and animals [37], but ATRs seem to be almost *Neisseria* specific. NCBI BLASTn searches revealed that the only non-neisserial ATR is found in *Peptoclostridum difficile* (assembly 7032989). In addition, in cyanobacteria there is also a MITE described, called '*Nezha',* which seems to be very similar to the neisserial 'ATRs' [176]. They show up the same features in their structure, size and distribution, suggesting that these kinds of MITEs are very successful systems, but species-specific [176].

7.4.1 **Genome distribution and mobility**

Little is known about the activity and transposition of MITEs, but there is evidence on how the 'ATRs' spread within the genome (this work, [37]). The distribution within the chromosome suggests that these genetic elements are not spread randomly (chapter 6.2.2).

In silico analysis revealed that the ATRs of MC58 are significantly placed in intergenic regions. Moreover, the large part of the ATRs was significantly inserted between convergent genes, although 74% of 2063 genes were collinear. With exception of ATR_{relA} in strain α522, no ATR was placed between divergent organized genes.

Together this indicates that the location in putative promoter regions might be under negative selection possibly due to disadvantageous effects on the expression of neighboring genes.

However, not only strain α522 has an insertion sequence in the *relA* upstream region. Twenty-three fully sequenced genomes of different *Neisseria* species were analyzed for putative inserted DNA sequences at their *relA/grxB* loci. Multiple alignments of intergenic regions of 23 *Neisseria* strains generated by ClustalW revealed that four different groups of intergenic regions are present at the *relA/grxB* locus (Figure 7.2).

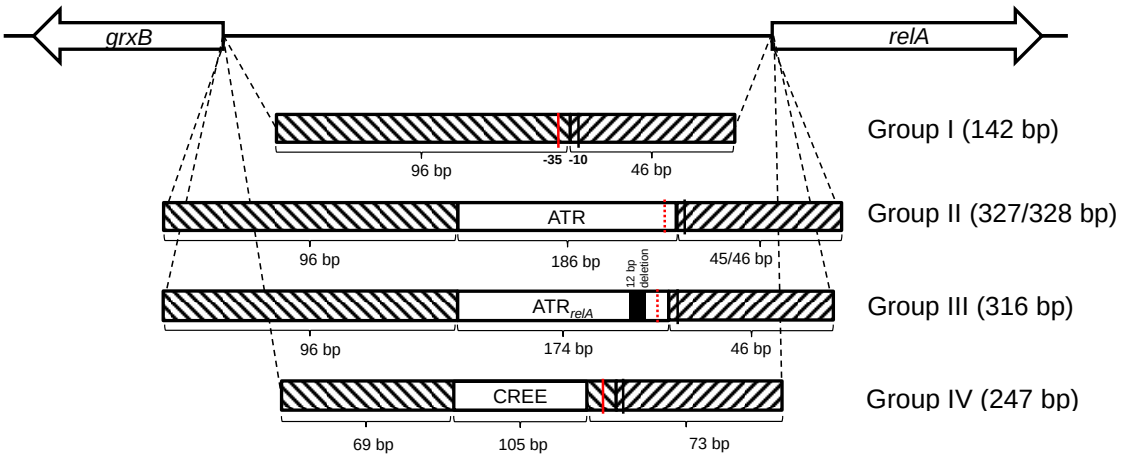

Figure 7.2 Schematic organizations of the *relA/grxB* loci in *Neisseriaceae*

Depicted is a schematic representation of four different intergenic regions at the *relA/grxB* locus, from 23 completely sequenced neisserial genomes. Promoter regions of *relA* and *grxB* were predicted by using BPROM (prediction of bacterial promoters, [108]). Black vertical lines indicate the -10 box of the *relA* promoter. Red vertical lines indicate the -35 box and red dotted lines indicate a changed -30 box of the *relA* promoter.

The *in silico* analysis revealed that three groups harbor an insertion element and in one group, where MC58 belongs to, no insertion was found. Seventy-four percent of the 23 neisserial strains harbor an insertion element at their *relA* locus. Three different DNA sequence elements were found, the already described ATRs, ATR_{relA} and CREE. Like ATRs, CREEs also belong to the group of MITEs [38]. Table 7.1 lists the different MITEs found at the *relA/grxB* locus from different *Neisseria* species.

Table 7.1 *Distribution of MITEs in Neisseriaceae at the relA/grxB locus.*

Group	Strain	SG	Accession No	IR (bp)	MITE
Group I	*Nm* MC58	B	AE002098.2	142	-
	Nm M04-240196	B	CP002423.1	142	-
	Nm H44/76	B	NC_017516	142	-
	Ng FA1090	-	AE004969.1	142	-
	Ng NCCP11945	-	CP001050.1	142	-
	Ng NG08107	-	NC_017511	142	-
Group II	*Nm* FAM18	C	AM421808.1	327	ATR
	Nm α153	E	Schoen *et al*., 2008 [31]	328	ATR
	Nm α275	W	Schoen *et al*., 2008 [31]	327	ATR
	Nm NZ-05/33	B	NC_017518	328	ATR
	Nm DE10444	Y	unpublished	327	ATR

Group	Strain	SG	Accession No	IR (bp)	MITE
Group II	*Nm* M01-240149	B	NC_017514	328	ATR
	Nm M01-240355	B	CP002422.1	327	ATR
	Nm G2136	B	CP002419.1	327	ATR
	Nm WUE2121	C	unpublished	327	ATR
	Nm 053443	C	CP000381.1	328	ATR
Group III	*Nm* α522	B	This work and Ampattu & Hagmann *et al*., 2016 (submitted)	316	ATR_{relA}
	Nm α710	B	CP001561.1	316	ATR_{relA}
	Nm WUE2594	A	FR774048.1	316	ATR_{relA}
	Nm Z2491	A	AL157959.1	316	ATR_{relA}
Group IV	*Nm* α14	cnl	AM889136.1	247	CREE
	Nm 8013	C	FM999788.1	247	CREE
	Nl 020-06	-	FN995097.1	247	CREE

Abbreviations: *Ng, N. gonorrhoeae*; *Nm, N. meningitidis*; *Nl, N. lactamica*; IR, intergenic region of *relA/grxB*.

The first group comprises six strains, including MC58, which do not have any insertion element at the *relA/grxB* locus. The second and biggest group comprises 10 *Neisseria* strains which all harbor a full length ATR in the *relA* promoter region. In the third group, where strain α522 belongs to, four strains with the 12 bp shorter ATR_{relA} were found. The last group consists of three strains which have a CREE integrated in the intergenic region. The high abundance of an insertion element at the *relA* locus in *Neisseria* indicates that strain α522 is not a special case.

Genome comparisons also provided some indication on how MITEs might spread within the bacterial chromosome. Genome analyses of strain MC58 revealed five transposases (NMB0919, NMB0991, NMB1399, NMB1539 and NMB1601) that possess the same TIRs as ATR/ATR_{relA}, suggesting that these transposases might be able to transpose ATRs *in trans* in the chromosome. All of these transposases belong to the *IS1106* family [130]. Salvatore *et al*. 2001 characterized the flanking regions of the *IS1106* copies in strain Z2491 and described the putative control elements [130].

They also could not find a consensus target site but a repeat element (5'-ATTCCC-3', RS3) which is located in the promoter region and downstream of several *IS1106* elements, suggesting a preferred target site selection. The IRL (inverted repeat left) contains a putative -35 (5'-TTTGCAA-3') box which is the same in the TIR of

ATR/ATR$_{relA,}$ a -10 (5'-TAAATT-3') and a Shine-Dalgarno (5'-AGGGGA-3') box as well as a 14 bp long IR (5'-AAAATCCCCTAAAT-3') which might affect expression of neighboring genes in a polar manner. These elements were all found in the upstream regions of the five *IS1106* transposases in strain MC58.

7.4.2 **Polar effect on gene expression**

In silico analysis, as already discussed above (chapter 7.4.1), revealed that ATR$_{relA}$ is preferentially integrated in intergenic regions downstream of the two flanking coding sequences. It is known that MITEs contain controlling elements such as strong promoters [45], terminators and IHF binding sites [177], but little is known about the transcriptional control of downstream genes encoding a crucial protein such as the (p)ppGpp synthetase. Therefore, qRT-PCR experiments analyzed the *in cis* effect of ATR$_{relA}$ on the transcription of *relA* and *grxB*. The experiments revealed that ATR$_{relA}$ can affect the expression in a strain- and growth phase- dependent manner. Whereas the integration of ATR$_{relA}$ led to a decrease in the mRNA levels of *grxB* in both growth phases compared to the strains without an ATR$_{relA}$, in mid logarithmic growth phase the expression of *relA* was significantly increased, independed of the genetic background of the strain. However, in late logarithmic growth phase the effect of ATR$_{relA}$ was strain specific. Whereas in strain α522 ATR$_{relA}$ led to a down regulation of *relA*, ATR$_{relA}$ in strain MC58 resulted in an increased expression of *relA* (Figure 6.29 A). The results confirm that ATR$_{relA}$ is able to effect the regulation of adjacent genes like *relA*. Further investigations should examine the expression in other growth phases and different conditions.

In the *ex vivo* survival assay, were the strains were exposed to human saliva, blood and CSF, the ATR$_{relA}$ mutants revealed differences only in blood compared to the wild-type strains. Survival of strain α522 in human blood depended on the presence of ATR$_{relA}$ at the *relA* - *grxB* locus, suggesting that ATR$_{relA}$ harbors binding sites for regulatory proteins, which might influence the transcription of *relA,* required for survival in human blood. The growth of strain MC58 harboring the ATR$_{relA}$ in the promoter region of *relA* was unaffected, which fits to the results that strain MC58 does not depend on *relA* in the survival in human whole blood.

7.5 Conclusion and outlook

In vitro experiments revealed that RelA is essential to invade into epithelial cells and that the stringent response is important for blood stream survival and contributes to virulence in a strain specific-manner. Since the stringent response contributes to meningococcal survival in human blood in strain specific manner it thus constitutes a novel virulence factor in this commensal pathogen.

Most studies focus on differences in the sequence of protein coding genes rather than on differences in intergenic regions changing gene expression. This study found that an intergenic element might affect virulence in a strain-dependent manner. The impaired growth of the α522ΔATR$_{relA}$ in whole human blood gives evidence that regulatory elements, such as the ATR upstream of *relA* can contribute to virulence in a strain- and condition-dependent manner. This provides an example of how regulatory evolution via the integration of non-coding MITEs into promoter regions might contribute to fitness and consequently virulence differences among bacterial strains.

Furthermore, the finding that L-glutamine or L-cysteine alone or in combination improved the growth of strain MC58 *prelA::p*ATR$_{relA}$ compared to the wild-type suggests that ATR/ATR$_{relA}$ might possess binding sites for different regulators and/or senses amino acid availability.

Moreover, this is the first time that a biological function of a MITE is described. In conclusion, these data suggest that virulence might be related to the way how meningococci accomplish growth with the host environment (Figure 7.3).

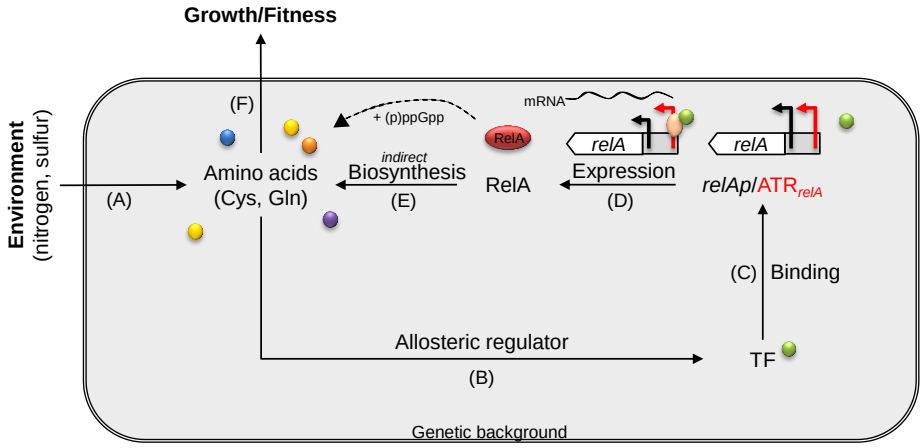

Figure 7.3 Hypothesis

In dependence of nutrient availability (for instance nitrogen and sulfur) and the genetic background of the strain, amino acids are synthesized (A). The availability of the amino acids in the cell is presumably mediated by an allosteric regulator that activates a TF (B). The specific TF binds to ATR$_{relA}$ (C) and activates the expression of *relA* (D). RelA indirectly leads to the stringent response and the biosynthesis of necessary amino acids (E) and thus decides on potential growth or the fitness of the cell.

In dependency of environmental conditions, amino acids such as the availability of amino acids and other nutrients, are either taken up or synthesized de novo within the bacterial cell (Figure 7.3 A). The availability of the amino acids like cysteine and glutamine in the cell is possibly sensed by an allosteric regulator that activates a TF (Figure 7.3 B). This specific TF binds either to ATR$_{relA}$ or outside of ATR$_{relA}$ within the *relA* promoter region and affects and the expression of *relA* (Figure 7.3 C). RelA in turn functions as a mediator for stresses such as amino acid starvation (Figure 7.3 D) and via the stringent response regulates the biosynthesis of necessary amino acids (Figure 7.3 E). It thus affects growth and fitness of the cell in response to environmental stimuli dependent on, amongst others, on the presence/absence of ATR$_{relA}$ (Figure 7.3 F).

Future work needs to focus on transcriptome analyses in a larger and genetically more representative set of meningococcal strains under different conditions. In addition, to unravel regulatory proteins which alter gene expression, electrophoretic mobility shift assays could be used to analyze binding partners to ATR.

8 References

1. Kawai M, Uchiyama I, Kobayashi I: **Genome comparison in silico in Neisseria suggests integration of filamentous bacteriophages by their own transposase**. *DNA research : an international journal for rapid publication of reports on genes and genomes* 2005, **12**(6):389-401.
2. Claus H, Maiden MC, Wilson DJ, McCarthy ND, Jolley KA, Urwin R, Hessler F, Frosch M, Vogel U: **Genetic analysis of meningococci carried by children and young adults**. *The Journal of infectious diseases* 2005, **191**(8):1263-1271.
3. Yazdankhah SP, Caugant DA: **Neisseria meningitidis: an overview of the carriage state**. *Journal of medical microbiology* 2004, **53**(Pt 9):821-832.
4. Stephens DS, Greenwood B, Brandtzaeg P: **Epidemic meningitis, meningococcaemia, and Neisseria meningitidis**. *Lancet (London, England)* 2007, **369**(9580):2196-2210.
5. Rosenstein NE, Perkins BA, Stephens DS, Popovic T, Hughes JM: **Meningococcal disease**. *The New England journal of medicine* 2001, **344**(18):1378-1388.
6. Yi K, Rasmussen AW, Gudlavalleti SK, Stephens DS, Stojiljkovic I: **Biofilm Formation by Neisseria meningitidis**. *Infection and immunity* 2004, **72**(10):6132-6138.
7. Coureuil M, Join-Lambert O, Lécuyer H, Bourdoulous S, Marullo S, Nassif X: **Pathogenesis of Meningococcemia**. *Cold Spring Harbor Perspectives in Medicine* 2013, **3**(6):a012393.
8. Rouphael NG, Stephens DS: **Neisseria meningitidis: biology, microbiology, and epidemiology**. *Methods in molecular biology (Clifton, NJ)* 2012, **799**:1-20.
9. Bosis S, Mayer A, Esposito S: **Meningococcal disease in childhood: epidemiology, clinical features and prevention**. *Journal of preventive medicine and hygiene* 2015, **56**(3):E121-124.
10. Halperin SA, Bettinger JA, Greenwood B, Harrison LH, Jelfs J, Ladhani SN, McIntyre P, Ramsay ME, Safadi MA: **The changing and dynamic epidemiology of meningococcal disease**. *Vaccine* 2012, **30 Suppl 2**:B26-36.
11. Tan LK, Carlone GM, Borrow R: **Advances in the development of vaccines against Neisseria meningitidis**. *The New England journal of medicine* 2010, **362**(16):1511-1520.
12. Morand P, Rudel T: **Genetics, Structure and Function of Pili**. *In: Frosch M, Maiden M, editors Handbook of Meningococcal Disease* 2006, **Wiley-VCH, Weinheim**:247.
13. Pallen MJ, Wren BW: **Bacterial pathogenomics**. *Nature* 2007, **449**(7164):835-842.
14. Schoen C, Tettelin H, Parkhill J, Frosch M: **Genome flexibility in Neisseria meningitidis**. *Vaccine* 2009, **27 Suppl 2**:B103-111.
15. Marri PR, Paniscus M, Weyand NJ, Rendon MA, Calton CM, Hernandez DR, Higashi DL, Sodergren E, Weinstock GM, Rounsley SD *et al*: **Genome sequencing reveals widespread virulence gene exchange among human Neisseria species**. *PLoS One* 2010, **5**(7):e11835.
16. Caugant DA, Maiden MC: **Meningococcal carriage and disease-population biology and evolution**. *Vaccine* 2009, **27 Suppl 2**:B64-70.
17. Buckee CO, Jolley KA, Recker M, Penman B, Kriz P, Gupta S, Maiden MC: **Role of selection in the emergence of lineages and the evolution of virulence in Neisseria meningitidis**. *Proceedings of the National Academy of Sciences of the United States of America* 2008, **105**(39):15082-15087.
18. Schoen C, Kischkies L, Elias J, Ampattu BJ: **Metabolism and virulence in Neisseria meningitidis**. *Frontiers in cellular and infection microbiology* 2014, **4**:114.

19. Tettelin H, Saunders NJ, Heidelberg J, Jeffries AC, Nelson KE, Eisen JA, Ketchum KA, Hood DW, Peden JF, Dodson RJ *et al*: **Complete genome sequence of Neisseria meningitidis serogroup B strain MC58**. *Science* 2000, **287**(5459):1809-1815.
20. McGuinness BT, Clarke IN, Lambden PR, Barlow AK, Heckels JE, Poolman JT, Jones DM: **Point mutation in meningococcal por A gene associated with increased endemic disease**. *The Lancet* 1991, **337**(8740):514-517.
21. Rutherford K, Parkhill J, Crook J, Horsnell T, Rice P, Rajandream MA, Barrell B: **Artemis: sequence visualization and annotation**. *Bioinformatics* 2000, **16**(10):944-945.
22. Joseph B, Schwarz RF, Linke B, Blom J, Becker A, Claus H, Goesmann A, Frosch M, Muller T, Vogel U *et al*: **Virulence evolution of the human pathogen Neisseria meningitidis by recombination in the core and accessory genome**. *PLoS One* 2011, **6**(4):e18441.
23. Maiden MC, Malorny B, Achtman M: **A global gene pool in the neisseriae**. *Mol Microbiol* 1996, **21**(6):1297-1298.
24. Rotman E, Seifert HS: **The genetics of Neisseria species**. *Annual review of genetics* 2014, **48**:405-431.
25. Parkhill J, Achtman M, James KD, Bentley SD, Churcher C, Klee SR, Morelli G, Basham D, Brown D, Chillingworth T *et al*: **Complete DNA sequence of a serogroup A strain of Neisseria meningitidis Z2491**. *Nature* 2000, **404**(6777):502-506.
26. Schoen C, Tettelin H, Parkhill J, Frosch M: **Genome flexibility in Neisseria meningitidis**. *Vaccine* 2009, **27**(Suppl 2):B103-B111.
27. Davidsen T, Rodland EA, Lagesen K, Seeberg E, Rognes T, Tonjum T: **Biased distribution of DNA uptake sequences towards genome maintenance genes**. *Nucleic acids research* 2004, **32**(3):1050-1058.
28. Spratt BG, Bowler LD, Zhang QY, Zhou J, Smith JM: **Role of interspecies transfer of chromosomal genes in the evolution of penicillin resistance in pathogenic and commensal Neisseria species**. *Journal of molecular evolution* 1992, **34**(2):115-125.
29. Frosch M, Meyer TF: **Transformation-mediated exchange of virulence determinants by co-cultivation of pathogenic Neisseriae**. *FEMS microbiology letters* 1992, **100**(1-3):345-349.
30. Linz B, Schenker M, Zhu P, Achtman M: **Frequent interspecific genetic exchange between commensal Neisseriae and Neisseria meningitidis**. *Mol Microbiol* 2000, **36**(5):1049-1058.
31. Schoen C, Blom J, Claus H, Schramm-Gluck A, Brandt P, Muller T, Goesmann A, Joseph B, Konietzny S, Kurzai O *et al*: **Whole-genome comparison of disease and carriage strains provides insights into virulence evolution in Neisseria meningitidis**. *Proceedings of the National Academy of Sciences of the United States of America* 2008, **105**(9):3473-3478.
32. Bentley SD, Vernikos GS, Snyder LA, Churcher C, Arrowsmith C, Chillingworth T, Cronin A, Davis PH, Holroyd NE, Jagels K *et al*: **Meningococcal genetic variation mechanisms viewed through comparative analysis of serogroup C strain FAM18**. *PLoS genetics* 2007, **3**(2):e23.
33. De Gregorio E, Abrescia C, Carlomagno MS, Di Nocera PP: **Asymmetrical distribution of Neisseria miniature insertion sequence DNA repeats among pathogenic and nonpathogenic Neisseria strains**. *Infection and immunity* 2003, **71**(7):4217-4221.
34. De Gregorio E, Abrescia C, Carlomagno MS, Di Nocera PP: **Ribonuclease III-mediated processing of specific Neisseria meningitidis mRNAs**. *The Biochemical journal* 2003, **374**(Pt 3):799-805.

35. Jiang N, Feschotte C, Zhang X, Wessler SR: **Using rice to understand the origin and amplification of miniature inverted repeat transposable elements (MITEs)**. *Current Opinion in Plant Biology* 2004, **7**(2):115-119.
36. Brugger K, Redder P, She Q, Confalonieri F, Zivanovic Y, Garrett RA: **Mobile elements in archaeal genomes**. *FEMS microbiology letters* 2002, **206**(2):131-141.
37. Fattash I, Rooke R, Wong A, Hui C, Luu T, Bhardwaj P, Yang G: **Miniature inverted-repeat transposable elements: discovery, distribution, and activity**. *Genome / National Research Council Canada = Genome / Conseil national de recherches Canada* 2013, **56**(9):475-486.
38. Delihas N: **Impact of small repeat sequences on bacterial genome evolution**. *Genome biology and evolution* 2011, **3**:959-973.
39. Mahillon J, Chandler M: **Insertion sequences**. *Microbiology and molecular biology reviews : MMBR* 1998, **62**(3):725-774.
40. Correia FF, Inouye S, Inouye M: **A family of small repeated elements with some transposon-like properties in the genome of Neisseria gonorrhoeae**. *The Journal of biological chemistry* 1988, **263**(25):12194-12198.
41. Buisine N, Tang CM, Chalmers R: **Transposon-like Correia elements: structure, distribution and genetic exchange between pathogenic Neisseria sp**. *FEBS letters* 2002, **522**(1-3):52-58.
42. Snyder LA, Cole JA, Pallen MJ: **Comparative analysis of two Neisseria gonorrhoeae genome sequences reveals evidence of mobilization of Correia Repeat Enclosed Elements and their role in regulation**. *BMC Genomics* 2009, **10**:70.
43. Black CG, Fyfe JA, Davies JK: **A promoter associated with the neisserial repeat can be used to transcribe the uvrB gene from Neisseria gonorrhoeae**. *J Bacteriol* 1995, **177**(8):1952-1958.
44. Snyder LA, Shafer WM, Saunders NJ: **Divergence and transcriptional analysis of the division cell wall (dcw) gene cluster in Neisseria spp**. *Mol Microbiol* 2003, **47**(2):431-442.
45. Siddique A, Buisine N, Chalmers R: **The transposon-like Correia elements encode numerous strong promoters and provide a potential new mechanism for phase variation in the meningococcus**. *PLoS genetics* 2011, **7**(1):e1001277.
46. De Gregorio E, Abrescia C, Carlomagno MS, Di Nocera PP: **The abundant class of nemis repeats provides RNA substrates for ribonuclease III in Neisseriae**. *Biochimica et biophysica acta* 2002, **1576**(1-2):39-44.
47. Finlay BB, Falkow S: **Common themes in microbial pathogenicity revisited**. *Microbiology and molecular biology reviews : MMBR* 1997, **61**(2):136-169.
48. Stock JB, Ninfa AJ, Stock AM: **Protein phosphorylation and regulation of adaptive responses in bacteria**. *Microbiological Reviews* 1989, **53**(4):450-490.
49. Oshima T, Aiba H, Masuda Y, Kanaya S, Sugiura M, Wanner BL, Mori H, Mizuno T: **Transcriptome analysis of all two-component regulatory system mutants of Escherichia coli K-12**. *Molecular Microbiology* 2002, **46**(1):281-291.
50. Yamamoto K, Hirao K, Oshima T, Aiba H, Utsumi R, Ishihama A: **Functional characterization in vitro of all two-component signal transduction systems from Escherichia coli**. *The Journal of biological chemistry* 2005, **280**(2):1448-1456.
51. Jamet A, Rousseau C, Monfort J-B, Frapy E, Nassif X, Martin P: **A two-component system is required for colonization of host cells by meningococcus**. *Microbiology (Reading, England)* 2009, **155**(7):2288-2295.
52. Tzeng Y-L, Zhou X, Bao S, Zhao S, Noble C, Stephens DS: **Autoregulation of the MisR/MisS Two-Component Signal Transduction System in Neisseria meningitidis**. *Journal of Bacteriology* 2006, **188**(14):5055-5065.

53. Newcombe J, Jeynes JC, Mendoza E, Hinds J, Marsden GL, Stabler RA, Marti M, McFadden JJ: **Phenotypic and Transcriptional Characterization of the Meningococcal PhoPQ System, a Magnesium-Sensing Two-Component Regulatory System That Controls Genes Involved in Remodeling the Meningococcal Cell Surface**. *Journal of Bacteriology* 2005, **187**(14):4967-4975.
54. Tzeng Y-L, Kahler CM, Zhang X, Stephens DS: **MisR/MisS Two-Component Regulon in Neisseria meningitidis**. *Infection and immunity* 2008, **76**(2):704-716.
55. Johnson CR, Newcombe J, Thorne S, Borde HA, Eales-Reynolds LJ, Gorringe AR, Funnell SGP, McFadden JJ: **Generation and characterization of a PhoP homologue mutant of Neisseria meningitidis**. *Molecular Microbiology* 2001, **39**(5):1345-1355.
56. Madan Babu M, Teichmann SA: **Evolution of transcription factors and the gene regulatory network in Escherichia coli**. *Nucleic acids research* 2003, **31**(4):1234-1244.
57. Vallenet D, Belda E, Calteau A, Cruveiller S, Engelen S, Lajus A, Le Fevre F, Longin C, Mornico D, Roche D *et al*: **MicroScope-an integrated microbial resource for the curation and comparative analysis of genomic and metabolic data**. *Nucleic acids research* 2013, **41**(Database issue):D636-647.
58. Delany I, Rappuoli R, Scarlato V: **Fur functions as an activator and as a repressor of putative virulence genes in Neisseria meningitidis**. *Mol Microbiol* 2004, **52**(4):1081-1090.
59. Sainsbury S, Ren J, Nettleship JE, Saunders NJ, Stuart DI, Owens RJ: **The structure of a reduced form of OxyR from Neisseria meningitidis**. *BMC structural biology* 2010, **10**:10.
60. Ieva R, Roncarati D, Metruccio MM, Seib KL, Scarlato V, Delany I: **OxyR tightly regulates catalase expression in Neisseria meningitidis through both repression and activation mechanisms**. *Mol Microbiol* 2008, **70**(5):1152-1165.
61. Ren J, Sainsbury S, Combs SE, Capper RG, Jordan PW, Berrow NS, Stammers DK, Saunders NJ, Owens RJ: **The structure and transcriptional analysis of a global regulator from Neisseria meningitidis**. *The Journal of biological chemistry* 2007, **282**(19):14655-14664.
62. Gunesekere IC, Kahler CM, Ryan CS, Snyder LAS, Saunders NJ, Rood JI, Davies JK: **Ecf, an Alternative Sigma Factor from Neisseria gonorrhoeae, Controls Expression of msrAB, Which Encodes Methionine Sulfoxide Reductase**. *Journal of Bacteriology* 2006, **188**(10):3463-3469.
63. Gruber TM, Gross CA: **Multiple sigma subunits and the partitioning of bacterial transcription space**. *Annual review of microbiology* 2003, **57**:441-466.
64. Sharma UK, Chatterji D: **Transcriptional switching in Escherichia coli during stress and starvation by modulation of sigma activity**. *FEMS microbiology reviews* 2010, **34**(5):646-657.
65. Gunesekere IC, Kahler CM, Powell DR, Snyder LAS, Saunders NJ, Rood JI, Davies JK: **Comparison of the RpoH-Dependent Regulon and General Stress Response in Neisseria gonorrhoeae**. *Journal of Bacteriology* 2006, **188**(13):4769-4776.
66. Laskos L, Dillard JP, Seifert HS, Fyfe JA, Davies JK: **The pathogenic neisseriae contain an inactive rpoN gene and do not utilize the pilE sigma54 promoter**. *Gene* 1998, **208**(1):95-102.
67. Hopman CT, Speijer D, van der Ende A, Pannekoek Y: **Identification of a novel anti-sigmaE factor in Neisseria meningitidis**. *BMC microbiology* 2010, **10**:164.
68. Huis in 't Veld RAG, Willemsen AM, van Kampen AHC, Bradley EJ, Baas F, Pannekoek Y, van der Ende A: **Deep Sequencing Whole Transcriptome Exploration of the σ(E) Regulon in Neisseria meningitidis**. *PLoS ONE* 2011, **6**(12):e29002.

69. Haines-Menges B, Whitaker WB, Boyd EF: **Alternative sigma factor RpoE is important for Vibrio parahaemolyticus cell envelope stress response and intestinal colonization**. *Infection and immunity* 2014, **82**(9):3667-3677.
70. Palonen E, Lindstrom M, Somervuo P, Korkeala H: **Alternative sigma factor sigmaE has an important role in stress tolerance of Yersinia pseudotuberculosis IP32953**. *Applied and environmental microbiology* 2013, **79**(19):5970-5977.
71. Abromaitis S, Koehler JE: **The Bartonella quintana extracytoplasmic function sigma factor RpoE has a role in bacterial adaptation to the arthropod vector environment**. *J Bacteriol* 2013, **195**(11):2662-2674.
72. Liu MC, Kuo KT, Chien HF, Tsai YL, Liaw SJ: **New aspects of RpoE in uropathogenic Proteus mirabilis**. *Infection and immunity* 2015, **83**(3):966-977.
73. Perez JC, Groisman EA: **Evolution of transcriptional regulatory circuits in bacteria**. *Cell* 2009, **138**(2):233-244.
74. Winfield MD, Groisman EA: **Phenotypic differences between Salmonella and Escherichia coli resulting from the disparate regulation of homologous genes**. *Proceedings of the National Academy of Sciences of the United States of America* 2004, **101**(49):17162-17167.
75. Escobar-Paramo P, Clermont O, Blanc-Potard AB, Bui H, Le Bouguenec C, Denamur E: **A specific genetic background is required for acquisition and expression of virulence factors in Escherichia coli**. *Molecular biology and evolution* 2004, **21**(6):1085-1094.
76. Methot PO, Alizon S: **What is a pathogen? Toward a process view of host-parasite interactions**. *Virulence* 2014, **5**(8):775-785.
77. Zhang YJ, Rubin EJ: **Feast or famine: the host-pathogen battle over amino acids**. *Cellular microbiology* 2013, **15**(7):1079-1087.
78. Cashel M: **The control of ribonucleic acid synthesis in Escherichia coli. IV. Relevance of unusual phosphorylated compounds from amino acid-starved stringent strains**. *The Journal of biological chemistry* 1969, **244**(12):3133-3141.
79. Ross W, Vrentas CE, Sanchez-Vazquez P, Gaal T, Gourse RL: **The Magic Spot: A ppGpp Binding Site on E. coli RNA Polymerase Responsible for Regulation of Transcription Initiation**. *Molecular cell* 2013, **50**(3):420-429.
80. Dalebroux ZD, Swanson MS: **ppGpp: magic beyond RNA polymerase**. *Nat Rev Micro* 2012, **10**(3):203-212.
81. Durfee T, Hansen AM, Zhi H, Blattner FR, Jin DJ: **Transcription profiling of the stringent response in Escherichia coli**. *J Bacteriol* 2008, **190**(3):1084-1096.
82. Traxler MF, Summers SM, Nguyen HT, Zacharia VM, Hightower GA, Smith JT, Conway T: **The global, ppGpp-mediated stringent response to amino acid starvation in Escherichia coli**. *Mol Microbiol* 2008, **68**(5):1128-1148.
83. Haseltine WA, Block R: **Synthesis of guanosine tetra- and pentaphosphate requires the presence of a codon-specific, uncharged transfer ribonucleic acid in the acceptor site of ribosomes**. *Proceedings of the National Academy of Sciences of the United States of America* 1973, **70**(5):1564-1568.
84. Battesti A, Bouveret E: **Acyl carrier protein/SpoT interaction, the switch linking SpoT-dependent stress response to fatty acid metabolism**. *Mol Microbiol* 2006, **62**(4):1048-1063.
85. Vinella D, Albrecht C, Cashel M, D'Ari R: **Iron limitation induces SpoT-dependent accumulation of ppGpp in Escherichia coli**. *Mol Microbiol* 2005, **56**(4):958-970.
86. Doniselli N, Rodriguez-Aliaga P, Amidani D, Bardales JA, Bustamante C, Guerra DG, Rivetti C: **New insights into the regulatory mechanisms of ppGpp and DksA on Escherichia coli RNA polymerase-promoter complex**. *Nucleic acids research* 2015, **43**(10):5249-5262.
87. Osterberg S, del Peso-Santos T, Shingler V: **Regulation of alternative sigma factor use**. *Annual review of microbiology* 2011, **65**:37-55.

88. Dalebroux ZD, Svensson SL, Gaynor EC, Swanson MS: **ppGpp conjures bacterial virulence**. *Microbiology and molecular biology reviews : MMBR* 2010, **74**(2):171-199.
89. Mittenhuber G: **Comparative genomics and evolution of genes encoding bacterial (p)ppGpp synthetases/hydrolases (the Rel, RelA and SpoT proteins)**. *Journal of molecular microbiology and biotechnology* 2001, **3**(4):585-600.
90. Pal RR, Das B, Dasgupta S, Bhadra RK: **Genetic components of stringent response in Vibrio cholerae**. *Indian J Med Res* 2011, **133**:212-217.
91. Pizarro-Cerda J, Tedin K: **The bacterial signal molecule, ppGpp, regulates Salmonella virulence gene expression**. *Mol Microbiol* 2004, **52**(6):1827-1844.
92. Klinkenberg LG, Lee JH, Bishai WR, Karakousis PC: **The stringent response is required for full virulence of Mycobacterium tuberculosis in guinea pigs**. *The Journal of infectious diseases* 2010, **202**(9):1397-1404.
93. Vogt SL, Green C, Stevens KM, Day B, Erickson DL, Woods DE, Storey DG: **The stringent response is essential for Pseudomonas aeruginosa virulence in the rat lung agar bead and Drosophila melanogaster feeding models of infection**. *Infection and immunity* 2011, **79**(10):4094-4104.
94. Lappann M, Haagensen JA, Claus H, Vogel U, Molin S: **Meningococcal biofilm formation: structure, development and phenotypes in a standardized continuous flow system**. *Mol Microbiol* 2006, **62**(5):1292-1309.
95. Baart GJ, Zomer B, de Haan A, van der Pol LA, Beuvery EC, Tramper J, Martens DE: **Modeling Neisseria meningitidis metabolism: from genome to metabolic fluxes**. *Genome biology* 2007, **8**(7):R136.
96. Archibald FS, DeVoe IW: **Iron in Neisseria meningitidis: minimum requirements, effects of limitation, and characteristics of uptake**. *J Bacteriol* 1978, **136**(1):35-48.
97. Peterson WD, Jr., Stulberg CS, Simpson WF: **A permanent heteroploid human cell line with type B glucose-6-phosphate dehydrogenase**. *Proceedings of the Society for Experimental Biology and Medicine Society for Experimental Biology and Medicine (New York, NY)* 1971, **136**(4):1187-1191.
98. Peterson WD, Jr., Stulberg CS, Swanborg NK, Robinson AR: **Glucose-6-phosphate dehydrogenase isoenzymes in human cell cultures determined by sucrose-agar gel and cellulose acetate zymograms**. *Proceedings of the Society for Experimental Biology and Medicine Society for Experimental Biology and Medicine (New York, NY)* 1968, **128**(3):772-776.
99. Sambrook J, Russell DW: **Rapid and Efficient Site-directed Mutagenesis by the Single-tube Megaprimer PCR Method**. *CSH protocols* 2006, **2006**(1).
100. Livak KJ, Schmittgen TD: **Analysis of relative gene expression data using real-time quantitative PCR and the 2(-Delta Delta C(T)) Method**. *Methods (San Diego, Calif)* 2001, **25**(4):402-408.
101. Schwarz R, Joseph B, Gerlach G, Schramm-Gluck A, Engelhard K, Frosch M, Muller T, Schoen C: **Evaluation of one- and two-color gene expression arrays for microbial comparative genome hybridization analyses in routine applications**. *Journal of clinical microbiology* 2010, **48**(9):3105-3110.
102. RC T: **R: A Language and Environment for Statistical Computing.** *Vienna, Austria: R Foundation for Statistical Computing* 2014.
103. Smyth G: **Limma: linear models for microarray data**. *Gentleman R, Carey V, Dudoit S, Irizarry R, Huber W Springer, New York* 2005, **Bioinformatics and Computational Biology Solutions using R and Bioconductor**:397–420.
104. Tatusov RL, Koonin EV, Lipman DJ: **A genomic perspective on protein families**. *Science* 1997, **278**(5338):631-637.
105. Fisher RA: **On the Interpretation of χ2 from Contingency Tables, and the Calculation of P**. *Journal of the Royal Statistical Society* 1922, **Vol. 85**(No. 1):87-94.

106. Holm S: **A Simple Sequentially Rejective Multiple Test Procedure**. *Scandinavian Journal of Statistics* 1979, **Vol. 6**(No. 2):65-70.
107. Mao F, Dam P, Chou J, Olman V, Xu Y: **DOOR: a database for prokaryotic operons**. *Nucleic acids research* 2009, **37**(Database issue):D459-463.
108. Solovyev V SA: **Automatic Annotation of Microbial Genomes and Metagenomic Sequences**. *In Metagenomics and its Applications in Agriculture, Biomedicine and Environmental Studies (Ed RW Li)* 2011, **Nova Science Publishers**:61-78.
109. Hall TA: **BioEdit: a user-friendly biological alignment editor and analysis program for Windows 95/98/NT**. *Oxford University Press* 1999, **Nucleic Acids Symposium Series No. 41**:95-98.
110. Carver TJ, Rutherford KM, Berriman M, Rajandream M-A, Barrell BG, Parkhill J: **ACT: the Artemis Comparison Tool**. *Bioinformatics* 2005, **21**(16):3422-3423.
111. Caspi R, Altman T, Billington R, Dreher K, Foerster H, Fulcher CA, Holland TA, Keseler IM, Kothari A, Kubo A *et al*: **The MetaCyc database of metabolic pathways and enzymes and the BioCyc collection of Pathway/Genome Databases**. *Nucleic acids research* 2014, **42**(D1):D459-D471.
112. Hofacker IL, Fontana W, Stadler PF, Bonhoeffer LS, Tacker M, Schuster P: **Fast folding and comparison of RNA secondary structures**. *Monatshefte für Chemie / Chemical Monthly*, **125**(2):167-188.
113. Hauryliuk V, Atkinson GC, Murakami KS, Tenson T, Gerdes K: **Recent functional insights into the role of (p)ppGpp in bacterial physiology**. *Nat Rev Micro* 2015, **13**(5):298-309.
114. Aravind L, Koonin EV: **The HD domain defines a new superfamily of metal-dependent phosphohydrolases**. *Trends in biochemical sciences* 1998, **23**(12):469-472.
115. Potrykus K, Cashel M: **(p)ppGpp: still magical?** *Annual review of microbiology* 2008, **62**:35-51.
116. Wolf YI, Aravind L, Grishin NV, Koonin EV: **Evolution of aminoacyl-tRNA synthetases-analysis of unique domain architectures and phylogenetic trees reveals a complex history of horizontal gene transfer events**. *Genome research* 1999, **9**(8):689-710.
117. Mechold U, Murphy H, Brown L, Cashel M: **Intramolecular regulation of the opposing (p)ppGpp catalytic activities of Rel(Seq), the Rel/Spo enzyme from Streptococcus equisimilis**. *J Bacteriol* 2002, **184**(11):2878-2888.
118. Xiao H, Kalman M, Ikehara K, Zemel S, Glaser G, Cashel M: **Residual guanosine 3',5'-bispyrophosphate synthetic activity of relA null mutants can be eliminated by spoT null mutations**. *The Journal of biological chemistry* 1991, **266**(9):5980-5990.
119. Fisher SD, Reger AD, Baum A, Hill SA: **RelA alone appears essential for (p)ppGpp production when Neisseria gonorrhoeae encounters nutritional stress**. *FEMS microbiology letters* 2005, **248**(1):1-8.
120. Tedin K, Bremer H: **Toxic effects of high levels of ppGpp in Escherichia coli are relieved by rpoB mutations**. *The Journal of biological chemistry* 1992, **267**(4):2337-2344.
121. Gaal T, Gourse RL: **Guanosine 3'-diphosphate 5'-diphosphate is not required for growth rate-dependent control of rRNA synthesis in Escherichia coli**. *Proceedings of the National Academy of Sciences of the United States of America* 1990, **87**(14):5533-5537.
122. Catlin BW: **Nutritional profiles of Neisseria gonorrhoeae, Neisseria meningitidis, and Neisseria lactamica in chemically defined media and the use of growth requirements for gonococcal typing**. *The Journal of infectious diseases* 1973, **128**(2):178-194.

123. Francis F, Ramirez-Arcos S, Salimnia H, Victor C, Dillon J-AR: **Organization and transcription of the division cell wall (dcw) cluster in Neisseria gonorrhoeae**. *Gene* 2000, **251**(2):141-151.
124. Rusniok C, Vallenet D, Floquet S, Ewles H, Mouze-Soulama C, Brown D, Lajus A, Buchrieser C, Medigue C, Glaser P *et al*: **NeMeSys: a biological resource for narrowing the gap between sequence and function in the human pathogen Neisseria meningitidis**. *Genome biology* 2009, **10**(10):R110.
125. Rhee SG, Park SC, Koo JH: **The role of adenylyltransferase and uridylyltransferase in the regulation of glutamine synthetase in Escherichia coli**. *Current topics in cellular regulation* 1985, **27**:221-232.
126. van Heeswijk WC, Westerhoff HV, Boogerd FC: **Nitrogen assimilation in Escherichia coli: putting molecular data into a systems perspective**. *Microbiology and molecular biology reviews : MMBR* 2013, **77**(4):628-695.
127. Pizer LI, Merlie JP: **Effect of serine hydroxamate on phospholipid synthesis in Escherichia coli**. *J Bacteriol* 1973, **114**(3):980-987.
128. Blumenthal RM, Lemaux PG, Neidhardt FC, Dennis PP: **The effects of the relA gene on the synthesis of aminoacyl-tRNA synthetases and other transcription and translation proteins in Escherichia coli A**. *Molecular & general genetics : MGG* 1976, **149**(3):291-296.
129. Grifantini R, Sebastian S, Frigimelica E, Draghi M, Bartolini E, Muzzi A, Rappuoli R, Grandi G, Genco CA: **Identification of iron-activated and -repressed Fur-dependent genes by transcriptome analysis of Neisseria meningitidis group B**. *Proceedings of the National Academy of Sciences of the United States of America* 2003, **100**(16):9542-9547.
130. Salvatore P, Pagliarulo C, Colicchio R, Zecca P, Cantalupo G, Tredici M, Lavitola A, Bucci C, Bruni CB, Alifano P: **Identification, characterization, and variable expression of a naturally occurring inhibitor protein of IS1106 transposase in clinical isolates of Neisseria meningitidis**. *Infection and immunity* 2001, **69**(12):7425-7436.
131. Wold S, Crooke E, Skarstad K: **The Escherichia coli Fis protein prevents initiation of DNA replication from oriC in vitro**. *Nucleic acids research* 1996, **24**(18):3527-3532.
132. Iggo R, Picksley S, Southgate J, McPheat J, Lane DP: **Identification of a putative RNA helicase in E. coli**. *Nucleic acids research* 1990, **18**(18):5413-5417.
133. Lappann M, Vogel U: **Biofilm formation by the human pathogen Neisseria meningitidis**. *Medical microbiology and immunology* 2010, **199**(3):173-183.
134. Joseph B: **Differential genome expression of serogroup B meningococci under *in vivo* mimicking conditions.** In., vol. 48: 17th International Pathogenic Neisseria Conference; 2010: 48.
135. Van 't Hof W, Veerman EC, Nieuw Amerongen AV, Ligtenberg AJ: **Antimicrobial defense systems in saliva**. *Monographs in oral science* 2014, **24**:40-51.
136. Carpenter GH: **The secretion, components, and properties of saliva**. *Annual review of food science and technology* 2013, **4**:267-276.
137. Crooks GE, Hon G, Chandonia JM, Brenner SE: **WebLogo: a sequence logo generator**. *Genome research* 2004, **14**(6):1188-1190.
138. Schneider TD, Stephens RM: **Sequence logos: a new way to display consensus sequences**. *Nucleic acids research* 1990, **18**(20):6097-6100.
139. Plague GR: **Intergenic transposable elements are not randomly distributed in bacteria**. *Genome biology and evolution* 2010, **2**:584-590.
140. Kredich NM: **Biosynthesis of Cysteine**. *EcoSal Plus* 2008, **3**(1).
141. Hryniewicz M, Sirko A, Palucha A, Bock A, Hulanicka D: **Sulfate and thiosulfate transport in Escherichia coli K-12: identification of a gene encoding a novel protein involved in thiosulfate binding**. *J Bacteriol* 1990, **172**(6):3358-3366.

142. Sirko A, Zatyka M, Sadowy E, Hulanicka D: **Sulfate and thiosulfate transport in Escherichia coli K-12: evidence for a functional overlapping of sulfate- and thiosulfate-binding proteins**. *J Bacteriol* 1995, **177**(14):4134-4136.
143. Sirko A, Hryniewicz M, Hulanicka D, Bock A: **Sulfate and thiosulfate transport in Escherichia coli K-12: nucleotide sequence and expression of the cysTWAM gene cluster**. *J Bacteriol* 1990, **172**(6):3351-3357.
144. Stern MJ, Ames GF, Smith NH, Robinson EC, Higgins CF: **Repetitive extragenic palindromic sequences: a major component of the bacterial genome**. *Cell* 1984, **37**(3):1015-1026.
145. Le Faou A: **Sulphur nutrition and metabolism in various species of Neisseria**. *Annales de microbiologie* 1984, **135b**(1):3-11.
146. Rhee SG, Ubom GA, Hunt JB, Chock PB: **Catalytic cycle of the biosynthetic reaction catalyzed by adenylylated glutamine synthetase from Escherichia coli**. *The Journal of biological chemistry* 1982, **257**(1):289-297.
147. Son HS, Rhee SG: **Cascade control of Escherichia coli glutamine synthetase. Purification and properties of PII protein and nucleotide sequence of its structural gene**. *The Journal of biological chemistry* 1987, **262**(18):8690-8695.
148. Leigh JA, Dodsworth JA: **Nitrogen regulation in bacteria and archaea**. *Annual review of microbiology* 2007, **61**:349-377.
149. Magnusson LU, Farewell A, Nyström T: **ppGpp: a global regulator in Escherichia coli**. *Trends in Microbiology* 2005, **13**(5):236-242.
150. Sarubbi E, Rudd KE, Xiao H, Ikehara K, Kalman M, Cashel M: **Characterization of the spoT gene of Escherichia coli**. *The Journal of biological chemistry* 1989, **264**(25):15074-15082.
151. Murray KD, Bremer H: **Control of spoT-dependent ppGpp synthesis and degradation in Escherichia coli**. *Journal of molecular biology* 1996, **259**(1):41-57.
152. Sajish M, Kalayil S, Verma SK, Nandicoori VK, Prakash B: **The significance of EXDD and RXKD motif conservation in Rel proteins**. *The Journal of biological chemistry* 2009, **284**(14):9115-9123.
153. Das B, Pal RR, Bag S, Bhadra RK: **Stringent response in Vibrio cholerae: genetic analysis of spoT gene function and identification of a novel (p)ppGpp synthetase gene**. *Mol Microbiol* 2009, **72**(2):380-398.
154. Boes N, Schreiber K, Schobert M: **SpoT-triggered stringent response controls usp gene expression in Pseudomonas aeruginosa**. *J Bacteriol* 2008, **190**(21):7189-7199.
155. Wendrich TM, Marahiel MA: **Cloning and characterization of a relA/spoT homologue from Bacillus subtilis**. *Mol Microbiol* 1997, **26**(1):65-79.
156. Mechold U, Malke H: **Characterization of the stringent and relaxed responses of Streptococcus equisimilis**. *J Bacteriol* 1997, **179**(8):2658-2667.
157. Hogg T, Mechold U, Malke H, Cashel M, Hilgenfeld R: **Conformational antagonism between opposing active sites in a bifunctional RelA/SpoT homolog modulates (p)ppGpp metabolism during the stringent response**. *Cell* 2004, **117**(1):57-68.
158. Varik V, Oliveira SRA, Hauryliuk V, Tenson T: **Composition of the outgrowth medium modulates wake-up kinetics and ampicillin sensitivity of stringent and relaxed Escherichia coli**. *Scientific Reports* 2016, **6**:22308.
159. Sørensen MA, Pedersen S: **Cysteine, even in low concentrations, induces transient amino acid starvation in Escherichia coli**. *Journal of Bacteriology* 1991, **173**(16):5244-5246.
160. Brockmann-Gretza O, Kalinowski J: **Global gene expression during stringent response in Corynebacterium glutamicum in presence and absence of the rel gene encoding (p)ppGpp synthase**. *BMC Genomics* 2006, **7**:230.

161. Gordon MH: **The inhibitory action of saliva on growth of the meningococcus**. *British medical journal* 1916, **1**(2894):849-851.
162. Orr HJ, Gray SJ, Macdonald M, Stuart JM: **Saliva and meningococcal transmission**. *Emerging infectious diseases* 2003, **9**(10):1314-1315.
163. Neil RB, Apicella MA: **Clinical and laboratory evidence for Neisseria meningitidis biofilms**. *Future microbiology* 2009, **4**(5):555-563.
164. Donlan RM, Costerton JW: **Biofilms: Survival Mechanisms of Clinically Relevant Microorganisms**. *Clinical microbiology reviews* 2002, **15**(2):167-193.
165. Balzer GJ, McLean RJ: **The stringent response genes relA and spoT are important for Escherichia coli biofilms under slow-growth conditions**. *Canadian journal of microbiology* 2002, **48**(7):675-680.
166. Sugisaki K, Hanawa T, Yonezawa H, Osaki T, Fukutomi T, Kawakami H, Yamamoto T, Kamiya S: **Role of (p)ppGpp in biofilm formation and expression of filamentous structures in Bordetella pertussis**. *Microbiology (Reading, England)* 2013, **159**(Pt 7):1379-1389.
167. He H, Cooper JN, Mishra A, Raskin DM: **Stringent response regulation of biofilm formation in Vibrio cholerae**. *J Bacteriol* 2012, **194**(11):2962-2972.
168. O'Dwyer CA, Li MS, Langford PR, Kroll JS: **Meningococcal biofilm growth on an abiotic surface - a model for epithelial colonization?** *Microbiology (Reading, England)* 2009, **155**(Pt 6):1940-1952.
169. Schmitt C, Turner D, Boesl M, Abele M, Frosch M, Kurzai O: **A functional two-partner secretion system contributes to adhesion of Neisseria meningitidis to epithelial cells**. *J Bacteriol* 2007, **189**(22):7968-7976.
170. Jeong J-H, Song M, Park S-I, Cho K-O, Rhee JH, Choy HE: **Salmonella enterica Serovar Gallinarum Requires ppGpp for Internalization and Survival in Animal Cells**. *Journal of Bacteriology* 2008, **190**(19):6340-6350.
171. Stintzi A, Marlow D, Palyada K, Naikare H, Panciera R, Whitworth L, Clarke C: **Use of Genome-Wide Expression Profiling and Mutagenesis To Study the Intestinal Lifestyle of Campylobacter jejuni**. *Infection and immunity* 2005, **73**(3):1797-1810.
172. Takahashi H, Yanagisawa T, Kim KS, Yokoyama S, Ohnishi M: **Multiple Functions of Glutamate Uptake via Meningococcal GltT-GltM L-Glutamate ABC Transporter in Neisseria meningitidis Internalization into Human Brain Microvascular Endothelial Cells**. *Infection and immunity* 2015, **83**(9):3555-3567.
173. Cross AS: **What is a virulence factor?** *Critical Care* 2008, **12**(6):196-196.
174. Casadevall A, Pirofski La: **Host-Pathogen Interactions: The Attributes of Virulence**. *Journal of Infectious Diseases* 2001, **184**(3):337-344.
175. Wexselblatt E, Oppenheimer-Shaanan Y, Kaspy I, London N, Schueler-Furman O, Yavin E, Glaser G, Katzhendler J, Ben-Yehuda S: **Relacin, a novel antibacterial agent targeting the Stringent Response**. *PLoS pathogens* 2012, **8**(9):e1002925.
176. Zhou F, Tran T, Xu Y: **Nezha, a novel active miniature inverted-repeat transposable element in cyanobacteria**. *Biochemical and biophysical research communications* 2008, **365**(4):790-794.
177. Rouquette-Loughlin CE, Balthazar JT, Hill SA, Shafer WM: **Modulation of the mtrCDE-encoded efflux pump gene complex of Neisseria meningitidis due to a Correia element insertion sequence**. *Mol Microbiol* 2004, **54**(3):731-741.

9 Annex

9.1 Abbreviations

APS……ammonium persulfate
ATR……AT-rich repeat
β-ME……beta-mercaptoethanol
bp……base pairs
BSA……bovine serum albumin
BSRP……BLASTP bio score ratio
CC……clonal complex
cDNA……complementary DNA
CE……Correia repeat element
CFU……colony forming units
COS plates……Colombia agar plates with 5% sheep blood
CREE……Correia repeat enclosed elements
CSPD……chloro-5-substituted adamantyl-1,2-dioxetane phosphate
CSF……cerebrospinal fluid
CTD……carboxy-terminal domain
Cy-3……cyanine 3
Cy-5……cyanine 5
DEPC……diethylpyrocarbonate
DIG……digoxygenine
DR……direct repeat
DUS……DNA uptake sequence
ddH_2O……double distilled water
DNA……desoxyribonucleic acid
dNTPs……desoxynucleotide triphosphates
DR……direct repeat
dsDNA……double-stranded DNA
DTT……dithiothreitol
EDTA……ethylenediamine-tetra-acetic acid
GCB……GC Medium Base
GCBL……*Neisseria gonorrhoeae* liquid medium
gDNA……genomic DNA
HCl……hydrogen chloride
IHF……integration host factor
IMD……invasive meningococcal disease

kb……..……...kilo base pairs
KCl……..……..potassium chloride
kDa……..……..…..kilo Dalton
LB……..……...lysogeny broth
LL……..……..……..……late logarithmic growth phase
LPS……..……lipopolysaccharides
M……..……...molar (mol/litre)
MFE……..…..……..minimum free energy
MITE…….....…….miniature inverted transposable elements
ML……...……...…….mid logarithmic growth phase
MLST……...…….……..multilocus sequence typing
MMM……..……Meningococcal minimal medium
mNDM……...…....Modified Neisseria Defined Medium
MOI……..……multiplicity of infection
MOPS……...……...3-(N-morpholino)propanesulfonic acid
NaCl……..…….Sodium chloride
NaOH……..……...Sodium hydroxide
Nf……..……neisserial filamentous phage
NIME……..…..neisserial intergenic mosaic elements
Nm……..…….*Neisseria meningitidis*
n.s.……..……..…not significant
NTD……..…..……amino-terminal domain
OD_{595}……..…….optical density measured at 595 nm
OD_{600}……...optical density measured at 600 nm
ORF……..……..….open reading frame
PABA……..……..4-Aminobenzoic acid
PAPS……..……3’-phosphoadenylsulfate
PBS……..……....phosphate-buffered saline
PBS-T……..……...…..…PBS-Tween
PCR……..…...polymerase chain reaction
PorA……..……...….porin A
PPi……..…….pyrophosphoryl
PPM……..……..….proteose peptone medium
PPM^{+}……..……..……proteose peptone medium with supplements
(p)ppGpp.....guanosine pentaphosphate or tetraphosphate
qRT-PCR……..……..quantitative real-time PCR
REP……..……...….repetitive extragenic palindromic sequence

RNA……..…..…ribonucleic acid
rpm……..……..……..…..rounds per minute
RT……..……..……....room temperature
SG……...……..……..…….serogroup
SDS……..……..……..sodium-dodecyl-sulfate
SDS-PAGE…….SDS-polyacrylamide gel electrophoresis
SOB……...……Super Optimal Broth
SOC……..……...SOB added with glucose
SR……..……stringent response
SSC……..……..…...saline-sodium-citrate buffer
SSPE……..……saline-sodium-phosphate-EDTA buffer
ST……..……..……sequence type
TAE……..……..….TRIS-acetate-EDTA
TBE……..…….…....TRIS-Borate-EDTA
TCS…….…….....……..two-component systems
TEMED…….….tetramethylethylenediamine
TIR……..…..…...terminal inverted repeat
TRIS…..……..…....trishydroxymethylaminomethane
TSD…….……target site duplications
U……..……...…units

9.2 List of Figures and Tables

9.2.1 Figures

9.2.2 **Tables**

9.3 Curriculum Vitae

9.4 Publications and Presentations

Publications

Schoen C, Kischkies L, Elias J, Ampattu BJ. Metabolism and virulence in *Neisseria meningitidis*. Front Cell Infect Microbiol. 2014; 4: 114.

Ampattu BJ & Hagmann L, *et. al.* Transcriptomic buffering of cryptic genetic variation contributes to meningococcal virulence. BMC. 2016 (submitted).

Presentations

Kischkies L, Joseph B, Frosch M, Schoen C. 'Stringent response in *ex vivo* survival of *Neisseria menigitidis*' XVIIth International Pathogenic Neisseria Conference (IPNC), Würzburg, Deutschland, 09.-14.09.2012

Kischkies L, Ampattu BJ, Schoen C. 'Impact of an intergenic sequence element and the stringent response on *ex vivo* virulence in the commensal pathogen *Neisseria meningitidis*', 13. Kongress für Infektionskrankheiten und Tropenmedizin, Würzburg, Deutschland, 15.-18.06.2016.

9.5 Danksagung